UNIVERSITY OF NOTTINGHAM
Institute of Engineering Surveying and Space Geodesy

HIGH PRECISION INTER-CONTINENTAL GPS NETWORK

João Francisco Galera Monico
BEng in Cartographic Engineering (Brazil), 1982
MSc in Geodesy (Brazil), 1988

Thesis submitted to the University of Nottingham
for the degree of Doctor of Philosophy

July 1995

ABSTRACT

GPS relative positioning provides precision of the order of 1 part per million (ppm) within relatively short periods of time. Considering this level of precision, together with the fact that the cost of GPS receivers is continuing to come down, it is now apparent that most of the future geodetic surveys will be performed by GPS. It is therefore important to establish geodetic control networks which are suitable for geodetic GPS activities. The Brazilian Institute of Geography and Statistics (IBGE), which is the National Geodetic Surveying organisation in Brazil, has proposed a high accuracy Brazilian GPS network, which has characteristics of an Active Control System (ACS). Such a system provides the users with the capability to perform relative positioning using only one receiver. An investigation of the methodology, algorithms and analysis, related to the IBGE network, has been carried out during this research. An initial investigation to assess the level of accuracy which can be obtained by a static user of the IBGE network, equipped with only one receiver and observing within different scenarios, has shown relative precision in the range of 2 to 0.1 ppm.

GPS positioning requires a global coordinate reference frame. The integration of a GPS network into such a global frame, requires stations already connected to the global reference frame to be observed simultaneously with the new network stations. The processing is then carried out involving the network stations together with those already connected to the global reference frame. The recently created International GPS Geodynamics Service (IGS) provides the capability for such easy integration. GPS data and ephemerides generated from the IGS Epoch '92 Campaign have been used in the processing carried out to integrate the Brazilian GPS network into the IERS Terrestrial Reference Frame 1993 (ITRF93). This data processing involved very large network, and the GPS processing software had to be expanded in order to provide higher accuracies. The results demonstrated repeatabilities of the order of 20 mm, for baseline lengths of up to 8200 km.

The expansion of the software mentioned above provided capability of processing very large or even global GPS networks. It allowed the investigation of several aspects related to global GPS, namely, free adjustment, the application of loose constraints to the parameters, and the use of internal constraints in the covariance matrix. The use of GPS to realise a global

reference frame has also been tested. In order to investigate all these aspects, an inter-continental network involving the Brazilian and IGS stations was used. Results have shown a level of agreement after the transformation between the *free network reference frame* and the ITRF93 coordinates, of the order of 6.4 mm.

To El for the encouragement and understanding,

and

to Gabriela.

Para a El pelo incentivo e compreensão

e

para a Gabriela.

ACKNOWLEDGEMENTS

This research was funded by the Conselho Nacional de Desenvolvimento Científico e Tecnológico - CNPq of the Ministry for Science and Technology of Brazil and the UNESP Universidade Estadual Paulista, Campus de Presidente Prudente, SP, Brazil. The author initiated his studies to pursue a PhD degree at the Delft University of Technology in June 1991 and transferred to the Institute of Engineering Surveying and Space Geodesy (IESSG) at the University of Nottingham in March 1993. The research has been conducted with the support of the Director of the IESSG, Professor V. Ashkenazi.

The author would like to thank his supervisors Professor V. Ashkenazi and Dr T. Moore for their support and encouragement. Acknowledgement is also extended to Dr W. Y. Ochieng, also from the IESSG, for his helpful comments and proof reading most of this thesis. In addition, many other present and past colleagues at the IESSG have contributed to this work. The author would like to express his gratitude to all of them and specially to Dr R. M. Bingley, Dr D. Lowe, Dr W. Chen, Dr P. Shadlow, Dr M. Dumville, Dr M. Stewart and Mr Nigel Penna. To all my PhD colleagues a big thank for a more helpful and entertaining research environment. Particular thanks are due to CCC, Po, Maria, Debbie and Jason.

During the early stages at Delft University of Technology, several people have contributed to the author's work. Thanks to Professor P. Teunissen and Dr. Hans Van der Marel for their supervision. Special thanks are also extended to Mr Paul de Jonge, for his help and friendship.

The author would like to thank all colleagues of the Department of Cartography at the UNESP Campus de Presidente Prudente, Sp, Brazil, for the support during this long period away from the duties of the Department. The author is grateful to Dr Denizar Blitzkow, from the Universidade de São Paulo, for his encouragement and advice, and to Mr L. P. S. Fortes, from the National Geodetic Survey of Brazil, IBGE (Instituto Brasileiro de Geografia e Estatistica), for providing information related to the Brazilian GPS Network (RMBC: Rede Brasileira de Monitoramento Continuo).

Finally and most important the author would like to express his utmost gratitude to his family, specially his parents and sisters, who despite his long absence from home, always offered total support and encouragement.

The author would like to mention the birth of his daughter Gabriela during the final stages of this work, a happening of great emotion and happiness.

Contents

List of Figures

List of Tables

Chapter 1

INTRODUCTION

Geodesy has experienced a remarkable progress in the last four decades. At the beginning of this century, conventional geodetic networks were generally surveyed by triangulation and later on, with the advent of Electronic Distance Measurement (EDM), by traversing and trilateration techniques. From the mid-seventies, just a decade and half after the birth of satellite geodesy, represented by the launch of the first Sputnik spacecraft in 1957, Transit-Doppler observations were used for the densification and control of geodetic networks. More recently, the advent of the Global Positioning System (GPS) in the late 1980s, has provided the geodetic community with a highly effective positioning tool. The development and refinement of algorithms and techniques associated with the introduction of low cost GPS receivers, have made GPS the most important geodetic positioning system at present, and probably at any time since the beginning of measurement science.

The association of GPS with communication systems has allowed the development of surveying techniques, which have changed the concept of a geodetic survey. An example is the Active Control System (ACS), which is a GPS-based system of fixed receivers, continuously tracking all visible satellites and relaying information to users via a communication link (Delikaraoglou *et al*, 1986), or even off-line via floppy disks. The GPS tracking stations are referred to as Active Control Points (ACP). A user accessing information from an ACP can estimate his position relative to the ACS reference frame. In such a case, a user equipped with only one receiver can perform relative positioning without having to occupy a reference station. If the user has a second receiver available, surveying of selected stations can be performed simultaneously.

On a global scale, the recent implementation of the International GPS Geodynamics Service (IGS) has created the opportunity of processing high precision global GPS networks within a few days after data collection (Mueller and Beutler, 1992). The IGS network has its stations referenced to the IERS

(International Earth Rotation Service) Terrestrial Reference Frame (ITRF) with all the core stations continuously tracking the GPS satellites. The data collected and the products generated (precise ephemeris, earth rotation parameters, etc.) by this network are available to the user community at the IGS global data centres. The data and products can be accessed using a file transfer medium via INTERNET, a world-wide network of computers. Such facilities provide the capability for easy integration of local networks into global reference frame.

Geodetic surveys performed by GPS have provided a precision of the order of 1 part per million (ppm) within relatively short periods of time. For longer periods, precision of a few parts per billion (ppb) is now achievable (Ashkenazi *et al*, 1994; Andersen *et al*, 1993; Dong and Bock, 1989). It is now apparent that as the cost of GPS continues reducing, most of the future geodetic surveys will be performed by GPS. The traditional geodetic networks are inadequate for GPS users. The precision of these networks is about 10 times worse than that provided by standard GPS, ie 10 ppm compared to 1 ppm. An extra inconvenience is that the control points of the networks are normally located on the high points of the area to be surveyed and often not easily accessible. It is therefore important to establish networks which are especially suitable for geodetic GPS activities.

The Brazilian Institute of Geography and Statistics (IBGE), that is charged with the responsibility of developing and maintaining of the Brazilian Geodetic System (SGB), has proposed the development of a high accuracy GPS network (Fortes and Godoy, 1991). The IBGE Network is referred to as the Brazilian Network for the Continuous Tracking of GPS Satellites (RBMC- Rede Brasileira de Monitoramento Contínuo). The RBMC, with some 9 tracking stations, has the characteristics of an ACS and is intended to support static relative positioning of the order of up to 0.1 ppm (Fortes, 1991). Taking into account the configuration of the network, GPS users will be able to place their receivers at a spacing of up to 500 km from the nearest station. Exceptions will occur in the Amazon region and Southern Brazil, where the range to a network station can reach about 1,700 and 900 km respectively.

The main aim of this research project was to investigate the methodology, algorithm and analysis procedures related to the RBMC. Considering the required accuracy of the Brazilian network and the spacing of the stations, it was therefore necessary to carry out some tests to try and project future GPS

user scenarios for Brazil. An initial investigation was directed towards a study to assess the quality of the results that could be obtained by users of the Brazilian GPS network, once the proposed RBMC becomes operational. This was restricted to the case of a static user with only one receiver. The assumption was that such a user would access GPS data of the (nearest) station of the network, either via a communication link or off-line via floppy disk.

GPS positioning is carried out within a global coordinate reference frame, such as the ITRF. It is therefore necessary to integrate the Brazilian GPS network into a global reference frame. In order to achieve this, the processing of the network has to be carried out jointly with other stations already integrated within ITRF, and observed simultaneously. To enable an initial definition of the Brazilian network in a global reference frame such as ITRF, three stations belonging to the proposed network were continuously occupied by GPS receivers for 14 days during the IGS Epoch '92 campaign. Additionally, four stations located in the state of São Paulo collected GPS data for a local project. The station CHUA, origin of the South American Datum 1969 (SAD-69), was also occupied for a whole day. The processing and analysis of the IGS Epoch '92 campaign in Brazil was an additional task carried out during this research project. Besides the Brazilian stations, three stations already connected to the ITRF were also involved in the joint processing.

In order to perform the processing of the IGS Epoch '92 campaign in Brazil, the capability of the software available at the University of Nottingham (GPS Analysis Software-GAS) had to be expanded. The processing of very large networks was only possible by sub-dividing the network. The software developments implemented during the course of this research were therefore directed towards providing GAS with the capability of processing global networks.

The above software developments enabled investigations to be carried out on the processing of inter-continental or even global GPS networks. Studies on global GPS network processing have been reported by several researchers. Blewitt *et al* (1992), Heflin *et al* (1992a), Heflin *et al* (1992b), Heflin *et al* (1993) and Blewitt *et al* (1993a) have applied the non-fiducial approach, in which no stations are held fixed in the adjustment. In the adjustment process, very loose constraints are applied to the ITRF coordinates of the stations. Internal constraints are also applied, but only to the covariance matrix of the

parameters. Comparisons between positions determined by GPS and the ITRF92 coordinates, showed agreement at the level of 1.8 cm for height (Heflin *et al*, 1993), the worst coordinate component. Mur *et al* (1993) have applied the complete free network (without loose constraints) and the fiducial approaches, and the level of agreement with the IGS/IERS coordinates in the ITRF91 in the height component was of about 14 and 2.2 cm respectively.

The level of accuracy reported above is at the same level of the precision obtained in the processing of the IGS Epoch '92 campaign in Brazil (Ashkenazi *et al*, 1995a; Ashkenazi *et al*, 1995b). The latter was obtained by simply carrying out an ordinary least squares adjustment, but the computed recovery (accuracy) was significantly higher than the obtained level of precision. Therefore, a further investigation was carried out within the context of an inter-continental (almost global) network involving data collected during the IGS Epoch' 92 campaign, including some of the Brazilian stations. For clarity, there follows a brief description of the three adjustment approaches used.

(i) **Ordinary Network Adjustment**: In this approach, the satellite positions are computed from the precise ephemeris and held fixed in the adjustment. The coordinates of some fiducial stations are either fixed or constrained to their known values, and the corrections to the approximate coordinates of the new stations and some bias parameters are estimated in the adjustment;

(ii) **Fiducial Network Adjustment**: It involves the simultaneous estimation of the corrections to the approximate values of the satellite state-vectors, the corrections to the approximate coordinates of the unknown stations and some other bias parameters. The coordinates of the fiducial sites have to provide at least the minimal constraints needed to realise the network reference frame, ie three translations, three rotations and one scale;

(iii) **Free Network Adjustment or Non-Fiducial Approach**: In this technique no stations are held fixed, as all the parameters involved in the adjustment (coordinates of all stations, satellite state-vectors and bias) are estimated during the adjustment process.

The non-fiducial approach provides the means to investigate the possibility of using GPS to realise a global reference frame. Theoretically, if all stations and

satellites state-vectors are held free in the adjustment, the model should have rank deficiency, and no solution can be obtained by using conventional least squares. However, the use of a dynamic approach to estimate the satellite orbits in a model where the earth orientation parameters (EOP) are fixed to the IERS Bulletin A values for instance, provides a non-singular system, but with a weak solution (Mur *et al*, 1993). A few of these aspects have been investigated during this research with the aim of analysing the internal accuracy of GPS in the realisation of a global reference frame.

Any alterations in the fiducial stations used in the ordinary and fiducial network adjustments necessitate that all the main steps in the processing are repeated. This is clearly a very time consuming task. In contrast, once a free solution is available, such alteration can be adapted by simply performing a transformation from the *free network reference frame* to the *fiducial stations reference frame*. Investigations of both approaches have also been carried out and the results compared.

The basic theory and software development are given in Chapters 2, 3, 4 and 5. Chapter 2 gives an overview of GPS, including the concepts involved in the GPS technique and a discussion of most of the error sources affecting the measurements. The basic mathematical models used in GPS data processing for ordinary network adjustment are fully described in Chapter 3. Chapter 4 addresses the fiducial and non-fiducial concepts with a brief description of the forces acting on the GPS satellites. Chapter 5 gives a detailed description of all modifications made to the GAS software and the development of additional programs.

Chapters 6, 7 and 8 present the results from the analyses of a number of experiments carried out during this investigation. Short description of GPS control networks and of the Brazilian geodetic system is given in Chapter 6. This is followed by the assessment of the expected accuracy achievable by a user of the RBMC equipped with only one receiver. Chapter 7 presents the results of the analysis of the IGS Epoch '92 campaign in Brazil. Chapter 8 outlines the several experiments carried out within the inter-continental network. They involve the ordinary network adjustment, the fiducial network adjustment and the non-fiducial approach. The thesis in concluded in Chapter 9, with suggestions for further work.

Chapter 2

THE GLOBAL POSITIONING SYSTEM: AN OVERVIEW

2.1 Basic Concepts

The NAVigation Satellite Timing And Ranging Global Positioning System (NAVSTAR-GPS) is a world-wide, satellite-based radio-navigation system. It has been developed by the United States (US) Department of Defence (DoD) to be the primary radio-navigation system within the US-military. Due to the high accuracy provided by the system and improvements in receiver technology, there is a growing community which utilises GPS for a variety of civilian applications (navigation, geodetic positioning, etc.).

The basic idea of the navigation principle consists of the measurement of the so called pseudoranges between the user and four satellites. Knowing the satellite coordinates within an appropriate reference frame, one can estimate the coordinates of the user antenna with respect to the same reference frame. From a geometric point of view, only three range measurements are sufficient. The fourth one is necessary in order to derive the clock offset between GPS time and the user clock.

The pseudorange observable is derived in the GPS receivers, which measure ranges to the satellites electronically by noting the transit time of a binary pseudo-random noise (PRN) code signal. There are two such codes employed in GPS, namely, the so-called P-code (Private or Precise), primarily for military use and the C/A-code (Coarse-Acquisition), mainly used by civilians. The satellite positions are determined from satellite ephemeris referenced to the World Geodetic System 1984 (WGS84).

GPS provides two levels of service, namely, a Standard Positioning Service (SPS) and a Precise Positioning Service (PPS). SPS is a positioning and timing service that will be available to all GPS users on a continuous, world-wide

basis with no direct charge. SPS will be provided on the GPS L1 signal which contains the C/A-code and the navigation data message. SPS is planned to provide, on a daily basis, the capability to obtain horizontal positioning accuracy within 100 meters (95% probability) and 300 meters (99.99% probability). The vertical positioning accuracy will be within 140 meters (95% probability), and timing accuracy within 340 nanoseconds (95% probability). The GPS L1 signal also contains the P-code that is not a part of the SPS. PPS employs the P-code to provide a highly accurate position, velocity, and timing information which will be available on a continuous, world-wide basis to users authorised by the DoD. The P-code is provided on both L1 and L2 signals. The service, with an accuracy of 10 to 20 m, was designed primarily for US military use. PPS is denied to unauthorised users by the use of cryptography.

The accuracy of the system is fulfilled by two modes of limitations, namely the Anti-Spoofing (A-S) and Selective Availability (SA). Anti-Spoofing entails the encryption of the P-code in order to protect it from imitations by unauthorised users (Seeber, 1993). A-S was exercised intermittently through 1993 and implemented on 31 January 1994. SA, the denial of full accuracy, is accomplished by manipulating navigation message orbit data (epsilon) and/or satellite clock frequency (dither). SA was activated on 4 July 1991 at 0400 UT.

GPS consists of three main segments: Space, Control and User.

2.2 Space Segment

The space segment consists of 24 satellites in six evenly spaced orbital planes, (four satellites in each plane) at an altitude of approximately 20,200 Km. The orbital planes are inclined at 55° to the earth's equator with an orbital period of 12 sidereal hours. The position is therefore the same at the same sidereal time each day, ie the satellites appear four minutes earlier each day. This configuration provides a minimum of 4 GPS satellites visible from anywhere on earth at any time.

Three types of satellites can be distinguished: Block I, Block II and Block IIR. Block I refers to the development (prototype) satellites. Eleven satellites were launched between 1978 and 1985. A total of 28 Block II operational satellites are planned to support the twenty-four satellite configuration. Twenty

replenishment satellites (Block IIR), will replace the Block II satellites as necessary. Two of the new design feature of the Block IIR satellites are the ability to measure distance between satellites (cross link ranges) and compute ephemeris on-board (Seeber, 1993).

Each satellite carries high performance frequency standards (Caesium and Rubidium) with a stability between 10^{-12} to 10^{-13} , forming a precise time base. Whereas the Block I satellites were equipped with quartz oscillators, the production satellites have been equipped with better frequency standards, namely two caesium and two rubidium oscillators.

The GPS satellites are identified by two different numbering schemes. The SVN (Space Vehicle Number) or NAVSTAR number, based on the launch sequence and the PRN (Pseudo-Random Noise) or SVID (Space Vehicle IDentification) numbers, related to the orbit arrangement and the particular PRN segment allocated to the individual satellites.

2.2.1 GPS Signal Characteristics

The satellites transmit on two L-band frequencies: L1=1575.42 MHz and L2=1227.6 MHz, which are generated by integer multiplication of the fundamental frequency (f_0) of 10.23 MHz. The corresponding wavelengths are approximately 19.05 cm and 24.45 cm for L1 and L2 frequencies respectively. The fundamental frequency is based on the output of highly stable atomic clocks. The carriers are modulated with PRN codes. These are sequences of binary digits (zeros and ones, or +1 and -1) which appear to have random character, but which can be identified unequivocally.

Three PRN codes are in use: the C/A-code, the P-code and the Y-code. The C/A-code has a frequency of 1.023 MHz, ie a sequence of 1.023 million binary digits or chips per second (bps). The period of the C/A-code is one millisecond and is used primarily to acquire the P-code. The corresponding wavelength of one chip is about 300 m. The P-code frequency is 10.23 MHz (wavelength of about 30 m) with a period of seven days. Under A-S conditions, the GPS satellites continue to broadcast the P-code, but it has been encrypted by having a relatively simple 50 bps W-code modulated on top of it. The resulting P+W code is what is commonly referred to as the Y-code.

The L1-band signal is modulated with the navigation data and the C/A- and P-codes. The L2-band only contains the P-code plus navigation data. The various satellites all transmit on the same frequencies, L1 and L2, but with individual code assignments. The navigation data contain the orbital elements, clock behaviour, system time and status messages. In addition, an almanac is also provided which gives the approximate data for each active satellite. This allows the user to find all satellites once the first has been acquired.

2.3 Control Segment

The Control segment consists of five Monitor Stations (Hawaii, Kwajalein, Ascension Island, Diego Garcia, Colorado Springs), three Ground Antennas, (Ascension Island, Diego Garcia, Kwajalein), and a Master Control Station (MCS) located at Colorado Springs, Colorado. Each monitor station possesses a dual-frequency receiver connected to an external caesium beam oscillator. The monitor stations passively track all satellites in view and transmit the data to the MCS. The data is processed at the MCS to determine satellite orbits (broadcast ephemerides) and satellite clock corrections in order to update each satellite's navigation message. The updated information is transmitted to each satellite via the Ground Antennas. The Monitor Station (MS) coordinates were precisely surveyed with respect to the World Geodetic System 1972 (WGS72) reference frame. The new standard is the World Geodetic System 1984 (WGS84), the transition taking place on January 10, 1987.

2.3.1 GPS Time System

GPS positioning involves the precise measurement of the signal time of flight from satellite to receiver. As such, the time measurement must be referenced to a very stable time frame. GPS uses its own time scale, which is called GPS time. It is an atomic time scale and differs from the Coordinated Universal Time (UTC) by a nearly integer number of seconds. Both time scales were identical on 6 January 1980. Because GPS time is not incremented by the leap seconds as in the case of UTC, the difference between the two systems is increasing. The relation between UTC and GPS time is available in time bulletins of the United State Naval Observatory (USNO) and International Bureau of Weights and Measures (BIPM) as well as within the GPS satellite messages. By applying the broadcast clock corrections, the GPS time is kept synchronised to UTC to within 100 ns (Wells *et al*, 1986).

2.3.2 GPS Reference Frame

The GPS reference frame is the Department of Defence (DoD) World Geodetic System 1984 (WGS84), which provides the basic reference frame and geometric figure for the earth, models the earth gravimetrically, and provides the means for relating positions on various local geodetic systems. Its origin is the earth's centre of mass with Cartesian axes identical to the Conventional Terrestrial System (CTS) as defined by the Bureau International de L'Heure (BIH) for the epoch 1984.0 (Figure 2.1). The Geodetic Reference System 1980 (GRS80) was adopted as the ellipsoid of reference. The realisation of WGS84 consists of 1591 stations determined by the Defence Mapping Agency (DMA) using the TRANSIT (Doppler) system, accurate to 1 to 2 m. Further information about the system can be found in White *et al* (1989).

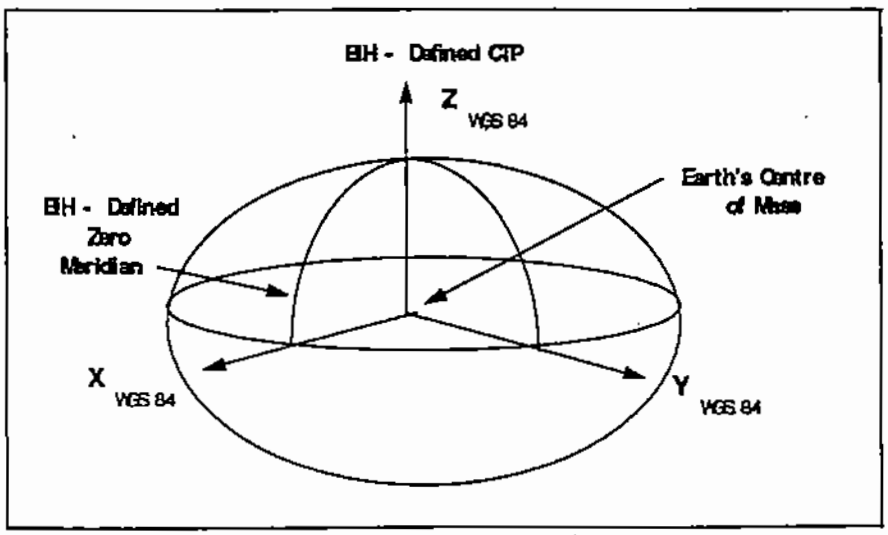

Figure 2.1: WGS84 Reference Frame

The broadcast ephemerides of the GPS satellites are given in the WGS84 coordinate system. The coordinates of ground stations derived by GPS measurements will therefore also be in the same reference frame. However, most of the GPS users will be interested in coordinates referenced to a particular local and/or regional datum. Therefore, precise and reliable transformation parameters between such geodetic datum and WGS84 should be available. For some applications, the transformation parameters between WGS84 and local geodetic system may require better precision than that provided by DoD. At such cases, the use of the International Terrestrial Reference System (ITRF) coordinates (§4.3.2) may be the best solution.

2.3.3 Satellite Ephemerides

In order to determine the receiver position in the navigation mode, the user must have real-time access to the satellite positions and the satellite system time. This information is accessed via the GPS satellites signal, which contains the broadcast ephemerides. For those users not requiring instantaneous positioning, but high accuracy, one option is to access the precise ephemerides.

(a) Broadcast Ephemerides

The procedure for producing the broadcast ephemeris has been described by several authors (Seeber, 1993; Ashkenazi and Moore, 1986; Wells *et al*, 1986). It involves the processing of pseudorange data of the monitor stations in conjunction with a satellite force model, using Kalman filter. The conversion to the Keplerian format is also involved in the procedure. The parameters describing the satellite orbit are the Keplerian elements and their related perturbations. They are valid for a time interval of about two hours before and two hours after a given reference epoch, without much degradation. Using these elements and the time parameters, the satellite positions for all epochs of observations can be computed (Moore, 1993).

A fresh data set is broadcast every 60 minute, causing different overlapping representations with steps that can reach a few decimetres. They may be smoothed by suitable approximation techniques (Ochieng, 1993) or neglected. When the broadcast ephemerides are derived from different data sets, these steps can be even larger. The expected accuracy of the satellite position represented by the broadcast ephemerides is about 10 m (Wells *et al*, 1986). However, the implemented SA can degrade the broadcast ephemerides for Block II satellites to about 100 m (Ochieng, 1990).

(b) Precise Ephemerides

One possibility of improving the quality of the satellite ephemerides is carrying out a posteriori estimation of the satellite orbits, the so-called precise ephemerides.

Traditionally, precise ephemerides were determined by the US Defence Mapping Agency (DMA) based on observations at 10 globally distributed stations. Besides the five monitor stations, data collected at five DMA stations (Austria, Ecuador, England, Argentina and Bahrain) are included in the

processing. The most recent developments include the Cooperative International GPS Network (CIGNET) operated under the coordinating responsibility of the US National Geodetic Survey (NGS) (Moore, 1993) and the International GPS Geodynamics Service (IGS) under the auspices of the International Association of Geodesy (IAG) (Muller and Beutler 1992). The IGS provides precise ephemerides computed from different analysis centres; namely JPL (Jet Propulsion Laboratory, Pasadena, California), UTX (University of Texas, Austin, Texas), SIO (Scripps Institute of Oceanography, La Jolla, California), EMR (Energy, Mines, and Resources, Ottawa, Canada), CODE (Centre of Orbit Determination in Europe, Bern, Switzerland), ESA (European Space Agency, Dasrmstadt, Germany) and GFZ (Zentralinstitut fur Physik der Erde, Postdam, Germany). IGS orbits are referenced to the ITRF.

Efforts have been made towards a production of an official IGS orbit by combining the results of all IGS processing centres (Springer and Beutler, 1993), which culminated to an official IGS satellite orbit ephemeris.

2.4 User Segment

The User Segment consists of the equipment required to receive the signals transmitted by the satellites. The user categories can be divided into military and civilian. Within the civilian sector, GPS receivers are being used for a wide range of applications: surveying, navigation, fleet management and control, intelligent vehicles, just to mention a few. The diversity of users is matched by the type of receivers available today. Taking into account the type of observables (ie, code pseudoranges or carrier phases) and on the availability of codes (ie, C/A-code or P-code), one can classify GPS receivers into three groups: (1) C/A-code pseudorange, (2) C/A-code carrier phase, and (3) P-code carrier phase measurement instruments (Hofmann-Wellenhof *et al*, 1992).

High precision application requires access to the code and carrier phase data, ie, a receiver of group (2) or (3). The technique usually applied to access the carrier phase when A-S is not activated is the code-correlation technique. Otherwise, the L2 carrier phase can be accessed by one of several techniques, namely signal squaring, code-correlation squaring, cross-correlation and P-W code tracking, depending on the receiver type. A brief description of these techniques follows below.

2.4.1 Code-correlation

In this technique, the receiver correlates the codes generated by itself with the codes received from the satellites. If there is initially no match between the codes, the code generated within the receiver is shifted until maximum correlation is obtained. Once the signals are aligned, a code tracking loop ensures that both code sequences remain aligned. The time shift in the two sequences of codes is a measure of the travel time of the signal, from the satellite to the receiver. As there is receiver and clock error, when the time is multiplied by the speed of light, it results in the so called pseudorange.

Once the lock has occurred, the receiver demodulates the carrier phase by the extraction of the navigation message. The carrier phase observable is the relative phase between the received carrier signal and the internal reference carrier signal derived from the local oscillator measured at pre-set epochs. During the interval of the pre-set epochs, the receiver keeps counting the integer number of wavelengths to be added or subtracted in the measurement as the satellite to receiver range changes. The carrier can be measured to an accuracy of about 3 millimetres.

This technique only works on L2 when the P-code is available (A-S not activated), or for authorised users with access to the Y-code.

2.4.2 Signal Squaring

In the signal squaring technique the incoming satellite signal is multiplied by itself and therefore generates a second harmonic of the original carrier. The codes and broadcast message are lost and the resulting signal, after filtering, is a sine wave with twice the original carrier frequency and increased signal-to-noise ratio. The advantage of this technique is that knowledge of the code is not required, making it suitable for L2 access in times of P-code denial (A-S activated).

The loss of the navigation message means that one requires an external ephemeris and satellite clock correction terms. The solution for this problem involves the use of the C/A-code to obtain the L1 pseudorange and carrier and hence the timing information and navigation message. By squaring the L2 signal, the carrier is obtained. Detection of outlier and cycle slip corrections are

usually more difficult on data collect by receivers using the squaring technique on L2 than those using the code-correlation technique.

2.4.3 Cross-Correlation

The cross-correlation technique is an option available in some receivers, such as Trimble 4000SSE and TurboRogue. They are automatically switched to the cross-correlation technique when Anti-Spoofing is on. It provides four observables: full-cycle on L1 and L2 carrier phase measurements, C/A-code and cross-correlated Y-code pseudorange.

The cross-correlation technique relies on the fact that the L1 and L2 Y-codes are identical but not necessarily known. Luckily, due to ionospheric delays, the L1 signal will always arrive before the L2 signal. By observing what the signal is on L1, one can use it to correlate with the L2 signal coming in slightly later. Therefore, the L1 Y-code signal is fed through a variable feed back loop until it correlates with the incoming L2 Y-code. The delay required is equivalent to the (Y2-Y1) pseudorange, ie the difference between the L1 and L2 P-code pseudoranges. This can be added to the L1 C/A-code pseudorange to provide the L2 pseudorange. After correlating the two incoming codes, they are precisely aligned and can be subtracted to give the L2 carrier signal. This leads to a 24 cm (full wavelength) L2 carrier phase (Talbot, 1992).

2.4.4 Code-Correlating Squaring

This technique uses the fact that most of the Y-code is made up of the P-code. Correlating the L2 Y-code signal with a locally generated replica of the underlying P-code and narrowing the bandwidth it is possible to measure the P-code pseudorange on L2. Then, the signal is squared to get a half wavelength L2 carrier phase. This is the technique used by Leica 200 GPS receivers.

2.4.5 P-W Code Tracking

This is the latest technique and has been developed by Ashtech, which uses a P-W code tracking technique in the Ashtech ZXII receiver. The Y-code signal under A-S can be broken down into two components; the original P-code and the W-code used to encrypt the P-code. This technique relies on the fact that the Y-code is the same on both the L1 and L2 frequencies. Furthermore, it uses

the knowledge that the W-code is a substantially lower rate encryption, at about 50 bps. The underlying P-code is correlated in the incoming P-W code signal, with a locally generated P-code. By reducing the bandwidths of the resulting signals to about 50 bps, and comparing the L1 and L2 signals, it is possible to estimate the current value of the encryption of the W-code. It can therefore be effectively removed, leaving the P-code. This technique provides a C/A and Y1 pseudorange on L1 and a Y2 pseudorange on L2 with full wavelength L2 carrier phase data (Ashjaee and Lorenz, 1992).

2.5 Current GPS Status

The current GPS constellation consists of 24 satellites. Eleven Block I satellites have been launched. They reflect the various stages of system development and are not identical with the operational satellites (Block II). The first Block II satellite was launched in February 1989 and twenty-four Block II/IIA satellites have been launched to date (June 1995).

The GPS Initial Operational Capability (IOC) was achieved on 8 December 1993 with a constellation of 24 GPS satellites (Block I/II/IIA). The GPS Full Operational Capability (FOC) was declared on 27 April 1995. It means that the 24 operational satellites (Block II/IIA) are effectively functioning in their assigned orbits, since they have been successfully tested for operational military functionality.

2.6 GPS Observables

Four basic observables can be identified in GPS (Seeber, 1993):

- pseudorange from code measurements,
- pseudorange difference from integrated Doppler counts,
- carrier phase or carrier phase difference and
- difference in signal travel time from interferometric measurement.

In practice, however, only two fundamental observables are used: code phases (pseudorange from code observations) and carrier phases. Hereafter they will be referred to as pseudorange and carrier phase observables respectively.

2.6.1 Pseudorange observable

The pseudorange observable (PR) is a measure of the distance between the satellite at the time of transmission and the receiver at the time of reception of the signal. The transit time of the signal is measured by either correlating identical pseudo-random-noise codes generated by the satellite and by the receiver (code-correlation technique) or by using some of the other techniques previously described (P-W tracking, Cross-Correlation, Code-Correlating Squaring) when A-S is activated. Depending on the receiver, one, two or three pseudoranges can be measured.

The codes are derived from the receiver and satellite clocks, which are not synchronised between themselves and with a basic time reference frame (GPS time). The GPS satellites have a precise atomic clock (oscillator) operating in the satellite time frame (t^s) to which all transmitted signals are referenced to. The receivers usually have less precise oscillators operating in the receiver time frame (τ_r) in which all received signals are referenced to. These two time frames can be related to the GPS time frame (T) by the following relationships:

$$T^s = t^s - \delta t^s(t^s) \tag{2.1}$$

$$T_r = \tau_r - \delta\tau_r(\tau_r) \tag{2.2}$$

where $\delta t^s(t^s)$ is the satellite clock offset at the satellite time frame t^s and $\delta\tau_r(\tau_r)$ is the receiver clock offset at the receiver time frame τ_r. Notice that a superscript denotes a satellite related quantity and a subscript denotes a receiver related quantity.

Effectively, pseudorange (PR) is the time difference (in the time frame of the receiver) between the reception time of the signal at the receiver (τ_r) and the time of transmission of this signal from the satellite (t^s) scaled by the speed of light in vacuum (c), ie,

$$PR_r^s(\tau_r) = c(\tau_r - t^s) \tag{2.3}$$

Introducing the transmission time of the signal t^s (equation 2.1) and the reception time of the signal τ_r (equation 2.2) in the last equation, one obtains

$$PR_r^s(\tau_r) = c(T_r - T^s) + c(\delta\tau_r(\tau_r) - \delta t^s(t^s)) \qquad (2.4)$$

The first element of the right hand side of this expression is the geometric distance between receiver and satellite at the epoch of transmission and reception of the signal in the GPS time frame, ie,

$$\rho_r^s(T_r, T^s) = c(T_r - T^s) \qquad (2.5)$$

This relation can be expressed in terms of three-dimensional coordinates of receiver (X_r, Y_r, Z_r) and satellite (X^s, Y^s, Z^s) as:

$$\rho_r^s = \sqrt{(X^s - X_r)^2 + (Y^s - Y_r)^2 + (Z^s - Z_r)^2} \qquad (2.6)$$

There are other terms that may be added to the pseudorange expression, particularly to account for ionospheric and tropospheric delay biases. A detailed discussion on errors and biases affecting GPS observations will be given in (§2.7). Assuming that whenever possible, most of the errors are modelled and eliminated, the full pseudorange observation equation is given by

$$PR(\tau_r)_r^s = \rho_r^s(T^s, T_r) + c(\delta\tau_r(\tau_r) - \delta t^s(t^s)) + v_{pr} \qquad (2.7)$$

where (v_{pr}) denotes the random (and unmodelled) error.

2.6.2 Carrier phase observable

The basic observable in precise GPS positioning is the carrier phase observable ϕ_r^s, which is obtained by measuring the difference between the phase of the signal arriving from the satellite (ϕ^s), and the phase of the signal generated locally at the receiver (ϕ_r). The observed phase ϕ_r^s or beat frequency (in cycles) is given as (King *et al*, 1985)

$$\phi_r^s(\tau_r) = \phi^s(\tau_r) - \phi_r(\tau_r) + N_r^s \qquad (2.8)$$

where τ_r is the time of reception of the satellite signal at station **r**,

$\phi^s(\tau_r)$ is the carrier phase received at station **r** from satellite **s** at receipt time τ_r,

$\phi_r(\tau_r)$ is the locally generated phase at the receiver receipt time τ_r and

N_r^s is an integer, representing the integer cycle ambiguity in the observed phase.

The term N_r^s represents the integer ambiguity for the first epoch of measurement. Receivers provide the accumulating phase ϕ_r^s over time at pre-set, equally spaced epochs in units of cycle. The precision of the measurements is about 1/100 of a cycle.

The time at which the signal is received, τ_r, is related to the time at which the signal is transmitted, τ^s, by

$$\tau^s = \tau_r - \tau \tag{2.9}$$

where τ is the travel time of the signal, which is a function of the geometric distance between the satellite and the receiver and of the effects of the ionosphere and troposphere. It is also referred to as propagation delay. Therefore, the phase of the received signal $\phi^s(\tau_r)$, is related to the phase of the transmitted signal Φ_r^s by

$$\phi^s(\tau_r) = \phi_r^s(\tau_r - \tau) = \phi_r^s(\tau_r) - f\tau \tag{2.10}$$

The transmitter frequency f is nominally constant but it varies due to instabilities and dithering (S-A) in the satellite's clock. In addition, the GPS time of the signal reception, T_r, differs from the receipt time τ_r. It can be shown that the carrier beat phase can be represented as (King *et al*, 1985)

$$\phi_r^s(\tau_r) = -f\tau - f[\delta_r(\tau_r) - \delta^s(\tau^s)] + \overline{N}_r^s \tag{2.11}$$

with

$$\overline{N}_r^s = N_r^s + \Phi^s(\tau_0) - \Phi_r(\tau_0) \tag{2.12}$$

not an integer any more. The second and third terms in the expression (2.12) are the unknown initial phases of the satellite and receiver oscillator, respectively.

Details of the errors affecting the carrier phase measurement are given in §2.7. As it was the case with the pseudorange observable, it is assumed that most of the errors are modelled and eliminated. Adding an extra term v_Φ, which contains the random (and unmodelled) errors due to clocks, propagation media, satellite ephemerides, fixed station coordinates, multipath and etc., to the expression (2.12), the resulting carrier phase observation equation is given as:

$$\phi_r^s(\tau_r) = -f\tau - f[\delta t_r(\tau_r) - \delta t^s(\tau^s)] + \overline{N}_r^s + v_\phi \qquad (2.13)$$

2.7 GPS Biases and Errors

The GPS observables, like any other observable in a measurement process, are subject to systematic error or biases, blunders and random noise. In order to obtain reliable results, the specified mathematical (stochastic and functional) model should hold and be able to detect model mis specifications. Therefore, the sources of errors/biases in the measurement process should be well known. Systematic errors (biases) can either be modelled as additional terms in the observation equation or eliminated by appropriate techniques. Random errors, in contrast, have no known relationship with the measurement and are normally the discrepancies remaining after all the blunders and systematic errors have been removed. In the following sections, the GPS error sources and their effects on the observable are described and the methods used to minimise them, highlighted. Table 2.1 realises a sub-division of the error sources and lists some of their effects.

The errors listed in Table 2.1 are conveniently grouped according to their sources. They are namely, satellite related errors, propagation medium related errors, receiver related errors, and station related errors.

Table 2.1: GPS Error Sources and Effects

SOURCE	EFFECT
Satellite	- Orbital error - Clock Bias - Relativity - Group Delay
Signal Propagation	- Troposphere Refraction - Ionosphere Refraction - Cycle Slips - Multipath
Receiver/Antenna	- Clock Bias - Interchannel Bias - Antenna Phase Centre
Station	- Coordinates - Earth Body Tides - Polar Motion - Ocean Tide Loading - Atmosphere Pressure Loading

2.7.1 Satellite Related Errors

(a) Orbital Errors

Orbital information can be obtained either from the broadcast ephemerides of the satellite messages or precise ephemerides from several sources (§2.3.3). The satellite positions derived from the ephemerides are normally held fixed in the processing of GPS data. Therefore, any error in satellite coordinates propagates into the user position. In point positioning, (§3.4), satellite positioning errors are strongly correlated with the user position error. Differencing the observables eliminates most of the orbital error (see §3.3.2), but the remaining error degrades the baseline accuracy. A useful rule-of-thumb expressing baseline error as a function of satellite positioning error (Wells *et al*, 1986) is

$$\Delta b = b \frac{\Delta r}{r} \tag{2.14}$$

where Δb is the baseline error,

b is the baseline length (km),

Δr is the satellite position error and,

r the satellite to receiver range ($\equiv$ 20,000 km).

The broadcast ephemeris is currently estimated to have an accuracy of 20 to 100 m (with 'Epsilon' type S-A). Precise ephemerides is claimed to have orbital accuracy of the order of 20 cm when processing 14-day-arcs (Beutler *et al*, 1994). The standard, however, is processing 1-3 days-arcs providing accuracy of about 2 m. Typical baseline errors (Δb) are tabulated in Table 2.2. For the broadcast ephemeris (BE) it is assumed an accuracy of 20 and 100 m and the precise ephemeris (PE), an accuracy of 2 and 0.2 m for baselines ranging from 10 to 5000 km. Over short baselines, orbital errors tend to cancel out if a differential approach is used. Precise ephemerides are capable of providing relative precision of about 0.01 parts per million (ppm) over long baselines. Such level of precision may support most of the GPS applications. However, for real time applications, broadcast ephemerides should be used, and the quality of the results depends on the accuracy of the ephemerides. Wide Area Differential GPS (WADGPS) has been receiving increasingly widespread attention and can provide a suitable answer to real-time applications (Mueller, 1994).

Table 2.2 Effect of Orbital Errors on Baseline Vector

Ephemerides	Orbital error Δr (m)	Baseline Length b (km)	Baseline error Δb (cm)	Relative Accuracy $\Delta b/b$ (ppm)
BE	100	10	5	5.0
		100	50	
		1 000	500	
		5 000	2 500	
BE	20	10	1	1.0
		100	10	
		1 000	100	
		5 000	500	
PE	2	10	0.10	0.1
		100	1	
		1 000	10	
		5 000	50	
PE	0.2	10	0.01	0.01
		100	0.1	
		1 000	1	
		5 000	5	

(b) Satellite Clock Bias

The satellite clock bias represents the difference (offset) between the time provided by the satellite and the highly stable GPS time. This difference can be as much as 1 millisecond (Wells *et al*, 1986).

GPS satellites carry a rubidium and a caesium atomic frequency standards, whose performance is monitored by the control segment. The amount by which they differ from the GPS time is included in the broadcast message in the form of coefficients of a second-order polynomial given as:

$$\delta t(t) = a_0 + a_1(t - t_{oc}) + a_2(t - t_{oc})^2 \qquad (2.15)$$

where t_{oc} is the satellite clock reference time,
a_0 is the clock offset at reference time,
a_1 is the clock drift term at reference time and
a_2 is the clock ageing term at reference time.

The SA 'dither' error ('Delta' -type SA) is implemented through the injection of errors in the a_1 satellite clock term (Lachapelle *et al*, 1992). Therefore, with SA turned on, the satellite clock error is not correctly modelled by this polynomial. The effects of the satellite clock error can be reduced by differencing the observables (§3.2.2). In the processing of IGS data to generate precise ephemerides, some IGS centres introduce the satellite clock error in the adjustment as a white noise parameter (Kouba *et al*, 1993).

(c) Relativity

The relativistic effects for GPS are not only restricted to the satellites (orbit and clock) but also to the signal propagation and receiver clock. The satellite clock, besides the error already mentioned, shifts due to the general and special relativity. The effects are compensated for by offsetting the fundamental frequency f_0 of the oscillator by -4.55×10^{-3} Hz (Spilker, 1980)

Most of the effects of the general relativity (accelerated reference systems, signal path is curved due to the gravity field) can be neglected. Besides this, they are cancelled out when differencing the observations (Hofmann-Wellenhof *et al*, 1992).

(d) Group Delay

This is due to signal retardation as it passes through the satellite hardware. These delays affect the travel time of the signal. However, calibration during ground test of the satellites, provides the magnitude of these delays and the corrections are included in the clock polynomial coefficients.

2.7.2 Propagation Medium Related Errors

The propagation media affect the electromagnetic radiation at all frequencies. The result is a bending or refraction associated with a time delay of arriving signal. The former is due to the fact that the signal passes through layers of varying density in the atmosphere and the latter due to the fact that the speed of the signal in the atmosphere differs from that in a vacuum. The propagation media consist of the troposphere and ionosphere. The troposphere extends from the earth's surface to about 50 km. For frequencies below 30 GHz the troposphere behaves mainly like a non-dispersive medium; ie the refraction is independent of the frequency of the signal passing through it. The ionosphere is a dispersive medium (the refraction depends of the signal frequency), meaning that the carrier phase as well as the modulation on it is affected differently. The ionosphere comprises the regions between approximately 50 and 1,000 km above the earth and contains free electrons. Due to the difference in behaviour, the ionosphere and troposphere are modelled separately.

(a) Ionospheric Refraction

The ionosphere is a dispersive medium at microwave frequencies. This means that its effects will vary with the signal frequency. The basic simplistic form of the relationship between the refractive index (**n**), and the frequency (**f**) is given by (Dodson *et al*, 1993; Hofmann-Wellenhof *et al*, 1992)

$$n = 1 \pm A_1 \frac{N_e}{f^2} + \text{high-order terms} \qquad (2.16)$$

where A_1 is a simple combination of physical constants (=40.3 Hz^{2}),

N_e is the free electron density in the ionosphere (approximatelly 10^{16} electrons / m^3) and

$\pm$ depends on whether the refraction index for the velocity of the code (+ for group refractive index) or for the phase of the signal (- for phase refractive index) is being determined.

From this expression one can see that the refractive index for the phase is less than unity, ie the phase is advanced when passing through the ionosphere, whilst the code is delayed. Therefore, the code pseudoranges are too long and the carrier phase too short compared to the geometric distance between the satellite and the receiver. The difference is identical in both cases. Apart from the frequency of the signal, the refractive index is also affected by the free electron density. This depends on the activity of the sun. However, magnetic storms superimpose an irregular pattern over the sun spot cycle, making the prediction of free electron density very difficult. During disturbed ionospheric conditions, the vertical ionospheric delay may reach as much as 100 m during the day on satellites at low elevation angles (Newby and Langley, 1992), reducing to 1 or 2 m at night (Dodson *et al*, 1993). The equatorial and polar regions are frequently the hosts for major disturbances.

The first order ionospheric refraction I_r^s (metres) is obtained from the expression

$$I_r^s = \pm \frac{A_1}{f^2} N_t \qquad (2.17)$$

where N_t is the total electron content (TEC), ie the number of electrons in a column through the ionosphere with a cross-sectional area of one square metre along the signal.

The dependency of the ionospheric refraction on the frequency makes it possible to eliminate the first order effects of the ionosphere by using the dual frequency technique (§3.3.1). However, experiments carried out with data collected in the equatorial region have shown that even for short baselines, the detection of cycle slips and determination of the double difference ambiguities become considerably more complicated during period of high ionospheric activity due to scintillation (Wanninger, 1993). Therefore, in the equatorial region, the GPS users need to be aware of severe ionospheric conditions.

For single frequency users, the ionosphere remains one of the largest sources of error. For relative positioning, over short baselines, most of this error is differenced away. However, single frequency receivers are widely used for precise surveying over baselines longer than what is expected to be reasonable for elimination of the ionosphere effects. Therefore, in order to improve the results, some of the reported models for correction of the ionospheric delay

(Newby and Langley, 1990; Georgiadou Y, 1990; Newby and Langley, 1992; Klobuchar, 1986) have to be used. In some of these models, the phase measurements from dual frequency receivers are used to estimate corrections for single frequency users operating in the same area. This approach seems ideally suited to the Brazilian Network for Continuous tracking of GPS satellites (§6.4.2), which would consist of a number of dual frequency receivers spread over the country. The information collected at these stations could be used with little cost or effort by single frequency users.

(b) Tropospheric Refraction

The troposphere is a non-dispersive medium at radio frequencies. Thus, its effects can not be estimated (or eliminated) from two-frequency measurements in the way that the ionospheric effects can. Instead, estimation of the delay relies on the use of one of the several established models.

The tropospheric path delay can be defined as:

$$T_r^s = 10^{-6} \int_a^b N ds \tag{2.18}$$

with **a** and **b** the limits of the troposphere boundary and **N** the refractivity. The basic requirement of such a model is the ability to estimate the integral of the refractivity along the ray path. This expression is commonly expressed as the sum of two effects; a dry (**d**) and a wet (**w**) component, which result from the dry atmosphere and the water vapour respectively.

One of the several expressions that exist for refractivity (Shardlow, 1994; Dodson *et al*, 1993) is

$$N = 77.6 \frac{P}{T} + 3.73 \times 10^5 \frac{e}{T^2} \tag{2.19}$$

where **P** is the total atmosphere pressure (mbars)
T is the absolute temperature (Kelvin) and
e is the partial water vapour pressure (mbars).

The first term of the right hand side of this expression refers to the dry component and the second one to the wet component.

The troposphere like the ionosphere, delays the signal's time of flight and hence the pseudorange increases but unlike the ionosphere, the phase measurement decreases. About 90% of the tropospheric delay arises from the dry component, which can be accurately modelled using surface measurements alone. The contribution of the wet term, although very small compared with the dry one, is more difficult to model. This is because the measurements of temperature and partial water vapour pressure at the antenna site are generally not representative of the conditions along the line of sight.

The distribution of the partial water vapour pressure in the atmosphere is extremely variable due to localised effects. This makes it difficult to obtain accurate values for the partial water vapour pressure from surface meteorological data, especially for the upper regions of the troposphere. Various methods are available for measurement of the amount of water vapour in the atmosphere, but the expense and inconvenience of these methods implies that they are rarely used for GPS observations. An example of such an instrument is the microwave radiometer (Dodson *et al*, 1993).

The usual approach for estimating the tropospheric effects is therefore to apply one of the several existing models of the troposphere, either using surface meteorological observations or a surface meteorological model. The better results are often found by using a surface meteorological model. Nevertheless, the surface meteorological observations are collected in order to identify any adverse atmospheric conditions. The empirical model, referred to as Magnet model, implemented by Texas Instruments, does not require any meteorological data (Curley, 1988). It uses a standard atmosphere and estimates the atmosphere pressure based on the Julian Day, station's latitude and height. Tests carried out in Nottingham indicated that this model will very often yield solutions that are better than those obtained with surface meteorological observations (Ffoulkes-Jones, 1990).

Another technique used in conjunction with the models outlined above is the introduction of a scale factor (α) as an extra unknown in the processing. It determines an offset to the model estimate of the delay using the strength of the GPS data. The estimated scale factor and the height component are strongly

correlated. The inclusion of such parameter can also compensate for other systematic effects in the GPS data, mainly those affecting the height component.

In the processing of long duration of GPS data (e.g. 24 hours), the scale factor may be defined by a polynomial to represent the time varying nature of the troposphere. In this case, the model is correlated through time via connection of the start epoch (To) to the current epoch (T) (Shardlow, 1994).

(c) Multipath

Multipath is the phenomenon whereby a transmitted signal arrives at the antenna via two or more different paths. It is mainly due to reflecting surfaces in the vicinity of the receiver, although reflection at the transmitting satellite is also possible. As a result, the received signals have relative phase offsets and the phase differences are proportional to the differences of the path lengths.

Multipath is dependent on the reflectivity of the antenna environment, antenna characteristics, antenna-to-satellite geometry and the multipath rejection techniques utilised. The arbitrary geometric situations make it difficult to model the multipath effects, although the level of multipath can be assessed by using appropriate combination of observables. As they are normally considered a random error, a more relaxed variance can be associated to the observables when high level of multipath is detected. There are, however, some cases in which the multipath effects have a systematic behaviour. Therefore, the most effective recommendation is to avoid using sites with reflective surface nearby.

(d) Cycle Slips

The phase measurements are normally continuous with respect to the time period of an observing session. A discontinuity in the phase measurement is referred to as cycle slip. It may occur due to signal blockage, antenna acceleration, excessive atmospheric disruption, interference from other radio sources and receiver and software problems. When a cycle slip occurs, the fractional part of the phase measurement is most likely to be still correct; only the integral count takes a big jump. It is necessary and may be possible to correct the wrong integral cycle by using some sort of cycle slip fixing techniques. Otherwise, a new ambiguity term must be included as unknown in the model. Numerous methods exist for detecting and repairing cycle slips (Ffoulkes-Jones, 1990).

2.7.3 Receiver and Antenna Related Errors

Receiver and Antenna dependent errors are those related to the receiver hardware (receiver clock offset, interchannel biases and noise) and antenna design (antenna phase centre and low elevation antenna response).

(a) Receiver Clock Offset

GPS receivers are normally equipped with high quality quartz crystal clocks, whose oscillators have very high internal quality but exhibit long term instabilities. Some receivers also accept an external timing of better quality, providing possibility of modelling the satellite clocks. This is important in the case of monitoring the level of SA. The deviation of the receiver clock from GPS time is the receiver clock offset. Each receiver has its own time frame. The options for modelling the clock biases depend on the quality of the receiver clocks and required precision of the survey. High quality clocks can be modelled as a polynomial or as a white noise parameter. Low accuracy surveying does not require a stable clock and normally the clock offset is ignored. In relative positioning, the receiver clock offset is differenced away but the satellite positions are dependent on its value. One can simply solve for an extra clock offset parameter along with coordinates using pseudorange solution and use this value to compute the satellite positions.

(b) Interchannel Biases

Interchannel biases may occur if the receiver has more than one tracking channel (multiple channel). Current geodetic receivers are multiple channel receivers, ie, they record measurements from each satellite at each frequency on dedicated channels. In order to correct for eventual biases between the different channels, the receiver performs an interchannel calibration at the beginning of each survey. This involves each channel simultaneously tracking a satellite and an offset is determined with respect to a reference channel. All subsequent measurements are adjusted for this offset.

(c) Antenna Phase Centre

The electrical phase centre of the antenna is the point to which the radio signal measurement is referred and generally is not identical to the physical centre of the antenna. The offset varies with the intensity and direction of the incident signals and is different for L1 and L2. For precise applications the offset of all antennas involved in one project have to be very well known in order to correct

the observations. Chamber tests performed by Schupler and Clark, (1991) provide corrections for a variety of antennas over a complete range of elevation angles.

2.7.4 Station Related Errors

Besides the station coordinates errors, the other station related errors arise from the geophysical phenomena causing the station coordinates to physically change during an observation period. This includes the effects of earth body tides, ocean tide loading and atmosphere pressure loading.

(a) Station Coordinates

GPS relative positioning lead to very precise three-dimensional coordinate vectors which do not contain any information about the geodetic datum. In order to introduce such information, at least one point in the network (baseline) should be held fixed to a known position. Since the satellite coordinates, either derived from broadcast or precise ephemerides, are held fixed in the adjustment, the coordinates of the fixed stations must also be related to the reference frame in which the satellite positions are computed. Otherwise, errors will be introduced in the geographical coordinates differences. It has been shown that an error of 5 m in the coordinates of Greenwich, produces errors of 1.0, 0.9 and 0.8 ppm in the difference of geographical coordinates ($\Delta\varphi, \Delta\lambda$ and ΔH) between Greenwich and Paris (Breach, 1990). This shows the importance of having stations compatible with WGS84 in order to support geodetic activities carried out by GPS.

(b) Earth Body Tides

The deformation of the earth due to the tidal forces (sun and moon) is referred to as earth body tides (EBT). At low latitudes, the surface moves through a range of over 40 cm over a period of 6 hours (Baker, 1984). It varies with time as a function of the position of sun and moon. The main periods of these variations are semidiurnal (approximately 12 hours) and diurnal (approximately 24 hours). In addition to being a function of time, it is also a function of position, ie, the position of the observer affects the magnitude of the deformation. The effect is similar for adjacent stations. For larger station separations, the differential effects have to be modelled in the parameter estimation process in order to correct the measurement. Details of the standard algorithm to be used are given in IERS Standards (McCarthy, 1992). The

periodicity of the EBT makes it possible to reduce some of the effects by collecting data continuously during such a period.

(c) Polar Motion

The variation of station coordinates caused by the polar motion may also be taken into account. They have a non-zero average over any given time span with maximum displacement of about 25 and 7 mm in the radial and horizontal components respectively (McCarthy, 1992). However, they can be greatly reduced in a relative positioning.

(d) Ocean Tide Loading

In addition to the deformation due to the earth body tides, the weight of the ocean tides produces a periodic loading on the earth's surface resulting in a further displacement (Baker, 1984). The magnitude of the effect depends on the alignment of the earth, sun and moon and position of the observer. The Ocean Tide Loading (OTL) deformation has range of more than 10 centimetres for the vertical displacement in some part of the world (Baker *et al*, 1995). On the continents, it typically decreases to 1 cm at distances of about 500 km away from the ocean, but in some areas it is still over 1 cm at distances of 1000 km from the ocean. This implies that for high precision GPS surveying, an ocean tide loading model should be incorporated in the software. The IERS Standards (McCarthy, 1992) gives some details of the computation of displacement due to ocean loading.

(e) Atmospheric Loading

The earth and the atmosphere interact through pressure loading at the earth surface and gravitational attraction of the atmospheric mass. Variations in the horizontal distribution of atmospheric mass, which can be inferred from surface atmospheric pressure measurements, induce deformations within the earth, mainly in the vertical direction. It has been reported that global seasonal fluctuations in barometric pressure contribute less than a centimetre to surface displacements. The largest displacements are associated with synoptic scale storms. In such cases, it is probable that the vertical displacements could be 10 mm or larger along a storm track (Van Dam and Wahr, 1987). It has been recommended (Blewitt *et al*, 1994) to extend site occupations of large regional campaigns for monitoring regional vertical deformation to 2 weeks rather than the usual 3-5 days, and calibrate the results using atmospheric loading models.

Chapter 3

BASIC MATHEMATICAL MODELS FOR GPS DATA PROCESSING

3.1 Introduction

A geodetic project involves a set of procedures related to the design, collection, initial analysis of data, processing of the data and, finally, the evaluation and presentation of the results. In the design of the project, as well as in the processing of the observed data, the mathematical model (functional and stochastic) is the central element, which relates the collected data to certain unknown parameters. It is usual to collect more data than is needed for a unique determination of the unknown parameters, which provides a means of assessing the accuracy and reliability of the results.

The estimation of the unknown parameters with redundant data is usually based on the least squares approach, which also provides the elements for the analysis of the results. A summary of basic least squares estimation and analysis theory, followed by a description of some basic mathematical models used in GPS data processing are given within this Chapter. The models are restricted to the case in which the satellite positions are known from broadcast or precise ephemerides and held fixed in the adjustment. The mathematical model relating to the case where the satellite positions are also estimated in the least squares estimation procedure is covered in Chapter 4.

3.2 Least Squares Adjustment

The least squares adjustment can be carried out using the model of observation equations, the model of condition equations and the mixed model representation. During this research, only the model of observation equations has been used. Therefore, no further reference is made regarding the other two models. For a full treatment of this subject, the reader is referred to Teunissen (1990), Vaníček and Krakiwsky (1986) and Cross (1983).

3.2.1 The Observation Equation Model

An inconsistent linear (or linearised) model, ie a system for which $\mathbf{L} \notin \mathbf{R(A)}$ holds true, can be made consistent by introducing an $(m \times 1)$ residual vector $\mathbf{V}$ as

$$\mathrm{L} = \mathrm{AX} + \mathrm{V} \quad \text{with} \quad m > n = \mathrm{rank(A)} \tag{3.1}$$

where m is the number of equations,
n is the number of unknowns,
$\mathbf{L}$ is a $(m \times 1)$ vector of observations,
$\mathbf{X}$ is an $(n \times 1)$ unknown vector of parameters,
$\mathbf{A}$ is a $(m \times n)$ matrix with known scalars, referred to as design matrix,
$\notin$ stands for 'does not belong to' and
$\mathbf{R(A)}$ stands for range space of $\mathbf{A}$, which is equal to n.

In order to obtain quality measures for the results of least squares estimation, a qualitative description of the input (measurement vector) should be introduced. The description is of a probabilistic nature because the measurements, when repeated under similar circumstances, can be described to a sufficient degree by stochastic random variable. Therefore, it will be assumed that the observation vector $\mathbf{L}$, which contains the numerical values of the measurements, constitutes a sample of the random vector of observables and can be written as the sum of a deterministic functional part $\mathbf{AX}$ and a random residual part $\mathbf{V}$, as given by expression (3.1)

Assuming that the probabilistic nature of the variability in the measurements is defined by the vector $\mathbf{V}$, it seems acceptable to assume that the expected value of this variability is zero on the average, ie $\mathrm{E\{V\}} = 0$ ($\mathrm{E\{.\}}$ stands for mathematical expectation operator). The measurement variability is modelled through the covariance matrix, which is assumed to be known and it is denoted by $\Sigma_{\mathbf{L}}$

$$\mathrm{D\{L\}} = \Sigma_{\mathrm{L}} \tag{3.2}$$

where $\mathbf{D\{.\}}$ stands for the dispersion operator. Equation (3.1) can be rewritten as:

$$E\{L\} = AX \quad D\{L\} = \Sigma_L \tag{3.3}$$

which is the mathematical model for the vector of observables **L**.

3.2.2 Least Squares Estimates

The general least squares principle states that

$$\Phi = (L - AX)^T W (L - AX) \rightarrow \text{minimum} \tag{3.4}$$

where **W** is a symmetric positive definite (*mxm*) weight matrix, which accounts for the difference in the observational accuracies. Once the minimization[5.1] problem is solved, one obtains the estimate parameter $\hat{X}$ (Teunissen, 1990):

$$\hat{X} = (A^T W A)^{-1} (A^T W L) \tag{3.5}$$

where the superscript T stands for the transpose of a matrix.

Using the estimate parameter $\hat{X}$, one can respectively determine the adjusted observations and residuals estimates from the expressions

$$\hat{L} = A\hat{X} \text{ and } \hat{V} = \hat{L} - A\hat{X} \tag{3.6}$$

The quality of the above estimates can be obtained from the first two moments of $\hat{L}$, ie the mean and standard deviation. With the assumption that the mathematical model given by the expression (3.3) holds, the least squares estimates are unbiased estimators[5.2] and this property is independent of the choice of the weight matrix **W**. If **W** is taken to be equal to the inverse of the covariance matrix of **L** and scaled by the *a priori* variance factor σ_0^2, ie

$$W = \sigma_0^2 \Sigma_L^{-1} \tag{3.7}$$

it can be shown that the Best Linear Unbiased Estimation (BLUE) of **X** is identical to the weighted least squares estimator (Teunissen, 1990). Hereafter,

---

5.1 $\frac{\partial \Phi}{\partial X} = 0$ and $\frac{\partial^2 \Phi}{\partial X^2}) 0$

5.2 An unbiased estimator $\hat{\Phi}$ is such that $E\{\hat{\Phi}\} = \Phi$

unless stated otherwise, the weight matrix **W** is assumed to be chosen as in equation (3.7). Application of the propagation law of covariance to equations (3.5) and (3.6) results in the expressions,

$$\begin{aligned} \Sigma_{\hat{x}} &= \hat{\sigma}_0^2 (A^T W A)^{-1} \\ \Sigma_{\hat{L}} &= A \Sigma_{\hat{x}} A^T \\ \Sigma_{\hat{v}} &= \Sigma_L - \Sigma_{\hat{L}} \end{aligned} \tag{3.8}$$

where $\Sigma_{\hat{x}}$ is the covariance matrix of the adjusted parameters,

$\Sigma_{\hat{L}}$ is the covariance matrix of the adjusted observations and

$\Sigma_{\hat{v}}$ is the covariance matrix of the estimated residuals.

The above results enables the description of the quality of the results of least squares estimations in terms of the mean and the covariance matrix. The term $\hat{\sigma}_0^2$ is referred to as unit variance (or estimated variance factor), and will be discussed further in the section (3.2.4).

3.2.3 Non Linear Models and Iterations

The results presented so far have involved linear estimation, however, the usual practice in resolving geodetic problems is that most of the applications involve non-linear estimation. The least squares criterion can, in principle, be applied directly to non-linear equations but the resulting normal equations would also be non-linear, which may pose considerable difficulties in seeking a unique solution. Furthermore, in the case of large geodetic projects, computational efforts to determine a solution may be impractical. These are the main reasons why in practice, the observation equations are first linearised before applying the least squares method. Starting from an approximate vector X_0 for the unknown parameters, close enough to **X**, a linearisation is applied by using a Taylor's series and the least squares solution is obtained from the linearised model. The linearised model is given as:

$$E\{\Delta L\} = A_L \Delta X \tag{3.9}$$

with

$$\begin{aligned} \Delta L &= L - L_0 \\ L_0 &= F(X_0) \\ A_L &= \frac{\partial F}{\partial X_0} \end{aligned} \tag{3.10}$$

where $\Delta \mathbf{L}$ is the vector of the observed measurements minus the measurement calculated using the provisional values of the parameters ($\mathbf{X_0}$),

$\mathbf{A_L}$ is the matrix of partial derivatives of the non-linear function F (hereafter referred as before, ie $\mathbf{A}$) and

$\Delta \mathbf{X}$ is the corrections to the provisional values $\mathbf{X_0}$.

Estimation from the linearised model provides an improved solution of the initial vector X_0. The process is repeated using the new improved solution, instead of X_0. This iterative process stops once the difference between successive solutions is not significant.

3.2.4 Assessment of the Observations and Results

The quality of the results presented in the previous section is only significant if the observation equation model represented by equation (3.3) holds, ie model errors are not present. If a meaningful description of the quality of the results is to be obtained, evidence of the presence or absence of errors in the model should be obtained. This is performed by means of statistical testing, where the original model is put forward as the null hypothesis, H_0, against an extended functional model, the alternative hypothesis H_a. At this point, an additional assumption must be taken into account. This is that the observables $\mathbf{L}$ have normal distribution with mathematical expectation $\mathbf{AX}$ and dispersion $\mathbf{\Sigma_L}$, ie,

$$H_0 : L \approx N(AX, \Sigma_L) \tag{3.11}$$

In order to obtain evidence that a model error is present, the size of the error ∇ is introduced as an extra unknown parameter to the null hypothesis. The extended functional model forms the alternative hypothesis and reads:

$$H_a : L \approx N(AX + C\nabla, \Sigma_L) \tag{3.12}$$

such that **C** is an (mxq) full rank matrix and ∇ is a ($qx1$) vector of unknowns. Notice that q is the number of errors to be tested in the model, whose range is given by $1 \leq q \leq (m\text{-}n)$. By estimating the value of ∇ and testing its critical significance, decision can be taken about whether a model error is likely to be present in the model.

The case where $q = 1$ has an important application in geodetic practice for blunder detection in the observations. It is applied following the convention that only one blunder is assumed to be present at a time. Then, the **C** matrix for the case where the observation **i** is being tested, is given by:

$$C_i = (0,\ldots,\underset{(i)}{1},0,\ldots,0)^T \tag{3.13}$$

and H_0 is rejected if $\hat{w}_i < -\sqrt{\chi^2_{1,\alpha}}$ or $\hat{w}_i > \sqrt{\chi^2_{1,\alpha}}$. The value of the test statistic $\hat{w}_i$ can be computed from the expression (Teunissen, 1989),

$$\hat{w}_i = \frac{C_i^T W \hat{V}}{\sqrt{C_i^T W \Sigma_{\hat{V}} W C_i}} \tag{3.14}$$

where $\chi^2_{1,\alpha}$ is obtained from the Chi-squared distribution with **1** degrees of freedom and level of significance α.

By applying the above tests on all the values in i ($1 \leq i \leq m$) the whole observation vector can be screened for observational blunders. This procedure is called 'data snooping'. For application in which the covariance matrix of the observables is a diagonal matrix, the equation (3.14) simplifies to:

$$\hat{w}_i = \hat{v}_i / \sigma_{\hat{v}_i} \tag{3.15}$$

with $\sigma_{\hat{v}_i}$ and $\hat{v}_i$ the estimated standard deviation of the residual and the residual of observation i respectively.

This test can be quite easily applied to GPS data, however, because of the considerable amount of data, some simplifications are necessary in order to make the tests more suitable. This is discussed further in (§5.2.1). In the

analysis of the repeatability of GPS results, such a test would provide an indication of a problematic solution.

The case where $q = m\text{-}n$ corresponds to the $\hat{\sigma}_0^2$ test statistic or *global test statistic* given by (Teunissen, 1989):

$$\hat{\sigma}_0^2 = \hat{V}^T W \hat{V}/q \tag{3.16}$$

with q degrees of freedom. The test is rejected if $\hat{\sigma}_0^2 > \chi^2_{q,\alpha}/q$. The practical importance of the above test is that the **C** matrix need not be specified in contrast with all other cases for which $q < m\text{-}n$. Since all the classes of alternative hypotheses for a practical problem can not be completely specified, the *global test* should be seen as an important safeguard. The test gives an indication of the validity of H_0 without the need to specify the alternative hypothesis.

Once the observations have been screened and the mathematical model examined, an assessment of the least squares estimator $\hat{X}$ can be performed if two or more estimations of the same unknown parameters have been calculated. Assuming k independent estimates for $\hat{X}$ (i=1,2,...,k) with n parameters each, one can rewrite the model given in expression (3.3) as,

$$E\left\{\begin{bmatrix}\hat{X}_1\\ \hat{X}_2\\ \dots\\ \hat{X}_k\end{bmatrix}\right\} = \begin{bmatrix}I_n\\ I_n\\ I_n\\ I_n\end{bmatrix}\left[\overline{X}\right] \; ; \; \Sigma_Y = \begin{bmatrix}\Sigma_{\hat{X}_1} & 0 & 0 & \dots & 0\\ 0 & \Sigma_{\hat{X}_2} & 0 & \dots & 0\\ \dots & & & & \\ 0 & 0 & \dots & 0 & \Sigma_{\hat{X}_k}\end{bmatrix} \tag{3.17}$$

where I_n is an (n x n) identity matrix and

$\Sigma_{\hat{X}_i}$ the covariance matrix of each independent solution and

$\overline{X}$ is the combined (final) solution.

In a similar manner to the procedure described in the previous section, one can obtain the least squares estimates of the final solution, as well as the associated covariance matrix. The *global test statistic* of this model will indicate the consistency of the independent solutions. If inconsistency is detected, it can be

identified by applying the tests given either by equation (3.14) or (3.15). By using some linear or linearised independent functions of the parameters, one can obtain the so-called repeatability (see Chapter 5) of the solution.

Additional analysis of the results can be carried out if some of the estimated parameters are known at a level of accuracy significantly better than that estimated in the least squares adjustment. In such cases, the recovery[5.3] of the parameter will give an indication of its accuracy.

3.3 Mathematical Model of the GPS Observables

The fundamental GPS observables, pseudorange and carrier phase, were described in (§2.6). Each observation generates one equation in the observation equation model given by expression (3.3). This implies that the errors affecting each observation are expected to have a zero mathematical expectation. Such results are mainly obtained by differencing the observables (single, double and triple differences) and using some special combination of observables. However, each differencing increases the noise of the resulting observable. For the purpose of this work, only combination of carrier phases is addressed, although it can also be formed between pseudoranges and a mixture of both (pseudorange and carrier phase). For details the reader is referred to Ffoulkes-Jones (1990).

The pseudorange and carrier phase observation equations including the main error sources (tropospheric (T_r^s) and ionospheric (I_r^s) refraction delays) are given by expressions (3.18) to (3.21). Notice that the GPS time frame (T) related to each constituent of the equation has been ignored. The observation equations for L1 and L2 pseudoranges are given by:

$$PR_{1r}^{s} = \rho_r^s + c(\delta\tau_r - \delta t^s) + T_r^s + I_r^s + v_{pr_1} \tag{3.18}$$

$$PR_{2r}^{s} = \rho_r^s + c(\delta\tau_r - \delta t^s) + T_r^s + \bar{I}_r^s + v_{pr_2} \tag{3.19}$$

where c is the speed of light in a vacuum,

ρ_r^s is the geometrical distance between receiver and satellite at the epoch of transmission and reception of the signal,

[5.3] Recovery has been used as the difference between the assumed 'true' and the estimated value of the parameter.

δt^s is the satellite clock offset from GPS time at the time of transmission of the signal, computed at receiver time frame,

$\delta\tau_r$ is the receiver clock offset from GPS time at the time of reception of the signal, computed at receiver time frame,

I_r^s is the ionospheric refraction delay (metres) on L1,

$\bar{I}_r^s$ is the ionospheric refraction delay (metres) on L2,

T_r^s is the tropospheric refraction delay (metres),

v_{PR_1} is the noise and other unmodelled effects affecting the pseudorange measurement on L1 and

v_{PR_2} as the previous one, but on L2.

The observation equations for L1 and L2 carrier phase are given by,

$$\Phi_{rL1}^s = \frac{f_{L1}}{c}\rho_r^s + f_{L1}[\delta\tau_r - \delta t^s] + \overline{N}_{L1} + \frac{f_{L1}}{c}T_r^s - \frac{f_{L1}}{c}I_r^s + v_{\Phi_1} \qquad (3.20)$$

$$\Phi_{rL2}^s = \frac{f_{L2}}{c}\rho_r^s + f_{L2}[\delta\tau_r - \delta t^s] + \overline{N}_{L2} + \frac{f_{L2}}{c}T_r^s - \frac{f_{L2}}{c}\bar{I}_r^s + v_{\Phi_2} \qquad (3.21)$$

where f_{L1} is the frequency of L1,

f_{L2} is the frequency of L2,

$\overline{N}_{L1}$ is the ambiguity of L1 plus the unknown initial phases of the satellite and receiver oscillator (see expression (2.12))

$\overline{N}_{L2}$ as the previous one, but of L2,

v_{Φ_1} is the noise and other unmodelled effects affecting the carrier phase measurements on L1 and

v_{Φ_2} as the previous term, but on L2.

3.3.1 Linear Combination of the GPS Observables

A linear combination LC_i of the carrier phase Φ_1 and Φ_2 is given by

$$LC_i = m_1\Phi_1 + m_2\Phi_2 \qquad (3.22)$$

Table 3.1 summarises the main properties of a few selected linear combinations, including the original ones (L1 and L2). The change in the

measurement noise relative to that on the L1 carrier phase (σ_{L1}) is represented as $\sigma_{m_1 m_2}$, which is obtained as (Ffoulkes-Jones, 1990):

$$\sigma_{m_1 m_2} = \lambda_{m_1 m_2} \sqrt{m_1^2 + m_2^2} \Big/ \sigma_{L1} \qquad (3.23)$$

Table 3.1 Linear Combination of the Carrier Phase Observables

Observable	m_1	m_2	$\cong\lambda_{m_1 m_2}$ (cm)	$\sigma_{m_1 m_2}$
L0	$f_{L1}^2/(f_{L1}^2 - f_{L2}^2)$	$-f_{L1}f_{L2}/(f_{L1}^2-f_{L2}^2)$	19.0	3.23
L1	1	0	19.0	2.0
L2	0	1	24.0	2.5
L3	1	-1	86.2	6.42
L4	1	1	10.5	0.80

A very important linear combination is the so-called ionospherically free observable, identified in Table 3.1 as the L0 observable. It greatly reduces the ionospheric effects and is the observable normally used in high precision positioning with long baselines. The combination of this observable with the so-called widelane (L3) is very useful in the detection of cycle slips (see §5.2.1). Over short baselines, where the ionosphere is effectively differenced away, the measurement noise of the L0 observable becomes dominant, offering no real advantage.

The long wavelength of the L3 observable makes it important in the resolution of integer ambiguities, however, the ionospheric delay and measurement noise may cause some problems (Hofmann-Wellenhof *et al*, 1992). The narrow lane (L4) observable when subtracted from the widelane (L3) is referred to as ionospheric signal (Seeber, 1993) and contains the complete ionospheric effect. It allows a detailed analysis of the ionospheric behaviour and is helpful in the ambiguity resolution strategies.

3.3.2 Differencing the Observables

A common strategy used in GPS data processing is the differencing technique. The resulting differenced observables are commonly referred to as single,

double and triple differences. The main advantage is that at each successive difference, an extra unknown (e.g. satellite and receiver clock errors) is eliminated, thus negating the need to rely solely on models. However, the drawback of the differencing approach is that the noise level generally increases and the uncorrelated observables provide a new set of correlated observables.

(a) The Single Difference Observable

Single differences can be formed between two receivers, two satellites, or two epochs. The most common single difference is calculated between two receivers, as illustrated in Figure 3.1. The fundamental assumption is that two receivers (r_1 and r_2) simultaneously track the same satellite (s^1).

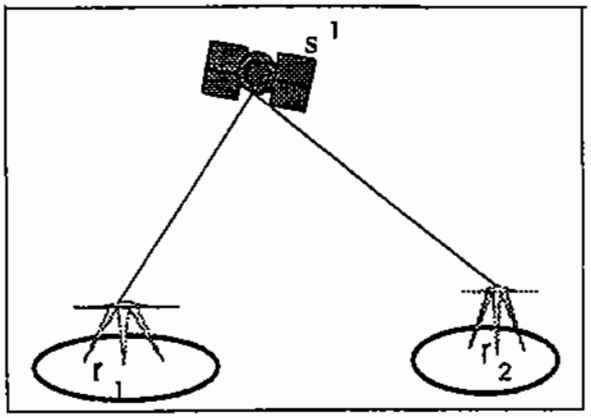

Figure 3.1: The Single Difference Observable

The difference between the simultaneous pseudorange measurements at both stations is the single difference pseudorange. The observation equation is given by,

$$\Delta PR^1_{1,2} = \Delta\rho^1_{1,2} + c(\delta\tau_1 - \delta\tau_2) + v_{PR_{SD}} \tag{3.24}$$

with

$$\Delta\rho^1_{1,2} = \rho^1_1 - \rho^1_2 \tag{3.25}$$

The single difference eliminates the satellite clock error δt^s. In addition, errors due to the ephemerides and atmosphere are minimised in this observable, especially for short baselines, since the tropospheric and ionospheric effects are

similar at each receiver. The remaining unmodelled errors are assumed to be of random nature and included as noise ($v_{PR_{SD}}$) in the observable.

The single difference carrier phase observation equation can be expressed as,

$$\Delta\Phi^{1}_{1,2} = \frac{f}{c}\Delta\rho^{1}_{1,2} + f[\delta\tau_1 - \delta\tau_2] + \overline{N}^{1}_{1,2} + v_{SD_\Phi} \tag{3.26}$$

where f is the correspondent frequency of the observable and $\overline{N}^{1}_{1,2}$ is given by

$$\overline{N}^{1}_{1,2} = N^{1}_{1} + \Phi_1(\tau_0) - N^{1}_{2} - \Phi_2(\tau_0) \tag{3.27}$$

This eliminates not only the satellite clock error, δt^s, but also the initial phase of the satellite oscillator, $\Phi^1(\tau_0)$ (see equation 2.12).

(b) The Double Difference Observable

This observable is derived by differencing two single differences. Figure 3.2 illustrates the double difference observable formed from the single differences between two receivers (r_1 and r_2) and the two satellites s_1 and s_2.

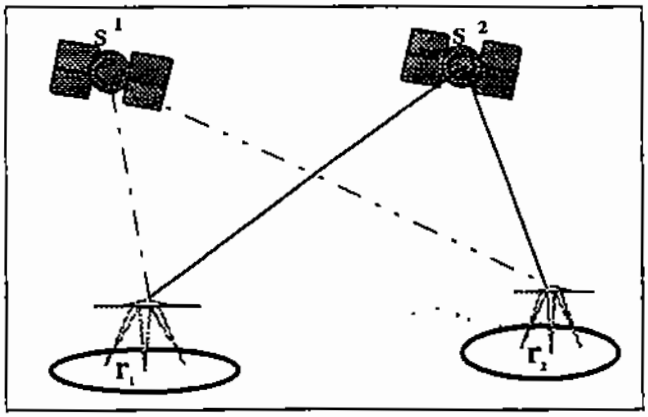

Figure 3.2: The Double Difference Observable

The double difference pseudorange observation equation is expressed as:

$$\Delta PR^{1,2}_{1,2} = \Delta\rho^{1,2}_{1,2} + v_{PR_{DD}} \tag{3.28}$$

where

$$\Delta\rho_{1,2}^{1,2} = \Delta\rho_{1,2}^{1} - \Delta\rho_{1,2}^{2} \tag{3.29}$$

The corresponding carrier phase observation equation is given as:

$$\Delta\Phi_{1,2}^{1,2} = \frac{f}{c}(\Delta\rho_{1,2}^{1,2}) + N_{1,2}^{1,2} + \nu_{\Phi_{DD}} \tag{3.30}$$

where,

$$N_{1,2}^{1,2} = \overline{N}_{1,2}^{1} - \overline{N}_{1,2}^{2} = N_1^1 - N_2^1 - N_1^2 + N_2^2 \tag{3.31}$$

The $N_{1,2}^{1,2}$ ambiguity is called the double difference ambiguity, which for some linear combinations is supposed to be an integer, since the initial phase of the receiver oscillators (see equation 3.27) have been vanished. The double difference equations (3.28) and (3.30) when compared to the single difference equations (3.24) and (3.26) show that the clock offset of both receivers (δt_1 and δt_2) have now been removed.

The double difference is normally the preferred observable in GPS data processing. It seems to provide the best compromise between the noise level of the observable and elimination of biases and errors.

(c) The Triple Difference Observable

The triple difference observable is given by the difference between a double difference at one epoch (τ_1) and the same double difference at a second epoch (τ_2). In the case of the pseudorange observable, the triple difference offers no significant advantage over the other combinations. For the carrier phase observable, the double difference ambiguity is now eliminated and the only unknowns left are the coordinates of the receivers. The triple difference carrier phase observation equation is given by,

$$\Delta\Phi_{1,2}^{1,2}(\tau_1) - \Delta\Phi_{1,2}^{1,2}(\tau_2) = \frac{f}{c}[\Delta\rho_{1,2}^{1,2}(\tau_1) - \Delta\rho_{1,2}^{1,2}(\tau_2)] \tag{3.32}$$

The triple difference observable is very sensitive to cycle slips and has accordingly been used as a method of detection prior to the final solution. The triple difference is not used for the final solution since the benefits of removing

the double difference ambiguity are outweighed by the increase in the noise of the observable.

3.3.3 Covariance of the Differenced Observables

The undifferenced observables are assumed to be uncorrelated in space and time. Since the differenced observables are combinations of various undifferenced observables, they become correlated, which should be accounted for in the adjustment.

The covariance matrix of a ($2nx1$) vector Φ_i containing the phase observables collected at two stations during a epoch τ_i and arranged as

$$\Phi_i^T = [\Phi_1^1, \Phi_1^2, \ldots, \Phi_1^n, \Phi_2^1, \Phi_2^2, \ldots, \Phi_2^n] \tag{3.33}$$

is given as

$$\Sigma_{\Phi_i} = \sigma^2 I \tag{3.34}$$

where I is an identity matrix of order equal the number of observations ($2n$) and σ^2 the variance of the pure phase observable. The single difference observables can be written as

$$\Phi_{SD_i} = [I, -I]\Phi_i \tag{3.35}$$

where Φ_{SD_i} is the vector containing the single difference observables and **I** is now an (nxn) identity matrix, where n is the number of single differences. The propagation covariance law applied to equation (3.35) yields

$$\Sigma_{SD_i} = 2\sigma^2 I \tag{3.36}$$

which is the covariance matrix of the carrier phase single differences.

The double difference observables are derived from the single difference observables, and can be written as

$$\Phi_{DD_i} = C\Phi_{SD_i} \tag{3.37}$$

where Φ_{DD_i} is the $((n-1)\text{x}1)$ vector containing the double difference observables. The $((n-1)\text{x}n)$ **C** matrix containing the double difference information can be chosen in different ways. In practice, however, only two are extensively used which are derived using the *sequential differencing method* and the *reference satellite differencing method* (Talbot, 1991). The latter is also referred to as base satellite method. For the former case, the C matrix has the following pattern,

$$C=\begin{bmatrix} 1 & -1 & 0 & \dots & 0 & 0 \\ 0 & 1 & -1 & 0 & \dots & 0 \\ \dots & & & & & \\ 0 & \dots & & 0 & 1 & -1 \end{bmatrix}. \tag{3.38}$$

In the *reference satellite differencing method*, the pattern of the **C** matrix depends on the reference (base) satellite. If satellite 1 is selected as base, the **C** matrix is given by

$$C=\begin{bmatrix} 1 & -1 & 0 & 0 & \dots & 0 \\ 1 & 0 & -1 & 0 & \dots & 0 \\ \dots & & & & & \\ 1 & 0 & 0 & & \dots & -1 \end{bmatrix} \tag{3.39}$$

Applying the propagation covariance law to equation (3.37) with the matrix **C** given by equation (3.38) yields

$$\Sigma_{DD_i}=2\sigma^2\begin{bmatrix} 2 & -1 & 0 & 0 & \dots & 0 & 0 \\ -1 & 2 & -1 & 0 & \dots & 0 & 0 \\ \dots & & & & & & \\ 0 & 0 & \dots & 0 & -1 & 2 & -1 \\ 0 & 0 & \dots & 0 & 0 & -1 & 2 \end{bmatrix} \tag{3.40}$$

If the *reference satellite differencing method* has been used (equation 3.39), the covariance matrix is given by

$$\Sigma_{DD_i} = 2\sigma^2 \begin{bmatrix} 2 & 1 & \dots & 1 & 1 \\ 1 & 2 & 1 & \dots & 1 \\ \dots & & & & \\ 1 & 1 & \dots & 1 & 2 \end{bmatrix} \tag{3.41}$$

and is independent of the base satellite selected.

At this point it should be pointed out that choice of method to form the double differences does not affect the results of the processing. However, in the event of an outlier occuring in the base satellite, all the double differences will be affected in the *reference satellite method*, whereas in the *sequential method*, only a maximum of two observables are affected.

The double differences are not correlated between epochs. Hence, the covariance matrix for let say, **k** epochs, is composed of **k** diagonal blocks similar to either equation (3.40) or (3.41).

The covariance matrices presented so far involve only one baseline, ie the observables of two receivers. If, however, a network of m receivers simultaneously observe to n satellites it is possible to form double differences between each baseline. The total number of possible baselines is $(m-1)*m/2$, but only $(m-1)$ baselines are independent. With (n) satellites being tracked at each station, a total of $(n-1)*(m-1)$ double differences is formed. To account for the correlation between the baselines, an $((m-1)xm)$ matrix Λ is defined. It contains elements only 0's, with two non-zero elements (+1, -1) per row, which identify the receivers forming each baseline. For a network defined by the baselines *1-2*; *2-3*, *3-4*, ..., *(m-1)-m*, the Λ matrix is given by,

$$\Lambda = \begin{bmatrix} 1 & -1 & 0 & 0 & \dots & 0 \\ 0 & 1 & -1 & 0 & \dots & 0 \\ \dots & & & & & \\ 0 & 0 & \dots & 0 & 1 & -1 \end{bmatrix}. \tag{3.42}$$

The double difference covariance matrix for a network at an epoch i, is given by (Ffoulkes-Jones, 1990) as:

$$\Sigma_{DD_i} = \sigma^2[\Lambda\Lambda^T] \otimes [CC^T] \tag{3.43}$$

where the **C** matrix is as defined in equation (3.38) or (3.39) and σ^2 is the variance of the pure phase observable. The symbol $\otimes$ stands for Kronecker product.

The covariance matrix of the triple difference observables can easily be obtained from the double difference observables. By forming the triple differences between successive epochs in a similar fashion to the sequential double difference technique, ie (τ_1 - τ_2 , τ_2 - τ_3, ...), the triple difference covariance matrix is computed as:

$$\Sigma_{TD} = \begin{bmatrix} 2\Sigma_{DD} & -\Sigma_{DD} & 0 & 0 & & \dots & 0 \\ -\Sigma_{DD} & 2\Sigma_{DD} & -\Sigma_{DD} & 0 & & \dots & 0 \\ \dots & & & & & & \\ 0 & 0 & \dots & 0 & -\Sigma_{DD} & 2\Sigma_{DD} & -\Sigma_{DD} \\ 0 & 0 & \dots & & 0 & -\Sigma_{DD} & 2\Sigma_{DD} \end{bmatrix} \tag{3.44}$$

3.3.4 Linearisation of the GPS Observables

The GPS observables discussed so far are non-linear with respect to the satellite's and receiver's coordinates, which form the geometric distance ρ. In this section the linearisation of ρ is discussed, starting from the formula given in equation (2.6):

$$\rho_i^j(T) = \sqrt{(X^j(T) - X_i)^2 + (Y^j(T) - Y_i)^2 + (Z^j(T) - Z_i)^2} \tag{3.45}$$

The coordinates of satellite **j**, $(X^j(T), Y^j(T), Z^j(T))$, are usually fixed to their known values from the broadcast or precise ephemerides. Assuming approximate values X_{i0}, Y_{i0}, Z_{i0} for the receiver **i** coordinates, an approximate distance $\rho_{i0}^j(T)$ can be calculated accordingly:

$$\rho_{i0}^j(T) = \sqrt{(X^j(T) - X_{i0})^2 + (Y^j(T) - Y_{i0})^2 + (Z^j(T) - Z_{i0})^2} \tag{3.46}$$

and the receiver coordinates can be represented by

$$\begin{aligned} X_i &= X_{i0} + \Delta X_i \\ Y_i &= Y_{i0} + \Delta Y_i \\ Z_i &= Z_{i0} + \Delta Z_i \end{aligned} \tag{3.47}$$

where ΔX_i , ΔY_i , ΔZ_i are the corrections to the approximate values and are, therefore, the new unknowns. Introducing equation (3.47) into equation (3.45), and expanding the resulting expression using a first order Taylor series this results in the following equation:

$$\rho_i^j(T) = \rho_{i0}^j(T) + \frac{\partial \rho_{i0}^j(T)}{\partial X_{i0}} \Delta X_i + \frac{\partial \rho_{i0}^j(T)}{\partial Y_{i0}} \Delta Y_i + \frac{\partial \rho_{i0}^j(T)}{\partial Z_{i0}} \Delta Z_i \tag{3.48}$$

with the partial differentials given as:

$$\begin{aligned} \frac{\partial \rho_{i0}^j(T)}{\partial X_{i0}} &= -\frac{X^j(T) - X_{i0}}{\rho_{i0}^j(T)} = a_i^j(T) \\ \frac{\partial \rho_{i0}^j(T)}{\partial Y_{i0}} &= -\frac{Y^j(T) - Y_{i0}}{\rho_{i0}^j(T)} = b_i^j(T) \\ \frac{\partial \rho_{i0}^j(T)}{\partial Z_{i0}} &= -\frac{Z^j(T) - Z_{i0}}{\rho_{i0}^j(T)} = c_i^j(T) \end{aligned} \tag{3.49}$$

Equation (3.48) is now linear with respect to the unknowns ΔX_i ,ΔY_i , ΔZ_i, ie:

$$\rho_i^j(T) = \rho_{i0}^j(T) + a_i^j(T)\Delta X_i + b_i^j(T)\Delta Y_i + c_i^j(T)\Delta Z_i \tag{3.50}$$

3.4 Absolute Point Positioning

Absolute point positioning can be carried out using the pseudorange observable, the carrier phase observable or a combination of both. For the purpose of this research only the first case will be described. The linearised pseudorange observation equation is obtained by substituting expression (3.50) into (3.18) or (3.19), which results in the equation given below:

$$PR_i^j - \rho_{i0}^j - T_i^j - I_i^j + c\delta t^j = a_i^j \Delta X_i + b_i^j \Delta Y_i + c_i^j \Delta Z_i + c\delta t_i + v_{PR} \tag{3.51}$$

where PR_i^j is the pseudorange measurement,

ρ_{i0}^j is the approximate geometrical distance between receiver and satellite,

T_i^j is the delay due to the troposphere,

I_i^j is the delay due to the ionosphere,

c is the speed of light in a vacuum,

δt^j is the satellite clock offset from GPS time,

a_i^j, b_i^j, and c_i^j are the coefficients of the corrections to the approximate coordinates (unknowns),

ΔX_i, ΔY_i, ΔZ_i are the corrections to the approximate coordinates of the receivers,

δt_i is the receiver clock offset from GPS time (also an unknown) and

v_{PR} is the noise of the measurement.

The components of the right hand side of equation (3.51) have already been described in this Chapter. The errors affecting the observables can either be modelled or neglected and the resulting value of the left hand side of equation (3.51) will be referred to as $\Delta l_i^j{}_{PR}$.

The number of unknowns in expression (3.51) is the three corrections to the receiver coordinates and the receiver clock term. For an instantaneous determination of one position it can be seen that a minimum of 4 satellites are required. If measurements from more than four satellites are available there is redundancy and least squares estimation can be carried out to estimate the corrections. If the receiver is static and accumulated point positioning is required some form of time varying clock parameter may be solved for, e.g. epoch by epoch receiver clock offset. In this mode it is no longer necessary to have a minimum four satellites every epoch because, over time, enough observations become available to perform the solution.

Assuming that a receiver (r_1) collected data for k epochs, with n satellites, the linearised model can be represented as:

$$E\left\{\begin{bmatrix}\Delta L_1\\ \Delta L_2\\ \cdots\\ \Delta L_k\end{bmatrix}\right\} = \begin{bmatrix}A_{1_1} & e & 0 & 0 & \cdots & 0\\ A_{1_2} & 0 & e & 0 & \cdots & 0\\ \cdots & & & & & \\ A_{1_k} & 0 & 0 & \cdots & 0 & e\end{bmatrix}\begin{bmatrix}\Delta R\\ c\delta t_1\\ \cdots\\ c\delta t_k\end{bmatrix} \tag{3.52}$$

where ΔL_i is a (n x *1*) vector of observed minus computed pseudoranges,

A_{1_i} is the i[th]-epoch (n x *3*) design matrix, composed by the coefficients of the corrections to the approximate coordinates of the receiver r_1,

e is a (n x *1*) unit vector, i.e. $e^T=[1,1,...,1]$,

ΔR is a (*3* x *1*) vector of corrections to the approximate values of the unknowns, i.e. $\Delta R^T=[\Delta X_i,\Delta Y_i ,\Delta Z_i]$ and

$c\delta t_i$ is the receiver clock offset (metres) for epoch i.

If the coordinates of the station are known, one can compute the correction to the pseudoranges or to the estimated coordinates of the station, that is the idea used in Differential GPS (DGPS).

The covariance matrix at a particular epoch i of equation (3.52) is given by

$$\Sigma_i = \sigma_{PR}^2 (A^T A)^{-1} \tag{3.53}$$

where $A = [A_{1_i} , e]$ is the design matrix of the considered epoch and σ_{PR}^2 the variance of the pseudorange observable.

3.5 Network Adjustment

The adjustment of GPS observables collected from more than one station can be carried out using either the undifferenced or differenced observables. The coordinates of one or more stations are usually held fixed (although not necessary) to their known values and the coordinates of the new stations are estimated relatively to the reference frame of the known stations. The satellite orbits can be computed from either the broadcast or precise ephemerides or even estimated as part of the adjustment. The first case is referred to as ordinary network adjustment and the coordinates of the fixed stations should

be given in the same reference frame of the satellite ephemerides. The last case, referred to as the fiducial network adjustment is discussed in the Chapter 4.

3.5.1 Ordinary GPS Network Adjustment

The network adjustment carried out during this research employed the carrier phase observable, which has precision better than the pseudorange observable. In a network of *m* stations, the *(m-1)* independent baselines are pre-processed in order to correct the observations of cycle slips and remove any detected outlier. At this stage, the single baseline model is used.

(a) The Single Baseline Model

The double difference carrier phase observable (equation 3.30) is now rewritten in the linear form using expression (3.50) and including the tropospheric scale factors (α_1 and α_2) to give:

$$\begin{aligned}\lambda\Delta\Phi_{1,2}^{1,2} - \Delta\rho_{1,2_0}^{1,2} - \Delta T_{1,2}^{1,2} = [&(a_1^{1,2})\Delta X_1 + (b_1^{1,2})\Delta Y_1 + (c_1^{1,2})\Delta Z_1 + \\ &+ (a_2^{2,1})\Delta X_2 + (b_2^{2,1})\Delta Y_2 + (c_2^{2,1})\Delta Z_2 + \lambda N_{1,2}^{1,2} + \\ &+ T_1^{1,2}(\tau - \tau_0)^n\alpha_1 - T_2^{1,2}(\tau - \tau_0)^n\alpha_2] + \nu_{\Phi_{DD}}\end{aligned} \qquad (3.54)$$

where

$$a_i^{1,2} = a_i^1 - a_i^2;\ \ b_i^{1,2} = b_i^1 - b_i^2;\ \ c_i^{1,2} = c_i^1 - c_i^2 \ \text{ with i = 1,2} \qquad (3.55)$$

The wavelength, $\lambda = (c/f)$, depends on the linear combination of the observable being used (see Table 3.1). The second two terms on the left hand side of expression (3.54) are obtained as follows:

$$\begin{aligned}\Delta\rho_{1,2_0}^{1,2} &= [\rho_{1,0}^1 - \rho_{2,0}^1 - \rho_{1,0}^2 + \rho_{2,0}^2] + \lambda N_{1,2_0}^{1,2} \\ \Delta T_{1,2}^{1,2} &= T_1^1 - T_2^1 - T_1^2 + T_2^2\end{aligned} \qquad (3.56)$$

The first expression is the double difference carrier phase (metres) computed from the satellite coordinates and approximate values of the receiver coordinates and double difference ambiguity. The second expression represents

the double difference tropospheric delay which can be computed from one of many available tropospheric models.

In addition to modelling the tropospheric delay, tropospheric scale factors ($\alpha_1$and α_2) are included in equation (3.54) as unknown parameters and can be estimate at each station using a polynomial model of order n (Shardlow, 1994). The model is correlated through time via the connection of the start epoch (τ_0) to the current epoch (τ). The coefficients $T_1^{1,2}$ and $T_2^{1,2}$ are computed from the tropospheric model.

Assuming that k epochs of data were collected at two stations (1 and 2) involving the same n satellites, the linearised model of the double difference carrier phase using first order polynomial model for the tropospheric scale factor can be represented as:

$$E\left\{\begin{bmatrix}\Delta L_1\\ \Delta L_2\\ \cdots\\ \Delta L_k\end{bmatrix}\right\} = \begin{bmatrix}A_{1,2_1} & A_{T_1} & I_{N-1}\\ A_{1,2_2} & A_{T_2} & I_{N-1}\\ \cdots & & \\ A_{1,2_K} & A_{T_K} & I_{N-1}\end{bmatrix}\begin{bmatrix}\Delta R_{1,2}\\ \Delta T\\ \Delta N\end{bmatrix} \qquad (3.57)$$

where ΔL_i is a ($(n\text{-}1)$ x 1) vector of differences between the double difference measurements (metres) and the double differences computed as a function of the approximate parameters,

$A_{1,2_i}$ is an ($(n\text{-}1)$ x 6) double difference design matrix composed by of the coefficients of the corrections to the approximate coordinates of stations 1 and 2,

A_{T_i} is an ($(n\text{-}1)$ x 4) matrix of the coefficients of the tropospheric scale factors,

I_{N-1} is an ($(n\text{-}1)$ x $(n\text{-}1)$) identity matrix of the coefficients of the ambiguities,

$\Delta R_{1,2}$ is a (6 x 1) vector with the corrections to the approximate values of the coordinates at both stations, ie $\Delta R_{1,2}^T = [\Delta X_1, \Delta Y_1, \Delta Z_1, \Delta X_2, \Delta Y_2, \Delta Z_2]$.

ΔT is a vector of the unknown tropospheric scale factors, which for a case of using a first order polynomial at each station is given by $\Delta T^T = [\alpha_1^0, \alpha_1^1, \alpha_2^0, \alpha_2^1]$,

ΔN is a $((n-1) \times 1)$ vector of ambiguities.

The weight matrix **W** (equation 3.7) is given by the inverse of the covariance matrix. Since the double difference observables are not correlated between epochs, the covariance matrix is block diagonal. At each epoch, when the *reference satellite method* is used, each block is given as equation (3.41). Therefore, only the inverse of the covariance matrix at a particular epoch needs be computed. This is given as (Hofmann-Wellenhof *et al*, 1992)

$$W_i = (2)^{-1}\frac{1}{n}\begin{bmatrix} (n-1) & -1 & -1 & \cdots \\ -1 & (n-1) & -1 & \cdots \\ \cdots & & & \\ -1 & \cdots & -1 & (n-1) \end{bmatrix} \tag{3.58}$$

where $(n-1)$ is the number of double differences of the epoch considered. For the case of a baseline, the term $(\Lambda\Lambda^T)$ of equation (3.43) is equal to 2. It can be seen that actually, there is no need to compute the inverse. It can be derived as a function of the number of double difference observables; $(n-1)$ for this particular case. Notice that the variance of the pure phase observable (see equation 3.43) was assumed being equal to the *a priori* variance factor (see equation 3.7).

Fixing the satellite positions provide means of obtaining solution, since the normal matrix has full rank. It is usual, however, that one station is held fixed in the baseline adjustment. This can be achieved by either removing the columns of $\mathbf{A}_{1,2}$ related to the fixed station or introducing an extra (fixing) observation into the model. It is the latter process that is generally used for data management purposes.

(b) The Network Model

In the processing of a single baseline, only two stations are assumed to simultaneously track the same satellites. For a network, the number of stations tracking the same n satellites will be represented by m. Therefore, the $(m-1)$ independent baselines are adjusted simultaneously. The selection of these baselines is usually made as a function of the shortest distances between stations.

The mathematical model is an extension of that presented for a baseline. Considering that the *(m-1)* independent baselines were defined as *(1-2; 2-3; ...; (m-1)-m)* and the tropospheric scale factor modelled as a first order polynomial per station, the model for a specific epoch **i** is given as:

$$E\{\Delta L_i\} = \begin{bmatrix} A_{X_i} & A_{T_i} & I_{(n-1)*(m-1)} \end{bmatrix} \begin{bmatrix} \Delta R \\ \Delta T \\ \Delta N \end{bmatrix} \tag{3.59}$$

where ΔL is a *((n-1)*(m-1)x1)* vector of observed minus computed double difference observations,

A_{X_i} is the design matrix composed by of the coefficients of the corrections to the approximate coordinates of the stations of the network,

A_{T_i} is the matrix of the coefficients of the tropospheric scale factors,

$I_{(n-1)*(m-1)}$ is an identity matrix of order *(n-1)*(m-1)* of the coefficients of the unknown ambiguities.

ΔR is a *(3*mx1)* vector of corrections to the approximate values of the coordinates,

ΔT is a *(2*mx1)* vector of tropospheric scale factors and

ΔN is a *((n-1)*(m-1)x1)* vector of ambiguities.

Finally, the weight matrix is given as: (Ffoukes-Jones, 1990)

$$W = (\Lambda\Lambda^T)^{-1} \otimes (CC^T)^{-1} \tag{3.60}$$

As in equation (3.58), the variance factor σ_0^2 (see equation 3.7) was assumed unknown but equal to the variance of the pure phase observable. Although the **W** matrix used in a network model can have very large dimension, ie *(n-1)*(m-1)*, its inverse is easily computed by applying the Kronecker product property[3.1]. The $(CC^T)^{-1}$ matrix can be computed as a function of the number of double differences (see equation 3.58). Therefore, in order to compute the weight matrix, only the matrix of order equal to the number of independent baselines *(m-1)* has to be inverted, ie $(\Lambda\Lambda^T)^{-1}$.

[3.1] $(A \otimes B)^{-1} = A^{-1} \otimes B^{-1}$

3.5.2 Handling of Missing Observations

In the computation of the weight matrix as given by equation (3.60), it is assumed that all the stations are tracking the same satellites. However, a few observations are occasionally 'missed' at one or more stations and for large network, such assumption may not hold. In this case, the double differences at each baseline can not be computed using the **C** matrix given by equations (3.38) or (3.39) as the matrix is then different for each baseline. Therefore, in principle the weight matrix can not be computed using the properties of the Kronecker product (equation (3.60)).

In order to overcome this problem the vector of double differences actually observed, Φ_{DD_R}, is written as a linear transformation of the complete set of double differences, Φ_{DD}; given by

$$\Phi_{DD_R} = L_R \Phi_{DD} \tag{3.61}$$

The coefficients of the transformation matrix are structured as follows:

$$L_R = \begin{bmatrix} L_{R,1} & 0 & 0 & \dots & 0 \\ 0 & L_{R,2} & 0 & \dots & 0 \\ \dots & & & & \\ 0 & 0 & 0 & 0 & L_{R,m-1} \end{bmatrix} \tag{3.62}$$

Each matrix $\mathbf{L_{R,i}}$, i = 1,2,...,m-1 corresponds to one of the $(m-1)$ independent baselines. The matrix $L_{R,i}$ has the number of rows equal to the actual number of double differences for baseline **i**, and the number of columns is equal to $(n-1)$ (the assumed number of double differences at each baseline). It is easy to see that the matrix $\mathbf{L_{R,i}}$ may only have elements 0 or 1. The covariance matrix of Φ_{DD_R} is then given as:

$$\Sigma_{DD_R} = L_R \Sigma_{DD} L_R^T \tag{3.63}$$

One solution at this point would be to compute the weight matrix by inverting the complete covariance matrix. This would require a lot of computer time, since the dimension of this matrix is rather high. Following the strategy

proposed by Beutler *et al*, (1986), one can make further use of the results given by equation (3.60). An additional step includes an auxiliary vector of double differences, Φ_{DD_A}, as follows

$$\Phi_{DD_A} = \left[\Phi_{DD_R}, \quad \Phi_{DD_m}\right]^T \tag{3.64}$$

The vector Φ_{DD_m} is composed of the 'missed' double differences. Thus this equation may be rewritten as,

$$\Phi_{DD_A} = L\Phi_{DD} \tag{3.65}$$

where

$$L = \left[L_R \quad L_M\right]^T \tag{3.66}$$

The rows of $\mathbf{L_M}$ are rows of a unit matrix. The covariance matrix of Φ_{DD_A} may now be written as,

$$\Sigma_{DD_A} = L\Sigma_{DD}L^T \tag{3.67}$$

The **L** matrix in the equation (3.67) is non-singular. Therefore, the weight matrix of the auxiliary vector can be computed as

$$W_A = (L^T)^{-1} W L^{-1} \tag{3.68}$$

where **W** is the weight matrix of the supposed complete set of double differences. This expression is easily computed since the inverse of **L** matrix is easy to compute.

Using equation (3.66), the right hand side of equation (3.67) may be rewritten as:

$$\Sigma_{DD_A} = \begin{bmatrix} L_R\Sigma_{DD}L_R^T & L_R\Sigma_{DD}L_M^T \\ L_M\Sigma_{DD}L_R^T & L_M\Sigma_{DD}L_M^T \end{bmatrix} = \begin{bmatrix} N_{11} & N_{12} \\ N_{21} & N_{22} \end{bmatrix} \tag{3.69}$$

From equation (3.63) it can be seen that it is the upper left matrix on the right hand side of equation (3.69) that has to be inverted. Restructuring the matrix $\mathbf{W_A}$ (equation 3.68) in a similar manner to the equation (3.69) gives:

$$W_A = \begin{bmatrix} W_{11} & W_{12} \\ W_{21} & W_{22} \end{bmatrix} \tag{3.70}$$

The required weight matrix is finally given by as (Beutler *et al*, 1986):

$$W_R = W_{11}\left[I_r + \underbrace{L_R \Sigma_{DD} L_M^T}_{N_{12}} \right]\left[W_{22} \underbrace{L_M \Sigma_{DD} L_M^T}_{N_{22}} \right]^{-1} W_{21} \tag{3.71}$$

where $\mathbf{I_r}$ is an identity matrix of dimension equal to the actual number of double differences.

The apparent advantage of this method is that one has only to invert the matrix $\mathbf{W_{22}N_{22}}$, which has dimensions equal to the number of 'missed' observations, usually a few, instead of inverting the complete covariance matrix. However, a large amount of multiplication has to be carried out to obtain the final required weight matrix, which may make the algorithm unattractive.

The idea behind this method is to start the process by assuming that all the observables are available. The weight matrix is then easily computed using the properties of Kronecker products (equation 3.60). If some observations are 'missed', the actual weight matrix is computed as given by equation (3.71). For successive epochs, the computation of the weight matrix is only necessary if the observation scenario has changed since the last epoch.

A more detailed analysis of equation (3.71) shows that it can be further simplified. Using the following relationship:

$$\Sigma_{DD_A} W_A = I \tag{3.72}$$

which implies

$$W_{11} N_{12} = - W_{12} N_{22} \tag{3.73}$$

In addition one can write

$$\left[W_{22}N_{22}\right]^{-1} = N_{22}^{-1}W_{22}^{-1} \tag{3.74}$$

since both matrices are not singular. Thus, introducing equation (3.73) into equation (3.71) and using relation (3.74), the required weight matrix is finally obtained as:

$$W_R = W_{11} - W_{12}W_{22}^{-1}W_{21} \tag{3.75}$$

This expression is a very simplified form of equation (3.71) and has also been described by Beutler *et al* (1987).

Chapter 4

THE FIDUCIAL AND FREE NETWORK TECHNIQUES

4.1 Introduction

The application of GPS depends essentially on knowing the satellite positions at the epoch of observation. For point positioning, the uncertainty in the satellite position is propagated directly into the estimated position. In the process of differencing the observables, relative baseline errors are approximately equal to the relative orbital errors. The broadcast ephemeris allows for the computation of the satellite coordinates at any epoch, providing relative precision of the order of 5 ppm under Selective Availability (SA) conditions. The use of precise ephemeris can significantly improve the quality of the results.

The quality of the precise ephemeris has significantly improved with the establishment of the International GPS Geodynamic Service (IGS). Goad (1993) claimed that orbit approaching 50 cm or better was indeed close by. Beutler *et al* (1994) reported orbit precision of the order of 20 cm, estimated using IGS data sets. Such a level of precision can provide relative baseline error of about 0.01 ppm, which should be sufficient for the needs of most of the GPS users. The high accuracy of the GPS satellite orbit is obtained by using the fiducial GPS approach.

The fiducial GPS technique involves the simultaneous observation of GPS data at a network incorporating three or more fiducial stations, and any other stations whose coordinates are required to be estimated. The fiducial station positions are known to a high accuracy in a global reference frame. The complete set of data is processed in a single adjustment, estimating corrections to the approximate satellite state-vectors, coordinates of the unknown stations and some other bias parameters (ambiguities, tropospheric scale factors, y-bias, etc.). The coordinates of the fiducial sites have to provide at least the minimal

constraints of the network, which are three translations, three rotations and one scale (Ashkenazi *et al*, 1990). This technique has been extensively used for regional orbit improvement.

The IGS permanent GPS network provides a global data set of precise GPS measurements. Using this data set, the fiducial concept can be applied to a global network. A recent development in GPS global network processing is the use of the concept of free network adjustment. In this technique, also referred in this thesis as non-fiducial approach, data processing is performed without fixing any fiducial station. Therefore, the main difference between the fiducial and free network techniques is that either some stations are held fixed in the fiducial approach or all stations are freed in the free network approach.

The basic principle of orbit estimation by the fiducial technique, as used in the Nottingham's GPS Analysis Software (GAS) is described in this chapter. The purpose is to provide the reader with a concise summary of the technique and stages involved, which are the results of research conducted in this field over the last eleven years at the University of Nottingham. Full descriptions of the technique can be found in Agrotis (1984), Moore (1986) and Whalley (1990). The basic concept of free network adjustment is also introduced in this Chapter.

4.2 Principles of Orbit Determination

Prior to the network adjustment stage, a theoretical 'integrated orbit' has to be computed for each of the satellites. This computation requires the precise modelling of the various forces acting on the satellite as a function of time, thus giving its time varying acceleration vector. These forces include the gravitational forces caused by gravitational attraction of the earth, moon, sun and other planets, surface forces (e.g. air drag, direct solar radiation, infrared radiation), and other perturbing influences (Ashkenazi and Moore, 1986). The resulting acceleration vector is numerically integrated in an inertial reference frame, once to obtain the velocity and twice to obtain the position of the satellite.

In order to perform the integration process, it is necessary to have provisional knowledge of the satellite's position and velocity vector at a reference epoch t_0, the so called initial state-vector. Using appropriate step length and algorithms,

the integration is carried out numerically, providing the 'integrated orbit', expressed in a geocentric inertial reference frame. The integrated orbits are improved during the network adjustment by introducing the observations collected from the tracking stations (fiducial and new). The network adjustment leads to improved solutions for the satellite initial state-vectors (position and velocity), some of the force model parameters, the coordinates of the tracking stations, and other unknown parameters. The improved satellite initial state-vector is used to re-integrate the orbit, the other corrections are applied to the corresponding unknowns, and an iterative process is followed until a convergence criterion is satisfied.

4.3 Reference Frame Considerations

Satellite orbit is performed in an Inertial reference Frame (IF), ie one which is either stationary or in a state of uniform motion. This is because the fundamental laws of mechanics are postulated with respect to an inertial coordinate system. However, the coordinates of the tracking stations and some force model components are given in an Earth Fixed (EF) reference frame which is a non-inertial frame. The EF parameters must therefore be transformed to the inertial reference frame, before the integration process can take place.

4.3.1 Inertial Reference Frame

The geocentric inertial reference frame adopted in the Nottingham software is the J 2000.0 (Moore, 1986), defined as follows:

- X axis directed towards the mean equinox of J 2000.0,
- Z axis normal to the equatorial plane of J 2000.0
- Y axis completes the right handed coordinate system.

This system is called the Conventional Inertial Frame because it is defined conventionally and the practical realisation does not necessary coincide with the theoretical system. Its reference epoch is January 1.5 of the year 2000.0 in the fundamental reference frame FK5, which describes the apparent positions of over 500 stars and extra-galactic radio sources at this reference epoch.

4.3.2 Earth Fixed Reference Frame

The EF reference frame used is based on the Conventional Terrestrial Reference System (CTRS), defined as follows (McCarthy, 1992):

- It is geocentric, the centre of mass being defined for the whole earth, including oceans and atmosphere,
- Its scale is that of a local earth frame, in the meaning of a relativistic theory of gravitation,
- Its orientation is given by the Bureau International de L'Heure (BIH) orientation at 1984.0,
- Its time evolution in orientation will create no residual global rotation with respect to the crust, ie a no-net-rotation (NNR).

The geocentric EF reference frame used for GPS is based on a CTRS, which is called WGS84 (§2.3.2). A more accurate reference frame is the realisation of the International Earth Rotation Service (IERS) Terrestrial Reference System (ITRS), referred to as IERS Terrestrial Reference Frame (ITRF). The IERS has also been responsible for computing the Earth Orientation Parameters (EOP), ie earth rotation and polar motion. They are estimated using Satellite Laser Ranging (SLR) and Very Long Baseline Interferometry (VLBI) observations and are published in the IERS Bulletin-A. Since August 1992, GPS observations have also been included in the processing. A brief description of the realisations of the ITRS is given below.

(a) Realisations of the IERS Terrestrial Reference System (ITRS)

The ITRS is annually realised by the IERS Central Bureau through a least squares adjustment of various Sets of Station Coordinates (SSC) obtained by spatial techniques such as SLR, LLR (Lunar Laser Range), VLBI, and more recently (1991), GPS. Different processing centres participate in the contribution of SSC. As a result, a list of coordinates and transformation parameters for the individual solutions are produced. A velocity field has also been included recently. The SLR, LLR and GPS provide the geocentre because their data can be modelled dynamically. The VLBI and LLR provide the scale whilst the orientation is defined by adopting the IERS earth orientation parameters at a reference epoch.

The activities of IERS started in 1988 replacing the BIH, which in 1985 initiated the realisation of CTRS. The realisations of the BIH Terrestrial System (BTS) are referred to as BTS84, BTS85, BTS86, and BTS87 (Boucher and Altamimi, 1989).

The initial realisation of the ITRS is the ITRF-0, which was linked to the BTS87. This was achieved by adopting the origin, orientation and scale of BTS87 (Boucher and Altamimi, 1989). To date (June 1995), the successive realisations of the ITRF, after the initial one, are ITRF88, ITRF89, ITRF90, ITRF91, ITRF92 and the up-to-date ITRF93.

The origin, scale and orientation adopted in the ITRF88 are those of ITRF-0. In the ITRF89, the origin was derived from SLR data and scale from VLBI and SLR data, whilst the orientation was such that no global rotation should exist with respect to ITRF88 (Boucher and Altamimi, 1991a). The minimal constraints adopted for the ITRF90, followed the same strategy as the previous implementations, but the orientation was such that no global rotation should exist with respect to ITRF89 (Boucher and Altamimi, 1991b). For all the above cases, no velocity field has been adjusted.

The origin of the ITRF91 was also obtained from SLR data. The scale came from VLBI and SLR data and the orientation defined in such way that no global orientation should exist with respect to ITRF90. An ITRF91 velocity field has also been estimated by the combination of several site velocity fields estimated by SLR and VLBI analysis centres. The NNR-NUVEL-1 was selected as a reference motion model and was included in the global adjustment of the ITRF91 velocity field (Boucher *et al*, 1992). For the first time, a GPS solution was included in the realisation of the ITRS, which is identified as SSC(JPL) 91 P 01. This solution was a contribution of the Jet Propulsion Laboratory (JPL).

The implementation of the ITRS referred to as ITRF92 was carried out in a similar manner to the ITRF91. The orientation was such that no-net-rotation should exist with respect to the ITRF91. Out of a total of 20 sets of solutions, six sets were derived from GPS data (Boucher *et al*, 1993a).

The up-to-date ITRF93 global combination solution is divided into 3 parts namely,

- a set of station coordinates at epoch 1988.0
- a set of station coordinates at epoch 1993.0
- a velocity field consistent with the above two sets.

The realisation of the ITRF93, which was achieved by the combination of 20 SSC submitted to the IERS was slightly different from the previous ones. The number of solutions for each technique was: (i) 6 VLBI, (ii) 4 LLR, (iii) 5 GPS, (iv) 4 SLR and (v) 1 GPS/SLR. So far, the orientation was defined such that no global rotation should exist with the previous realisation. The orientation and rate of change of the ITRF93 have been constrained to be consistent with the IERS series of Earth Orientation Parameters (EOP) at two epochs (88.0 and 93.0), thus defining the orientation and the time evolution. The origin and scale of the ITRF93 are defined by holding to zero the translations and the scale of the SLR solution (SSC(CSR) 94 L 01) in the two adjustments at both epochs (Boucher *et al*, 1994).

An ITRF93 velocity field has been estimated by combining ten site velocity fields estimated by SLR, VLBI and GPS analysis centres. The NNR-NUVEL1A, was selected as a reference motion model, instead of the previous one NNR-NUVEL1.

4.3.3 Transformation Between Reference Frames

The two reference frames involved in the process of orbit determination, ie inertial and EF, need be transformed between them. The transformation from inertial to EF coordinates and vice-versa requires successive transformation between several intermediate reference frames.

In order to transform the resultant satellite acceleration in the EF frame ($\ddot{\underline{r}}_{EF}$) to the inertial frame ($\ddot{\underline{r}}_{IF}$), four transformation matrices are applied. The transformation is achieved via the expression

$$\ddot{\underline{r}}_{IF} = Q^T N^T E^T P^T \ddot{\underline{r}}_{EF} \tag{4.1}$$

where **P**, **E**, **N** and **Q** are polar motion, earth rotation, nutation and precession matrices respectively (Moore, 1986; McCarthy, 1992).

4.4 Force Modelling

All the significant forces acting on the satellite should be correctly modelled and included in the resultant force model, in order to obtain a precise satellite orbit. This force model essentially consists of two different types of forces namely the gravitational and the surface-forces. Although all major forces are usually included in the force model, there are some other smaller forces normally neglected. These include the thrusts caused by the satellite's stabilising rockets firing, the reaction on the satellite caused by emitting a radio wave with a certain energy, etc. A brief description of the major force model components is given below.

4.4.1 Gravitational Forces

The gravitational forces consist of the gravitational attraction of the earth, moon, sun and all the other planetary bodies, as well as tidal effects.

(a) Earth's Gravitational Attraction

The gravitational attraction of the earth is the main constituent of the force model. It is modelled as a function of the satellite position in an EF reference frame and made up of equipotential surfaces radiating outwards from the earth's mass centre. As the density and shape of the earth are non-uniform, the equipotential surfaces are not spherical, but a complex shape, which is usually expressed in terms of a spherical harmonic expansion. The gravitational potential, U, at all points external to the earth is given as a function of their spherical polar EF coordinates (Φ, λ, and R for latitude, longitude and radius respectively) (Ashkenazi and Moore, 1986). The potential gravitational (U) is given by:

$$U = \frac{GM}{R}\left[1 + \sum_{n=2}^{\infty}\sum_{m=0}^{n}\left[\frac{a}{R}\right]^n P_n^m[C_{n,m}Cos(m\lambda) - S_{n,m}Sin(m\lambda)]\right] \qquad (4.2)$$

where GM is the earth's gravitational constant

n, m are the degree and order of spherical harmonic expansion,

a is the earth's equatorial radius,

P_n^m is the associated Legendre polynomial of degree n and order m and

$C_{n,m}$, $S_{n,m}$ are the spherical harmonic coefficients.

In order to compute the gravitational potential, as given by expression (4.2) an earth's gravitational model is required. The models available have been derived using satellite tracking data and terrestrial gravity measurements.

An example of these models is the WGS84 Earth Gravitational Model (EGM) (DMA, 1987). In theory, the expansion of the spherical harmonic expression of the gravitational potential results in an infinite series, which must be truncated at a certain point, for practical application. It has been shown (Whalley, 1990) that coefficients up to the order and degree 8 are sufficient for GPS satellite orbit determination.

The components of the force acting on the satellite due to the gravitational attraction of the earth are given in EF frame by the gradient of the potential, U, in the respective directions. As the potential is given in terms of spherical polar coordinates, the chain rule is used to relate this to the EF Cartesian components by the expression:

$$\ddot{\underline{r}}_{EF} = \frac{\partial U}{\partial R}\left(\frac{\partial R}{\partial R_i}\right) + \frac{\partial U}{\partial \lambda}\left(\frac{\partial \lambda}{\partial R_i}\right) + \frac{\partial U}{\partial \Phi}\left(\frac{\partial \Phi}{\partial R_i}\right) \qquad (4.3)$$

where R_i is the vector of satellite position (X, Y, Z) in the EF reference system and

$\ddot{\underline{r}}_{EF}$ is the vector of satellite instantaneous EF acceleration $(\ddot{X}, \ddot{Y}, \ddot{Z})$.

Notice that the acceleration vector at an instant $\mathbf{t_i}$ is a function of the satellite position at the same instant. Once the acceleration vector is computed, a new satellite position at an instant $\mathbf{t_{i+1}}$ can be computed. This process is repeated forward to the full considered interval. Derivations of the partial derivatives involved in the equation (4.3) are given in Moore (1986). The EF acceleration components must be transformed into an inertial frame for the purpose of orbit integration.

(b) Third Body Attraction

The moon, sun and other planets also exert an attraction on the satellite, resulting in an acceleration vector $\ddot{\underline{r}}$, of the satellite towards the 'third body', P_j, as illustrated in Figure 4.1. The earth is similarly attracted towards the third body P_j, resulting the acceleration vector $\ddot{\underline{r}}_E$.

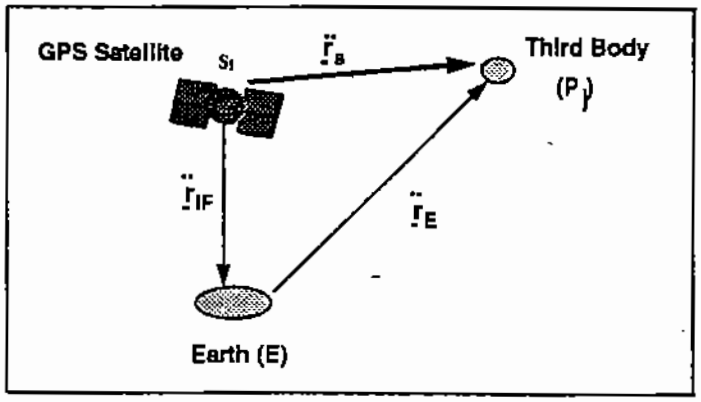

Figure 4.1: Third Body Gravitational Attraction

The resultant acceleration of the satellite, $\ddot{\underline{r}}_{IF}$, with respect to the earth (in the geocentric inertial frame) is given by:

$$\ddot{\underline{r}}_{IF} = \ddot{\underline{r}}_S - \ddot{\underline{r}}_E \tag{4.4}$$

which is represented as

$$\ddot{\underline{r}}_{IF} = -GM_j\left[\frac{\underline{r}_S - \underline{r}_j}{(\underline{r}_S - \underline{r}_j)^3} + \frac{\underline{r}_j}{\underline{r}_j^3}\right] \tag{4.5}$$

where G is the universal gravitational constant,
M_j is the mass of the third body P_j
$\underline{r}_s$ is the satellite position vector and
$\underline{r}_j$ is the third body position vector.

It can be seen from this expression that the positions of the so called third bodies must be known in an inertial reference frame. Their masses are also required in the computation. These are obtained from a planetary and lunar ephemeris developed by the Jet Propulsion Laboratory (JPL) known as DE200/LE200. It gives the daily positions of the moon and planets in a heliocentric inertial frame together with the masses of the planets and the constants associated with the ephemeris. In order to use this ephemeris, the coordinates have to be converted to the geocentric inertial frame by subtracting the coordinates of the earth from those of the moon and planets. The geocentric coordinates of the sun are obtained by multiplying the heliocentric position vector of the earth by -1. The positions at the required epochs are computed by interpolation.

(c) Earth Body and Ocean Tides

The gravitational attraction of the sun and moon on the earth varies continuously due to their different apparent orbits, with respect to the earth. As the earth is not a rigid body, these forces cause deformation on the earth, resulting in changes in the earth's gravitational field and consequently similar changes in the acceleration of the satellite. The coordinates of the tracking stations also change because of this effect, which can lead to movements of up to 32 cm and 15 cm for lunar and solar tides respectively. The ocean surface is an equipotential one (except for the effects of temperature, pressure, salinity and currents). The attraction of the moon, sun and other planet's forces leads to a rise in the tidal potential, causing the level of the ocean to fluctuate with time. This causes the ocean to apply a variable load on the body of the earth, which responds by deforming, resulting in a change in the gravitational field of the earth. Therefore, a similar change occurs in the acceleration of the satellites, which is much less than that due to the solid earth tides. The additional potential outside the earth arising from a deformed earth due the solid and ocean tides can be expressed in terms of a series of spherical harmonic coefficients, similar to those of the earth's gravitational potential. Their effects are normally introduced as corrections to the earth's gravitational potential spherical harmonic coefficients (Moore, 1986).

4.4.2 Surface Forces

Satellite surface forces are the result of solar radiation and atmospheric drag. The latter is negligible due to the high altitude of the GPS satellites. Unfortunately, this high altitude exposes the satellite to the bombardment of the radiation emitted from the sun. The resulting force is one of the most difficult to model because of large fluctuation in solar activity.

The model used in the Nottingham program for spherical satellites is described by Agrotis 1984 and Moore 1986. The inertial frame acceleration caused by the solar radiation pressure ($\ddot{\underline{r}}_{SR}$) in the direction of the sun, is given by:

$$\ddot{\underline{r}}_{SR} = C_R\left(\frac{I_0}{c}\right)\left[\frac{A}{|\underline{r}_S - \underline{r}_j|}\right]^2\left(\frac{a}{m}\right)\vec{e}_{ss} \qquad (4.6)$$

where C_R is a solar radiation reflectance coefficient, which will absorb certain deficiencies in the model and it can be determined as an unknown in the adjustment process,

I_0 the intensity of the radiation at a distance A nominally equal to 1367.2 W/m^2, but depending of the solar activity,

c is the speed of light,

A is the Astronomical unit (1.4959787 10^{11}m),

$\underline{r}_s$ is the satellite position vector in an inertial frame,

$\underline{r}_j$ is the sun position vector in an inertial frame,

a/m is the area to mass ratio of the satellite and

$\bar{e}_{ss}$ is the unit vector in the direction of the satellite from the sun.

This model has been satisfactory when applied to spherical satellites. However, GPS satellite has a complex shape, with two large panels attached to either side. As such, the model must take into account the shape, reflectivity of each surface of the satellite. The model adopted in the Nottingham software is a simple model, which is an improved version of that given by equation (4.6), since only short arcs are normally involved in the GPS data processing (Whalley, 1990). The model includes a y-bias acceleration term to account for the force along the y-axis of the solar panels. It is suspected that this y-bias acceleration may possibly be due to misalignment of the solar panels, the satellite altitude sensing mechanism, or thermal re-radiation effects. Besides this, a shadow factor, η, was introduced in order to take into account the eclipsing of the satellites, which occurs twice a year. The value of η varies between 1.0 (full sunlight) and 0.0 (full shadow). Introducing the y-bias acceleration term, C_y and the shadow factor, η in the expression (4.6) results

$$\ddot{\underline{r}}_{SR} = \eta\left[C_R\left(\frac{I_0}{c}\right)\left[\frac{A}{|\underline{r}_S - \underline{r}_j|}\right]^2\left(\frac{a}{m}\right)\bar{e}_{ss} + C_y\bar{e}_y\right] \qquad (4.7)$$

where $\bar{e}_y$ is a unit vector in the satellite coordinate system axes pointing along the satellite's positive y-axis (Fliegel *et al*, 1992)

4.5 Numerical Integration

The resultant acceleration due to the forces acting on the satellite is given by summing all the individual accelerations, each one of them properly evaluated

in the same inertial frame. This represents the equation of motion which is a second order differential equation and is a function of position, velocity and time.

$$\ddot{\underline{r}} = f(\dot{\underline{r}}, \underline{r}; t) \tag{4.8}$$

where $\ddot{\underline{r}}$ is the resultant acceleration vector in the inertial frame,
$\dot{\underline{r}}$ is the satellite velocity vector in the inertial frame,
$\underline{r}$ is the satellite position vector in the inertial frame and
t is the time.

By assuming an initial position, $\underline{r}(t_0)$, and velocity, $\dot{\underline{r}}(t_0)$, at a starting epoch, t_0, the position and velocity at another epoch, t, are given by numerical integration. The initial satellite state-vector components, $\underline{r}_{sv}(t_0) = [\underline{r}(t_0), \dot{\underline{r}}(t_0)]^T$, needs not be known precisely, as they can be improved by least squares adjustment. The integration is carried out with a 'step length' $(t_i - t_{i-1})$, resulting in a satellite ephemeris consisting of position and velocity vector at discrete epochs. This can be written as

$$\begin{aligned} \dot{\underline{r}}(t_i) &= \dot{\underline{r}}(t_{i-1}) + \int_{t_{i-1}}^{t_i} \ddot{\underline{r}}(t_{i-1})dt \\ \underline{r}(t_i) &= \underline{r}(t_{i-1}) + \int_{t_{i-1}}^{t_i} \dot{\underline{r}}(t_{i-1})dt \end{aligned} \tag{4.9}$$

The position and velocity of the satellite at any specific epoch may be computed by interpolation between the discrete values. For details the reader is referred to Agrotis (1984) and Moore (1986).

4.6 Mathematical Model for Orbit Improvement

In the ordinary GPS network adjustment (§3.5.1), the double difference carrier phase observable was used. This observable has also been used for the estimation of improved satellite initial state-vector and some model parameters, e.g. y-bias and solar radiation, as well as the usual parameters involved in ordinary GPS network adjustment. The linearised double difference carrier phase observation equation given by expression (3.54) must then be extended in order to include the corrections to the satellite initial state-vector ($\Delta\underline{r}_{sv}$), as

well as the coefficients of the solar radiation reflectance (ΔC_R) and y-bias acceleration (ΔC_y).

The expanded double difference carrier phase observation equation linearised about the unknown parameters, for the case involving stations r_1 and r_2 and the satellites s^i and s^j, is given by,

$$
\begin{aligned}
E\{\Delta l_{DD_o}\} = {} & a_1^{i,j}\Delta X_1 + b_1^{i,j}\Delta Y_1 + c_1^{i,j}\Delta Z_1 + \\
& + a_2^{i,j}\Delta X_2 + b_2^{i,j}\Delta Y_2 + c_2^{i,j}\Delta Z_2 + \lambda\Delta N_{1,2}^{i,j} + \\
& + T_1^{1,2}(\tau-\tau_0)^n\alpha_{1,n} - T_2^{1,2}(\tau-\tau_0)^n\alpha_{2,n} + \\
& + \sum_{n=1}^{6}\left[\left(\frac{\partial\rho_1^i}{(\partial\underline{r}_{sv}^i)_n} - \frac{\partial\rho_2^i}{(\partial\underline{r}_{sv}^i)_n}\right)(\Delta\underline{r}_{sv}^i)_n + \left(\frac{\partial\rho_2^j}{(\partial\underline{r}_{sv}^i)_n} - \frac{\partial\rho_1^j}{(\partial\underline{r}_{sv}^i)_n}\right)(\Delta\underline{r}_{sv}^j)_n\right] + \\
& + \left[\frac{\partial\rho_1^i}{\partial C_R^i} - \frac{\partial\rho_2^i}{\partial C_R^i}\right]\Delta C_R^i + \left[\frac{\partial\rho_2^j}{\partial C_R^j} - \frac{\partial\rho_1^j}{\partial C_R^j}\right]\Delta C_R^j + \\
& + \left[\frac{\partial\rho_1^i}{\partial C_y^i} - \frac{\partial\rho_2^i}{\partial C_y^i}\right]\Delta C_y^i + \left[\frac{\partial\rho_2^j}{\partial C_y^j} - \frac{\partial\rho_1^j}{\partial C_y^j}\right]\Delta C_y^j + v_{DD_o}
\end{aligned}
$$

...Equation (4.10)

The first three lines correspond to the ordinary model for double difference carrier phase observation equation (given by equation (3.54)), where Δl_{DD_o} is the computed minus observed double difference carrier phase. The last three lines represent the extension of the previous model. The partial derivatives with respect to each of the *(n=6)* elements of the satellite state-vector are obtained via the chain rule, ie

$$
\frac{\partial\rho_1^i}{\partial\underline{r}_{sv}^i} = \frac{\partial\rho_1^i}{\partial X^i}\left(\frac{\partial X_i}{\partial\underline{r}_{sv}^i}\right) + \frac{\partial\rho_1^i}{\partial Y^i}\left(\frac{\partial Y_i}{\partial\underline{r}_{sv}^i}\right) + \frac{\partial\rho_1^i}{\partial Z^i}\left(\frac{\partial Z_i}{\partial\underline{r}_{sv}^i}\right) \qquad (4.11)
$$

The partial derivatives of the form $\frac{\partial\rho_1^i}{\partial X^i}$ are computed in a similar way as for $\frac{\partial\rho_1^i}{\partial X_1}$ (see §3.3.4) , yielding the same value but of opposite sign. The partials derivatives of the satellite position with respect to the satellite state vector,

$\frac{\partial X^i}{\partial \underline{r}^i_{sv}}$, cannot be derived analytically, instead they are computed during numerical integration. A similar procedure is used in the derivation of the various partial derivatives for the solar-radiation reflectance, C_R as well as y-bias acceleration coefficients, C_y. Further details can be found in Whalley (1990). A more simple form of expression (4.10) can be written as

$$E\{\Delta l_{DD_o}\} = \begin{bmatrix} A_R & A^S & A_B^B \end{bmatrix} \begin{bmatrix} \Delta R \\ \underline{\Delta r}_{sv} \\ \Delta B \end{bmatrix} \tag{4.12}$$

which has an associated covariance matrix. The matrix $\mathbf{A_R}$ is composed of the coefficients of station coordinates, $\mathbf{A^S}$ of the coefficients of the satellites state-vectors and A_B^B of the coefficients of the bias parameters, either for the satellites, stations, or both. The vectors $\Delta\mathbf{R}$, $\underline{\Delta r}_{sv}$ and ΔB contain the corrections to the approximate coordinates of the stations, satellite state-vectors and bias parameters respectively.

4.7 The Fiducial Network Concept

In the least squares adjustment of a network by fiducial technique, the coordinates of the fiducial stations have to be included in the adjustment as either additional observation equations (constraints) or fixed values. They are supposed to be known at a level of accuracy of the order of 0.01 ppm. Such a level of accuracy has only usually been achieved by either the VLBI or SLR techniques, and more recently by GPS as well. In the fiducial GPS approach, mainly for regional orbit improvement, the network incorporates three or more points of known (fiducial) coordinates. Theoretically, only a minimum of seven coordinate values (ie a minimum of three fiducial stations) has to be held fixed, in order to provide the minimal constraints of the reference frame, which are three translations, three rotations and one scale (Ashkenazi *et al*, 1993a). However, depending on the internal consistency of the global reference framework, any subset of three fiducial stations held fixed will define a slightly difference reference frame from the global one.

Simultaneous measurements are made to the satellites at the fiducial stations and all the other unknown stations in the network. The complete set of data is

processed in a single adjustment, estimating corrections to the satellites state-vectors, coordinates of the unknown stations and some other bias parameters (ambiguities, tropospheric scale factors, y-bias, etc.). The resulting adjusted network of ground stations and satellite orbits is positioned, scaled and oriented to the reference frame defined by the adopted coordinates of the fiducial stations held fixed, thus transferring the high accuracy of the fiducial station coordinates, via the satellite orbits, to the new stations. The fiducial technique has been extensively used in regional orbit improvement, producing satisfactory results.

4.8 The Free Network Concept

The use of the concept of a GPS network without fiducial sites, referred to as free network or non-fiducial approach has been reported by several researchers [Hering *et al*, (1991); Blewitt *et al*, (1992); Heflin *et al*, (1992a and 1992b), Mur *et al*, (1993) and Heflin *et al*, (1993)]. This concept has been applied to global GPS experiments, in which fiducial stations are not necessary to provide an origin and scale. Instead, they are provided by the satellite force model, radio propagation model, and GPS data. It follows that only the orientation provided by the fiducial coordinates is missing, but the direction of the Z-axis is further constrained by the earth's daily rotation. Some quantities such as baseline lengths and geocentric radius are invariant with respect to the orientation of the network and can therefore be examined without the use of fiducial sites.

If the orientation of the network is missing, the functional model involved in the adjustment, represented by the design matrix **A**, has rank deficiency. In such a case, the system of normal equations in the least squares adjustment is singular, and no solution is possible of being estimated using conventional least squares adjustment. By constraining the approximate coordinates of the stations and satellites state vectors with very loose standard deviation, this problem can be solved. This concept, in case of providing acceptable results, could make GPS independent of the other techniques, which provide the coordinates of the fiducial station (e.g. SLR and VLBI). Blewitt *et al* (1992), Heflin *et al* (1992a and 1992b) and Heflin *et al* (1993) have used this concept together with the use of internal constraints applied to the covariance matrix of the station coordinates.

Tests carried out during this work have shown that a solution is possible even without applying loose constraints. This shows that the model has a *quasi* rank defect. However, differently to the cases cited above, the earth pole position was not estimated in the adjustment. The use of a dynamic approach to compute the satellite orbits in a model where the earth orientation parameters (EOP) are neglected (computed or fixed to IERS Bulletin-A values), provides a non-singular system (Mur *et al*, 1993).

4.8.1 Transformation of the Free Network Solution to the ITRF

In order to make the free or the non-fiducial solution consistent with the ITRF's scale, origin, and orientation, a similarity transformation is applied to the former solution. It involves the estimation of the seven parameters as follows:

$$\begin{bmatrix} x \\ y \\ z \end{bmatrix}_{GPS} = \begin{bmatrix} X \\ Y \\ Z \end{bmatrix}_{ITRF} + \begin{bmatrix} t_x \\ t_y \\ t_z \end{bmatrix} + \begin{bmatrix} s & -\Theta_z & \Theta_y \\ \Theta_z & s & -\Theta_x \\ -\Theta_y & \Theta_x & s \end{bmatrix} \begin{bmatrix} X \\ Y \\ Z \end{bmatrix}_{ITRF} \qquad (4.13$$

where **x**, **y** and **z** are the coordinates derived from the free GPS network;
X, **Y** and **Z** are ITRF coordinates of the known stations mapped to the time of the campaign;
$\mathbf{t_x}$, $\mathbf{t_y}$ and $\mathbf{t_z}$ represent the offsets in origin;
s represents a difference in scale and
Θ_x ,Θ_y and Θ_z represent differences in orientation.

Since the ITRF geocentric origin is generally believed to be accurate at the 2 cm level (Blewitt *et al*, 1992) and a geocentric origin is also adopted in the GPS models, the origin offsets should be consistent with the precision of the ITRF origin. The scale difference should also be consistent with zero, if both systems adopt the same speed of light and gravitational coefficients. The orientation differences have no physical significance, since in the GPS solution they are constrained by loose variances.

To estimate the transformation parameters, equation (4.13) should be rearranged and rewritten in the form of observation equation model (see equation (3.1)). The vector of observables is given by the differences between

GPS and ITRF coordinates and the vector of unknown parameters is composed by the seven parameters $\left[t_x \quad t_y \quad t_z \quad s \quad \Theta_x \quad \Theta_y \quad \Theta_z\right]^T$. The elements of the **A** matrix are given as:

$$A = \begin{bmatrix} 1 & 0 & 0 & X_1 & 0 & Z_1 & -Y_1 \\ 0 & 1 & 0 & Y_1 & -Z_1 & 0 & X_1 \\ 0 & 0 & 1 & Z_1 & Y_1 & -X_1 & 0 \\ \cdots & \cdots & \cdots & \cdots & \cdots & \cdots & \cdots \end{bmatrix} \tag{4.14}$$

The least squares estimation of the transformation parameters requires the weight matrix of the observables. The corresponding covariance matrix of the observables involved in the transformation is given as:

$$\Sigma_T = \Sigma_{X_{GPS}} + \Sigma_{X_{ITRF}} \tag{4.15}$$

ie the sum of the covariance matrix of the GPS and ITRF stations coordinates. The weight matrix is obtained from the inverse of equation (4.15). The residuals of the observables after the transformation give an indication of the quality of the transformation.

Once the transformation parameters have been estimated, those sites not included in the transformation may be transformed to the required reference frame.

The transformation is the last step involved in the free network approach. It means that only this step need be recomputed if the choice of the reference frame changes. In the traditional fiducial technique, however, all the main steps must be recomputed.

4.8.2 Internal Constraints

The covariance matrix estimated from the free network solution ($\Sigma_{X_{GPS}}$) is poorly determined if only loose constraints are applied to the station coordinates and initial satellite position components. Heflin *et al* (1992a), report 5 m for x and y and 4 cm for z, as the typical standard deviation for the station coordinates. Tests conducted in Nottingham (§8.5.1), showed values of about 12 m for x and y and 4 cm for z, for the cases in which all stations were

left free. Thus, the covariance matrix expressed by equation (4.15) will also have similar values. As the transformation parameters are estimated from observables with this level of precision, it is expected that the same level of precision would be obtained when they are applied to the other sites. Such level of precision should be improved to the same level as the ITRF stations in order to obtain consistent transformation parameters.

The approach adopted by Blewitt *et al* (1992) to tackle this problem was to modify the GPS covariance matrix in such way that the covariances are relative to an internally defined frame, as opposed to the a priori loosely constrained frame. This is obtained by applying an orthogonal projection operator, B, which projects GPS coordinate variations onto a space orthogonal to a reference frame that is implicitly defined through the approximate coordinates of the GPS stations. This is equivalent to applying the inner constraints in a model with rank deficiency, which intuitively corresponds to fixing the directions, origin and scale of the coordinates axes in an average sense to the initial approximate coordinates. Applying such constraints to the free solution yields

$$\Sigma_{X_{GPS\perp}} = B\Sigma_{X_{GPS}}B \tag{4.16}$$

with

$$B = I - A(A^T A)^{-1}A^T \tag{4.17}$$

The A matrix of equation (4.17) is obtained in a similar manner to equation (4.14), in which all the stations of the network are included. Therefore, the A matrix has dimension $n*3 \times 7$, with n equal to the number of stations. The coordinates are given by the approximate values used to linearise the observation equations in the adjustment. The equation (4.15) is rewritten as

$$\Sigma_T = \Sigma_{X_{GPS\perp}} + \Sigma_{X_{ITRF}} \tag{4.18}$$

This approach has been tested during this research without providing reasonable results. After applying the orthogonal projection represented by matrix B, the precision of the parameters was at the same level as it was before.

In this research, this problem was also tackled by applying internal constraints only to the covariance matrix, but in a different manner. Using the concepts of free adjustment described by Koch (1987) and Monico (1988), the internal constraints are represented by:

$$A^T \Delta R = 0 \tag{4.19}$$

where ΔR is the vector of corrections to the approximate coordinates.

The covariance matrix of the parameters after applying these constraints is given as (Vaníc̆ek and Krakiwsky (1982); Monico (1988) and Koch (1987)):

$$\Sigma_{\perp GPS} = \Sigma_{GPS} - \Sigma_{GPS} A \left(A^T \Sigma_{GPS} A \right)^{-1} A^T \Sigma_{GPS} \tag{4.20}$$

From this expression it can be clearly seen that the covariance matrix after applying the constraints are better than the previous one, but it is a singular matrix. Nevertheless, a weight matrix can be formed from blocks of $\Sigma_{\perp GPS}$ using the 3x3 covariance sub-matrices between the coordinates of individual stations. It should not be a problem since only diagonal terms for the ITRF are available. The use of the pseudo-inverse (Koch, 1987; Monico, 1988), in which the full inverse could be taken into account, is also an option for being used.

It has to be pointed out that as only the orientation of the network was missing, it seems reasonable to apply the internal constraints restricted only to the orientation. In this case, the A matrix would contain only elements associated with orientation ie, its last 3 columns of equation (4.14). This matrix has been identified as $\mathbf{A_I}$ and is given by:

$$A_I = \begin{bmatrix} 0 & Z_1 & -Y_1 \\ -Z_1 & 0 & X_1 \\ Y_1 & -X_1 & 0 \\ \cdots & \cdots & \cdots \end{bmatrix} \tag{4.21}$$

4.8.3 An Alternative Proposed Approach

Another approach, also based on the theory of free network adjustment, and closely related to the solution previously described, may also be used for GPS

network adjustment. As already pointed out, the model represented by equation (4.12) has a *quasi* rank defect. In the fiducial technique, this problem was solved by fixing the coordinates of the fiducial stations. The solution adopted in the non-fiducial approach was to apply loose constraints to the approximate coordinates of the stations and satellites. Furthermore, internal constraints were applied to the covariance matrix of the free solution.

An alternative approach would be to apply internal constraints directly to the model given by equation (4.12). The extended model would be:

$$E\{\begin{bmatrix} \Delta L_{DD_o} \\ 0 \end{bmatrix}\} = \begin{bmatrix} A_R & A^S & A_B^B \\ A_I^T & 0 & 0 \end{bmatrix} \begin{bmatrix} \Delta R \\ \underline{\Delta r}_{sv} \\ \Delta B \end{bmatrix} \tag{4.22}$$

where A_i represents the internal constraints and is given as equation (4.21). The system of normal equation of model (4.22) is given as (Monico, 1984):

$$\begin{bmatrix} N_{RR} & N_{RS} & N_{RB} & A_I \\ & N_{SS} & N_{SB} & 0 \\ & Symmetric & N_{BB} & 0 \\ & & & 0 \end{bmatrix} \begin{bmatrix} \Delta R \\ \underline{\Delta r}_{sv} \\ \Delta B \\ K \end{bmatrix} = \begin{bmatrix} (A_R)^T W(\Delta L_{DD_o}) \\ (A^S)^T W(\Delta L_{DD_o}) \\ (A_B^B)^T W(\Delta L_{DD_o}) \\ 0 \end{bmatrix} \tag{4.23}$$

The sub-matrices involved in the left hand side of this system of normal equation are as follows:

$$\begin{aligned} N_{RR} &= (A_R)^T W A_R \\ N_{RS} &= (A_R)^T W A^S \\ N_{RB} &= (A_R)^T W A_B^B \\ N_{SS} &= (A^S)^T W A^S \\ N_{SB} &= (A^S)^T W A_B^B \\ N_{BB} &= (A_B^B)^T W A_B^B \end{aligned} \tag{4.24}$$

with **W** as the weight matrix of the double difference carrier phase observables.

This approach was not applied in this research since it requires significant modifications in the software. Nevertheless the approach has been presented as a topic for future investigation.

Chapter 5

GPS DATA PROCESSING SOFTWARE: DESCRIPTION AND DEVELOPMENTS

5.1 Introduction

The mathematical models for GPS data processing addressed in the previous chapters have to be converted into computer processing algorithms. Numerous GPS software packages are currently available and used for different applications. They are usually general purpose software suitable for several applications, including small network adjustment, high accuracy surveys over short or long baselines and scientific investigation for geodynamics research.

A multi-purpose software package consists of several parts. The three main parts can be identified as,

(i) pre-processor,
(ii) the main processor and
(iii) the post-processor.

The pre-processing stage involves preparing the raw GPS data for the main processing. This stage may involve activities such as detection and repair of cycle slip, point positioning by using pseudorange observations, etc. Once the data has been pre-processed, network adjustment is undertaken in the main processing stage. The results of the main processing are subsequently used as input in the post-processing stage that may involve further analysis, such as the repeatability and the recovery of the network.

The University of Nottingham's GPS Analysis Software (GAS) has been used for this research. The software has been developed in-house at the Institute of Engineering Surveying and Space Geodesy (IESSG) (Stewart *et al*, 1993). GAS performs the twin tasks of pre-processing and actual processing of GPS

data. The post-processing, including the combination of sessions or days and estimation and application of transformations parameters (e.g. translations, rotations and scale) has been carried out using the GAS ancillary software CARNET (CARtesian NETwork adjustment program) (Lowe, 1992 and Lowe, 1994). In order to assess the results in terms of repeatabilities and recoveries the REPDIF (vector REPeatability or DIFferences) program was used (Bingley,1994).

A brief description of the software and the limitations encountered during this research are presented in this Chapter. The developments performed to expand the capabilities of the software are also presented.

5.2 The GPS Analysis Software (GAS)

The GPS Analysis Software (GAS) has been developed as a result of GPS research over the past eleven years at the University of Nottingham. It was designed primarily for processing multi-station static GPS surveys in a single network adjustment, using double difference carrier phase data. In such a case, a network of m stations consists of $(m-1)$ independent baselines and is adjusted with a full network covariance matrix.

5.2.1 Pre-processing

The first two operations in the pre-processing stage within GAS are:

(i) to convert RINEX (Receiver INdependent EXchange) format broadcast ephemeris files into SP3 format ephemeris file and
(ii) to convert raw RINEX GPS data to the Nottingham (NOT) format.

Two software modules, CON2SP3 (CONvert to SP3 format) and FILTER, are involved in these operations. They are followed by the detection and correction of cycle slip and outliers, which is carried out using the module PANIC (Program for the Adjustment of Network using Interferometric Carrier phase).

(a) CON2SP3

The module CON2SP3 has the function of converting RINEX format broadcast ephemeris files into SP3 format ephemeris files, which must be created before running the module FILTER or the processing module PANIC.

The SP3 format is the format used by the US National Geodetic Survey (NGS) to distribute precise ephemeris. It has also been used in the ephemerides distributed by the IGS (International GPS Geodynamics Service) processing centres.

In cases where the SP3 format ephemeris does not contain satellite clock correction values, the CON2SP3 module can also be used to insert these values, using the clock parameters from the broadcast ephemeris. Currently (June 1995), all the IGS centres provide the precise ephemeris with satellite clock corrections. The program CON2SP3 is also used for inserting satellite clock correction values for SP3 format ephemeris resulting from orbit integration with the GAS orbit module, referred to as GPSORBIT (§5.2.2).

(b) FILTER

The primary function of FILTER is to convert raw RINEX GPS data to the NOTtingham (NOT) format, which is the GAS GPS data file format. NOT is an ASCII .data format, which has a degree of similarity to the international accepted RINEX format. During data conversion, FILTER also detects and corrects for large cycle slip in the carrier phase data by comparing the change in the phase and pseudorange measurements for adjacent epochs. A point positioning pseudorange solution option can also be invoked. This provides a preliminary judgement of the quality of the data sets to be processed. The following additional options are also available in the filtering stage:

- discarding epochs which contain less than a certain number of satellites,
- selection of a new data interval,
- removal of data from unhealthy satellites and
- specification of a time-span for a session.

(c) Detection, Identification and Correction of cycle slip and Outlier

A cycle slip is a sudden jump in the carrier phase observable by an integer number of cycles, without affecting the fractional portion of the phase (Leick , 1990), whereas an outlier may affect the fractional part of the cycle. Either cycle slip or outlier has to be detected, identified and corrected during the early stages of data processing of a GPS network.

The cycle slip detection within GAS is carried out using PANIC module. This is an iterative process conducted on a baseline by baseline basis. Although slips

occur in the undifferenced phase observables, they are corrected in the double difference observable. It is not possible to identify the affected undifferenced phase observable using only a baseline. By convention, the cleaning process is undertaken relative to a pre-defined station and satellite, which are assumed to be clean. Furthermore, it should be noted that there is a risk of new cycle slip if the selected station and satellite change during the processing stage. For this reason, the definition of the independent baselines and base (reference) satellites for actual processing is conducted as part of this stage.

In the data cleaning mode, each run of PANIC generates a successively updated output file of estimated slips for the second station. These cycle slip are detected using an L1 or L2 triple difference residual algorithm. Over long baselines, the L1 or L2 triple difference residual algorithm is used in conjunction with other combination of observables, normally L0 (ionospherically free) and L3 (widelane). The slip file is automatically read as input into successive iterations, whereby PANIC internally corrects for any slips specified in the slip file and produces new slip estimates. Over long baselines, where the data noise may be high, or in the case of spurious data measurements, the detection of cycle slip is very difficult, if not impossible. In such cases, it may be necessary to manually correct the slip file generated by PANIC. The estimated factor of variance, ($\hat{\sigma}_0^2$), can give an indication about further cycle slips. Once it has an acceptable value, the GPS data file (for the second station) is corrected using SLIPCOR (SLIP CORrection) module, which reads information from the slip files and applies the correction to the GPS data file.

By making some assumptions, a simple strategy for outliers detection can be developed from the rigorous expression given in Chapter three (§3.2.4). The test statistic represented by equation (3.14), which is used for outliers detection, is given as:

$$\hat{w}_i = \frac{C_i^T W \hat{V}}{\sqrt{C_i^T W \Sigma_{\hat{v}} W C_i}}$$

where W is the weight matrix,

$\hat{V}$ is the vector of residuals,

$\Sigma_{\hat{v}}$ is the covariance matrix of the residuals, and

C is a vector given as $C = (0,...,1,...,0)^T$, with the no-null value identifying the observation being tested.

Results documented in the GPS literature show that the denominator of the above expression is almost a constant (Kösters ,1992). It is only marginally influenced by the changes in satellite configuration, the extension of the area of the network, the interval between observations and the observation period.

Tests carried out to detect outliers in a baseline, with level of significance, α, equal to 5%, showed that the minimum detectable double difference outlier was on average, 8 times the standard deviation of an undifferenced phase observation (Kösters ,1992). This value may be used to detect outliers during cycle slip detection process. As the residuals are normally analysed using the triple difference, one has to multiply the average value of the minimal detectable double difference outlier by $\sqrt{2}$, in order to take into account the error propagation from double to triple difference. Therefore, a triple difference residual between two adjacent epochs, $\mathbf{V_{TD}}$, may be considered as resulting from observations containing an outlier if,

$$V_{TD} > 11\sigma \qquad (5.1)$$

where σ is the standard deviation of the considered observable. This is an approximate value, which can be useful during the pre-processing stage. This shows that for the L1 carrier phase, assuming σ = 4 mm, the rejection of one observation will occur if the triple difference residual is about 44 mm, ie 0.23 cycles. This value may be used to analyse the residual file generated in PANIC during the cycle slip and outlier detection.

5.2.2 GAS Main Processor

The main processor in the GAS software is the PANIC module, which is run in the network adjustment or single baseline processing modes. In order to perform the above two tasks, several options are available. They include pseudorange or carrier phase solutions, simultaneous frequency combination solutions, varying tropospheric models, etc. The adjustment of a network can be carried out as an ordinary network adjustment, fiducial network adjustment and free network adjustment.

(a) Ordinary Network Adjustment

After the pre-processing has been carried out, all the clean data files are input into PANIC, which provides the network solution. The satellite positions are computed either from broadcast or precise ephemerides, and the coordinates of the known stations are held fixed in the adjustment. Some of the tasks performed by the PANIC module in the network adjustment mode are illustrated in Figure 5.1.

The observable showed in Figure 5.1 is the ionospherically free double difference, although other linear combinations can also be used. There are four options of corrections to be applied to the double difference observations. They are the Earth Body Tide (EBT), Ocean Tide Loading (OTL), Troposphere refraction and Antenna Phase Centre corrections.

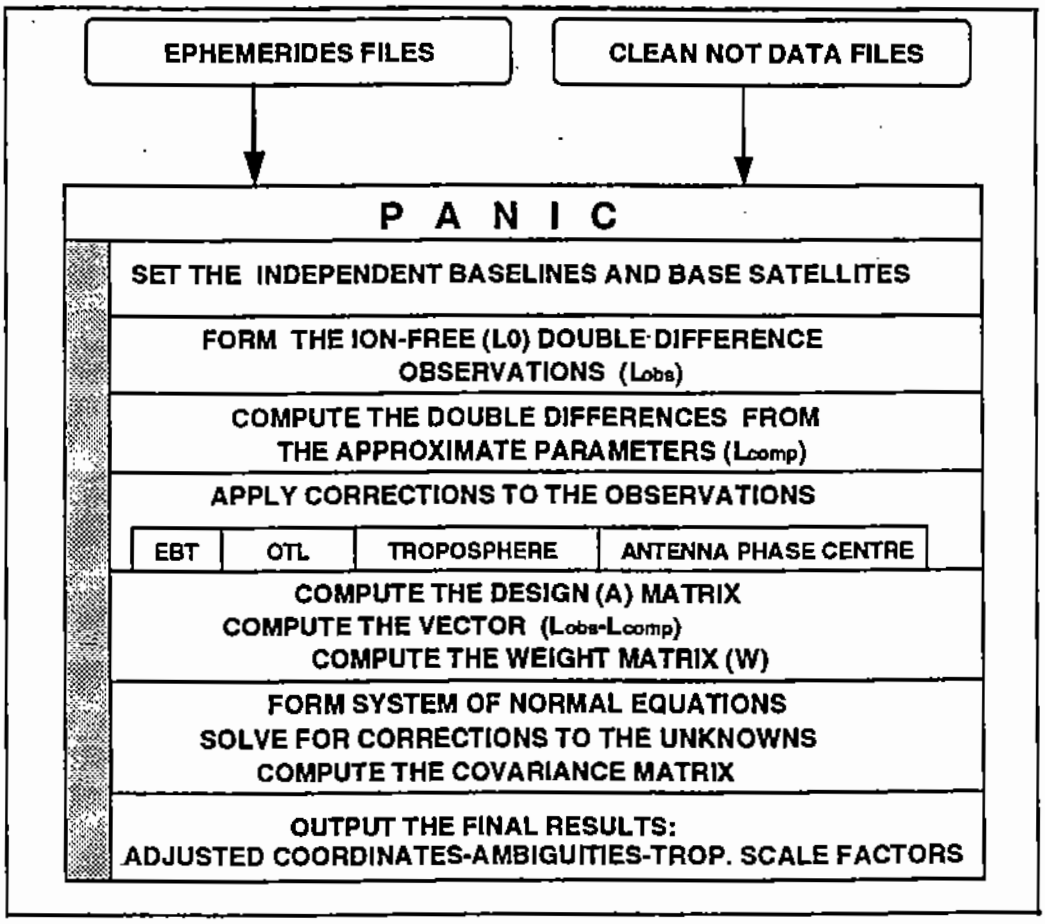

Figure 5.1 : Main Stages of an Ordinary GPS Network Adjustment With PANIC

In order to apply EBT corrections, a GAS Ancillary File (GAF) is required before running PANIC. This file contains information about the position of the

sun, moon and planets, which are used by PANIC to compute the EBT corrections. It is created by the GAS module MKGAF (MaKe GAF File).

If OTL corrections are to be applied, the ocean loading model has to be defined by the user. In this case, the amplitude and phase of the ocean loading crustal displacement (Height, North and East) related to the stations to be corrected must be included in a file containing all possible eleven tidal constituents or less. The tide is expressed as simple harmonic functions of time. The tidal constituents (M_2, S_2, N_2, K_2, K_1, O_1, P_1, Q_1, M_1, M_m and S_{sa}) used during this research were obtained from the IERS Standards (McCarthy, 1992). The OTL GAS option also allows for applying a single vertical OTL correction (height), horizontal OTL component corrections, or both.

The tropospheric delay correction may be applied either by using a standard atmosphere (ie without meteorological data) or using meteorological data. For the latter case, the meteorological data files have to be given by the user.

The antenna height models used in PANIC to correct for errors in antenna phase centre were based on tests outlined by Schupler and Clark (1991). The software contains models for Trimble, Rogue and Ashtech receivers. Nevertheless, the user may also specify his own antenna phase centre model.

The user can select as output of PANIC either Cartesian positions or Cartesian coordinates differences, both with the corresponding covariance matrix. The former is referred to as GAS Position File and the latter as GAS Baseline File.

(b) Fiducial Network Adjustment

The fiducial data processing with GAS is also carried out using the PANIC module. However, more information than for a basic network processing is required. In particular, it is necessary to generate an integrated orbit and the appropriate partial derivatives for the orbital unknowns, which are improved in the least squares adjustment. The integrated orbit and partial derivatives are generated by the GAS module GPSORBIT. GPSORBIT module requires a Global Gravity model file, a tidal model file and the GAF file, which may already be available, if the EBT corrections were applied during the basic network adjustment. Otherwise, the module MKGAF has to be run to produce the GAF file, which is valid for a 40-day period. The GAF file contains the

Chebychev polynomial coefficients that represent the nutation and precession matrices as well as the planetary ephemerides (Ffoulkes-Jones, 1990).

Before attempting to run a fiducial solution, the user must first ensure that there are no problems with the basic network solution. Whilst running the final network solution using fixed satellite positions (Figure 5.1), it is necessary to generate an initial satellite state-vector file. This contains the start time of orbit integration for each satellite, the initial state-vector for each satellite (position and velocity) and the corresponding rotation matrices (set to arbitrary values) necessary to transform the initial state-vector from the earth fixed reference frame to the inertial reference frame (§4.3.3). The rotation matrices are updated in GPSORBIT. Figure 5.2 is a flow diagram outlining the procedure for fiducial GPS data processing.

The Geopotential model of the earth's gravity field used in GPSORBIT is the WGS84 global gravity model with degree and order 8 (DMA, 1987) and the Schwiderski model for ocean tide corrections (McCarthy, 1992).

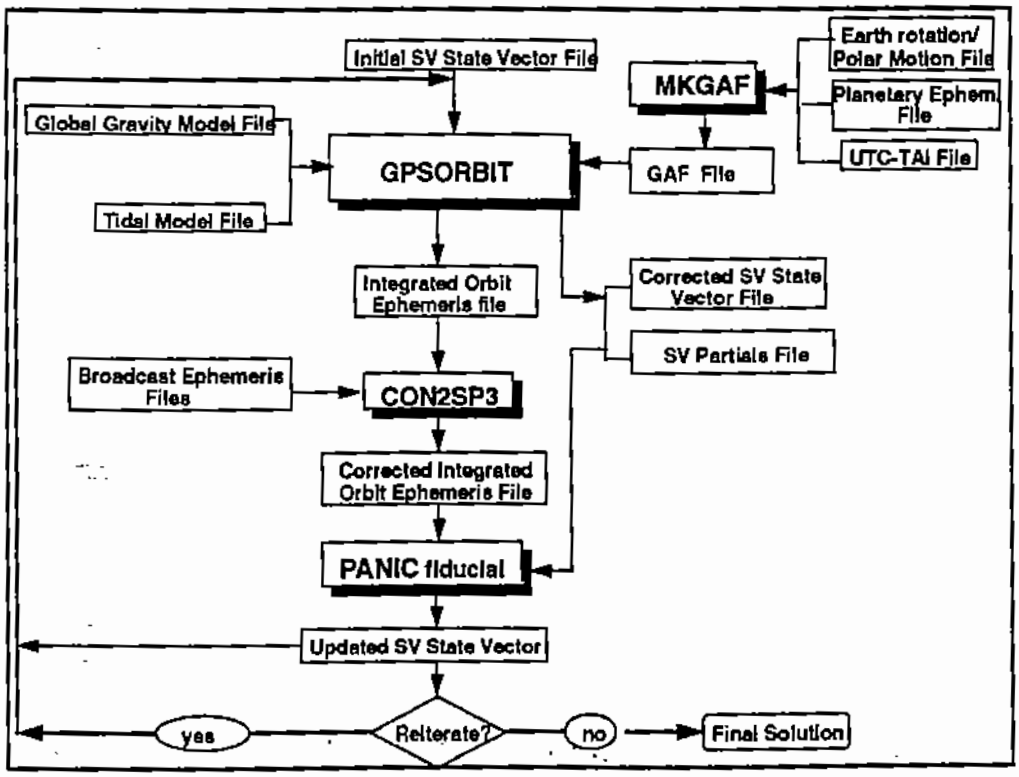

Figure 5.2 Fiducial GAS Flow Diagram (After Stewart *et al*, 1994)

(c) Free Network Adjustment

The network adjustment without fiducial stations, referred to as the free network adjustment, is carried out in a similar manner to the fiducial technique. Instead of holding the fiducial stations fixed, all stations are held free or loose constrained. The GAS main processor can, therefore, be used to carry out this adjustment. One of the results of the free network adjustment is an output file containing the Cartesian coordinates of the stations and respective covariance matrix. In the ordinary and fiducial network adjustments, it is usual that such a file contains the Cartesian positions differences together with the associated covariance matrix.

5.2.3 Post-Processing Software

The results obtained from the network adjustment process are normally available for various sessions or days and a unique solution is normally required. The network analysis software, CARNET, has been used to provide the required solution. The software has also been used to perform the transformation from the free network solution to a selected reference frame. At this stage, the software DEGRADE (degrade covariance matrix) had to be used for a few tests. The assessment of the quality of the results, in terms of repeatability and recovery, has been performed using the REPDIF software.

(a) Cartesian Network Adjustment Program (CARNET)

CARNET enables the integration of several types of conventional observations with GPS and other space geodetic techniques. These observations can be adjusted together, providing a 3-dimensional solution (Lowe, 1994). Several options can be invoked during the network adjustment, e.g. the estimation of transformation parameters or their application once they have been determined.

The Cartesian coordinates or Cartesian coordinate differences estimated in the network adjustment using PANIC from several sessions or days can be combined together to produce a final solution using CARNET. The observation equation model in this case is a very simple one, similar to that given by expression (3.17) in the Chapter 3. The final result is a set of weighted mean values.

The main output of CARNET is a list of Cartesian and geodetic coordinates with the respective estimated standard deviations as well as information related

to the quality of the processing. The information contains, among others, the estimated variance factor, ($\hat{\sigma}_0^2$), and a simplified test statistic $\hat{w}$, (expression 3.15), which are suitable to perform the 'data-snooping' tests. The output of specific matrices (e.g. design matrix, covariance matrix) can also be invoked by the user.

(b) DEGRADE Software

The DEGRADE software is used to modify a full covariance matrix to a diagonal or block diagonal covariance matrix. The input is a GAS position file (Cartesian coordinates with corresponding full covariance matrix) and the output will contain the degraded covariance matrix.

(c) REPDIF Software

The REPDIF software has been developed at the University of Nottingham to assess the quality of the estimated results by using the concept of repeatability and recovery of the results. It computes the root mean squares (RMS) of the baseline coordinate components [(**dN**, **dE** and **dh**) and (**dX**, **dY** and **dZ**)] and the length component (**dL**) for all possible baselines. The RMS of the baseline components are derived from the RMS of the Cartesian coordinates, which are also given by the REPDIF program. The input files are the CARNET file containing the final solution, and each session or day solution file generated by PANIC. The repeatability R_{X_i} as computed in REPDIF is given for a specific component (eg X) of a baseline **i** by the RMS of the solution ie:

$$R_{X_i} = \sqrt{\frac{\sum_{j=1}^{n}(X_j - \overline{X})^2}{n}} \qquad (5.2)$$

where n is the number of solutions
$\overline{X}$ is the final solution estimated by CARNET
X_i is the j^{th} solution from PANIC.

It is important to note that to compute the repeatability of the baseline components, (**dN**, **dE**, **dh**), a transformation from geocentric Cartesian to local coordinates has to be carried out. After computing the repeatability for all the baseline components, an average value $R_{X_{AV}}$ is estimated by:

$$R_{X_{AV}} = \sqrt{\frac{\sum_{i=1}^{k} R_{X_i}^{\,2}}{k}} \tag{5.3}$$

where

k is the number of all possible baselines,

R_{X_i} is the repeatability of the baseline i.

One should be aware that expression (5.2) would provide repeatability zero for the case in which only one sample is available, indicating a result of good quality. However, in such a case the computation of the repeatability is not possible. A more appropriate measure of the repeatability is given by (Blewitt, 1989):

$$R_{X_i} = \sqrt{\frac{n}{n-1}\frac{\sum_{j=1}^{n}\frac{(X_i - \overline{X})^2}{\sigma_j^2}}{\sum_{i=1}^{j}\sigma_j^{-2}}} \tag{5.4}$$

where σ_j^2 is the variance of the j^{th} estimate. Notice that an implicit condition to compute the repeatability is that n must be at least 2.

A careful analysis of the last expression shows that it is an approximation of the square root of the estimated variance factor, ($\hat{\sigma}_0$), estimated from an adjustment involving the combination of different session solutions. The difference is that in such a case whilst the variance factor estimation involves the full weight matrix and all three coordinates, the repeatability is expressed for each of the 3 Cartesian coordinates and neglects the non-diagonal elements of the weight matrix. The estimated variance factor of the combined solution model is, therefore, a good indication of the repeatability of the network in all the three components (**X**, **Y** and **Z**).

The recovery, defined in this research as the difference between the assumed 'true'[5.1] value of the position of a station and the estimated one, is also obtained using the REPDIF software. In order to obtain such values, the coordinates of

[5.1] True value refers to a position with an accuracy better than the esimated one

one or more very well known stations are estimated in the adjustment. The recovery, Rec_{X_i}, is then given by:

$$\mathrm{Rec}_{X_i} = X_i - \overline{X_i} \tag{5.5}$$

where $\mathbf{X_i}$ and $\overline{X_i}$ are the assumed 'true' and estimated coordinate of the considered station respectively, and similarly for the other two coordinates **Y** and **Z**.

5.3 Limitations of the Software

The GAS software has successfully been used in the processing of data for high accuracy surveys (Ashkenazi *et al*, 1994; Whitmore, 1995; Beamson, 1995). The data processing has been, however, limited to continental networks, where most of the satellites (or at least two) can be simultaneously tracked from all the stations. The double differences are formed in GAS by using the concept of base satellite which has to be the same for all the baselines (§3.3.3).

The project carried out in this research involved the processing of GPS data for inter-continental networks. A typical network was composed of stations located in Brazil and Chile (South America) and United States of America (North America). Over this network, the constellation of GPS satellites being tracked in South America differs from that in North America. Therefore, the limitation of having the same base satellite for all baselines of the network, as it was the case in GAS, does not allow the processing of the complete network. One option was to divide the network into sub-networks. Otherwise, a new module had to be developed to provide GAS with the capability of processing the complete network. The network processing was, therefore, undertaken in two stages. Firstly, the network was processed as two sub-networks. Secondly, a new software module implementing the option of using different base satellite per baseline, referred to as *base satellite per baseline*, was developed. This provides capability of processing very large (even global) networks.

The computation of the weight matrix is made very simple by the use of the Kronecker product properties (§3.5.1). However, in the application of such properties it is assumed that the same satellites are being tracked by all the stations of the network. However, a few observations are sometimes 'missed'. The solution to this problem was either to invert the complete covariance

matrix of the observations (time consuming) or to apply some linear transformation to the original weight matrix in order to still apply the properties of Kronecker product (§3.5.2). The latter was implemented in PANIC. It was found, however, that the algorithm aiming to speed up the computation of the weight matrix in case of 'missing' observations, was very much slower than the classical way of computing the weight matrix (complete inversion of the covariance matrix). Therefore, an improved algorithm was proposed and subsequently implemented in PANIC.

The GAS module for cycle slip detection needs to be added with some extra software in order to improve the manual detection of slips and outliers. It is a very time consuming task that could be less tedious, if plots of the residuals were available. By visually inspecting the residuals graphs, it would become very easy to identify undetected cycle slips and outliers, as they produce distinct patterns in the double and triple difference residuals. For instance, an outlier produces one peak in the double difference, and two, of opposite signs in the triple difference residuals (Monico, 1992). On the other hand, a cycle slip produces a step in the double difference and a peak in the triple difference. Although the non availability of this facility in the Nottingham software is not a limitation, its implementation would enhance significantly the system.

5.4 Software Developments

5.4.1 Handling of 'Missing' Observations

The algorithm used in GAS software at the beginning of this research to handle 'missed' observations has already been described (§3.5.2). It starts by assuming that all the observations are available and the weight matrix is computed using Kronecker products (see equation 3.60). If there are some 'missing' observations, the actual weight matrix is obtained by applying a linear transformation on the original set of observations. The resulting weight matrix is given by equation (3.71) as:

$$W_R = W_{11} + W_{11} N_{12} \left[W_{22} N_{22} \right]^{-1} W_{21}$$

Some tests were carried out in order to evaluate the performance in terms of computational time of this algorithm with respect to the 'conventional' one (full inverse of the covariance matrix). The tests were performed using a Personal Computer PC 486-33 and the Lahey compiler with the software coded in

FORTRAN-77. The simulated network consisted of 20 stations and 10 satellites, with the possibility of forming 171 double differences at one epoch. Table 5.1 gives the CPU time to compute the weight matrix by full inversion of the covariance matrix and by using the algorithm given by the above expression. These two methods will be referred to as 'conventional' and 'alternative' methods respectively.

From Table 5.1 it can be seen that the 'alternative' algorithm is more efficient than the 'conventional' method only for the case without any 'missing' observations. This case corresponds to obtaining the weight matrix using the Kronecker product (see equation 3.60) and shows a very significant advantage over the full inversion. However, in the cases whit 'missing' observations, the 'alternative' algorithm consumes more than twice the time of the 'conventional' algorithm. This is due to the matrix multiplication $W_{11}(...)$ involved in the last expression. Once the number of 'missing' observations increases, the efficiency of the 'conventional' method improves. This occurs because the dimension of the matrix to be inverted, which is equal to the number of double difference observations, decreases.

Table 5.1 CPU Time (seconds) to Compute the Weight Matrix ('Conventional' x 'Alternative' Algorithm)

'Missing' Observations	'Conventional' Method	'Alternative' Method
0	12.36	0.33
2	11.75	27.30
8	10.49	25.05
12	9.50	23.70
20	8.13	20.65
30	6.30	17.47
44	4.67	14.01
51	3.90	11.19
75	2.04	10.80
82	1.60	10.77
87	1.36	10.88
94	1.04	11.30

The computation time of the 'alternative' method decreases as long as the number of 'missing' observations increased to about half (82) of the total number of possible observations (171). From then on, it starts to increase again. This is related to the matrices multiplication and inversion involved in the algorithm. Whereas the number of operations involved in the multiplication decreases with 'missed' observations, it increases in the inversion. Therefore, the computation time reaches a minimum, and then starts to increase again.

A 'modified' algorithm that substantially reduces the number of matrix operations has been proposed (§3.5.2). The algorithm is given by expression (3.75) as:

$$W_R = W_{11} - W_{12} W_{22}^{-1} W_{21}$$

Each component of this expression is given by the original weight matrix (without 'missing' observations), which as shown in Table 5.1 is very quick to compute. The matrix to be inverted (W_{22}) has dimension equal to the number of 'missing' observations. Therefore, as the number of 'missing' observations increases, the algorithm becomes less attractive. Fortunately, for most of applications, only few observations are missed.

The same tests as carried out before (Table 5.1) were repeated to evaluate the performance of the 'modified' algorithm. The CPU time required for computing the weight matrix using the 'conventional' method (full inverse of the covariance matrix) and using the 'modified' algorithm as a function of the number of 'missing' observations is listed in Table 5.2.

From Table 5.2 one can see that the 'conventional' method becomes more efficient with the increase in the number of 'missing' observations, (m_0), whereas the 'modified' algorithm becomes less efficient. This is because the matrix $\mathbf{W_{22}}$ to be inverted is of dimension m_0 and the matrix $\mathbf{W_{12}}$ grows linearly with m_0. The 'conventional' method will certainly be more efficient for the case when the number of 'missing' observations is equal to the number of observations available. Notice that with m_0 = 75, approximately half of the total number of original observations (171), the 'conventional' method is about twice as fast as the 'modified' algorithm. The reason for this is that the matrices to be inverted are approximately of the same dimension in both methods but in the 'modified' algorithm there are extra multiplication operations.

Table 5.2 CPU Time (seconds) to Compute the Weight Matrix ('Conventional' x 'Modified' Algorithm)

'Missing' Observations	'Conventional' Algorithm	'Modified' Algorithm
0	12.36	0.33
2	11.75	0.82
8	10.49	1.05
12	9.50	1.30
20	8.13	1.59
30	6.30	1.98
44	4.67	2.50
51	3.90	2.90
75	2.04	4.22
82	1.60	4.61
87	1.36	4.94
94	1.04	5.45

The conclusion from the results showed in Table 5.2 is, therefore, that in cases where the actual number of observations in a specific epoch is about half the assumed number of observations, it is more efficient to compute the weight matrix by the 'conventional' method (full inversion). Nevertheless, the real advantage of the 'modified' algorithm over the so called 'alternative' method is quite clear from the analysis of Table 5.1 and 5.2.

The performance of each of the three algorithms is illustrated in Figure 5.3. The real advantage of the 'modified' algorithm over the 'alternative' algorithm is immediately clear from Figure 5.3, as it is about 20 times faster. It should be pointed out that once the number of stations in the network increases, the gain in time of the 'modified' algorithm, over the 'alternative' one, may even be larger. The efficiency of the former algorithm is also better than the 'conventional' one, since the number of 'missing' observations does not become very high (for this particular test, about 30% of the assumed number of observations).

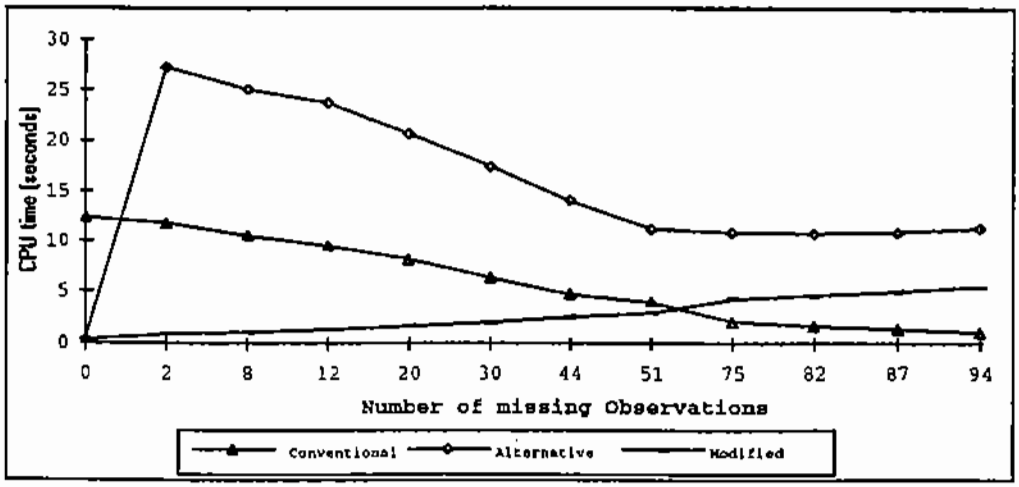

Figure 5.3: Performance of the Tested Algorithms

Tests carried out to analyse the total amount of time gained by using the 'modified' algorithm over the 'alternative' one during the complete processing of a network, showed values of the order of 10% to 30%. The 'modified' algorithm has successfully been implemented in the PANIC software as a substitute to the so called 'alternative' algorithm.

5.4.2 Base Satellite Per Baseline

The *base satellite per baseline* algorithm was implemented as an extra option in the PANIC software. It is suitable for the processing of very large or even global networks. The concepts of *base* or *sequential satellite differencing* could be used in the algorithms used to handle 'missing' observations ('alternative' or 'modified'). As PANIC has most of its subroutines developed using the base satellite concept, it was decided to implement the 'modified' algorithm using the same concept. However, for a large or global network, the concept of base satellite, as implemented in PANIC, has to be modified. In a global network the satellite constellation is likely to be different at most of the stations and the same satellite cannot be applied as base satellite for all the baselines. Otherwise, no double differences will be available on those baselines without the base satellite at one of the stations.

It was decided to continue using the concept of base satellite, but with the option of having a different one for each baseline. In this way, the **C** matrix (see equation 3.38), which relates the satellites involved in the double difference equations, will not be the same for all the baselines of the network.

Therefore, the double difference covariance matrix and consequently the weight matrix cannot be obtained using the concept of Kronecker product. The weight matrix has to be computed by full inversion of the covariance matrix, without assumptions about the number of observations collected, ie only the actual observations are taken into account.

In order to show how to the covariance matrix is obtained, expressions (3.35) and (3.37) are repeated here for simplicity. They are given as:

$$\Phi_{SD_i} = [I, \quad -I]\Phi_i$$
$$\Phi_{DD_i} = C\Phi_{SD_i}$$

These expressions represent the single and double difference carrier phase equations respectively, for a particular baseline at an epoch **i**. From these expressions one can see that the double differences can be rewritten as:

$$\Phi_{DD_i} = D\Phi_i \quad \text{with} \quad D = [C \quad -C] \tag{5.6}$$

and the covariance matrix is given as,

$$\Sigma_{\Phi_{DD}} = \sigma_0^2[DD^T] \tag{5.7}$$

The **D** matrix will be specific for each baseline and only the actual observations are taken into account. Considering a network with $(m\text{-}1)$ independent baselines, $(1\text{-}2; 2\text{-}3; \ldots; (m\text{-}1)\text{-}m)$, the covariance matrix for a specific epoch is given as:

$$\Sigma_{\Phi_{DD}} = \begin{bmatrix} D_1D_1^T & D_1D_2^T & 0 & 0 & 0 & \ldots & & & & 0 \\ D_2D_1^T & D_2D_2^T & D_2D_3^T & 0 & 0 & \ldots & \ddots & & & 0 \\ 0 & D_3D_2^T & D_3D_3^T & D_3D_4^T & 0 & \ldots & & & & 0 \\ \ldots & & & & \ldots & & & & & \\ 0 & \ldots & & & 0 & D_{m-3}D_{m-4}^T & D_{m-3}D_{m-3}^T & D_{m-3}D_{m-2}^T & 0 \\ 0 & \ldots & & & 0 & 0 & D_{m-2}D_{m-3}^T & D_{m-2}D_{m-2}^T & D_{m-2}D_{m-1}^T \\ 0 & \ldots & & & 0 & 0 & 0 & D_{m-1}D_{m-2}^T & D_{m-1}D_{m-1}^T \end{bmatrix} \tag{5.8}$$

It should be pointed out that the properties of Kronecker product (§3.5.2) could also be used, if the *sequential differencing method* (equation 3.38) was applied. In such a case, for a global network, one would have to assume that all the satellites have been tracked for all the stations and would treat those not observed as generating 'missed' observations. As the total number of GPS satellites is 24 and the average number of satellite being tracked at one station is about 8, the number of 'missing' observations would be higher than the actual number of observations. It was shown (§5.4.1) that in such a case is more efficient to make use of the full inversion of the covariance matrix than to handle the 'missed' observations.

Therefore, the *base satellite per baseline* option implemented in PANIC makes use of the full inversion of the covariance matrix to obtain the weight matrix. The user has to define a list of potential base satellites for each baseline, and PANIC automatically chooses the satellite with the highest elevation angle at the middle point of the baseline.

5.4.3 Internal Constraints

The concept of internal constraints was addressed in Chapter 4 (see §4.8.2), and a program was developed to apply this concept. The constraints are applied only to the covariance matrix of the station coordinates, which is given by equation (4.20), ie:

$$\Sigma_{\perp GPS} = \Sigma_{GPS} - \Sigma_{GPS} A \left(A^T \Sigma_{GPS} A \right)^{-1} A^T \Sigma_{GPS}$$

Two similar programs were developed and coded in FORTRAN 77. They are referred to as CONSCOV7 (CONStraints to the COVariance matrix applying 7 internal constraints) and CONSCOV3 (CONStraints to the COVariance matrix applying 3 internal constraints). In the former program the A matrix is given as equation (4.14), meaning that in this case, seven internal constraints are applied to the covariance matrix. The latter, as equation (4.21) and therefore, three internal constraints are applied (those related to orientation).

The inputs of both programs are a file of the Cartesian coordinates of the stations and a file with the corresponding covariance matrix. The output is a file type GAS Position File, which contains the Cartesian coordinates and the upper covariance matrix.

5.5 Summary

An efficient algorithm for handling 'missing' observations has been implemented in GAS. This algorithm is about 20 times faster than the one previously used in GAS.

The *base satellite per baseline* option, which allows for the processing of very large (even global) networks has also been implemented in GAS.

Two programs (CONSCOV3 and CONSCOV7) have been developed in order to apply internal constraints to the covariance matrix of the station coordinates estimated by GAS.

Chapter 6

ACCURACY ESTIMATES OF THE PROPOSED BRAZILIAN GPS NETWORK

6.1 Introduction

The Global Positioning System (GPS) has revolutionised the positioning industry (surveying, mapping and navigation) and changed the concept of a geodetic control network, mainly because of the high accuracy (relative positioning) and cost-effectiveness of the system. Surveys performed by GPS have provided precision of the order of 1 part per million (ppm) within a relatively short period of time. For longer periods, a precision of a few parts per billion (ppb) has been reported (Dong and Bock, 1989; Ashkenazi *et al*, 1994). It is also conceivable that as the cost of GPS receivers reduce, almost all future geodetic (horizontal) surveys will be performed by GPS. However, the traditional geodetic networks, which have been extensively used so far, are inadequate for GPS users. This is not only with respect to precision but also because most of the network control points are normally located on the high points of the area to be surveyed and often not easily accessible. It is therefore important that the organisations responsible for the establishment and maintenance of these networks provide suitable solutions to the geodetic GPS users. This has been tackled either by establishing an array of new (passive) control points or by the so-called Active Control System (ACS).

In this Chapter, a brief summary of the GPS positioning techniques is presented followed by a description of the solutions adopted in some countries for the provision of geodetic networks suitable for GPS users, with special attention given to the Brazilian solution. Some tests carried out to assess the accuracy that can be obtained by the users of the Brazilian network are described, taking into account the observable and the use of either precise or broadcast ephemerides for baselines ranging from 9 to 1000 Km.

6.2 GPS Positioning

GPS positioning can be performed either absolutely (only one receiver) or relatively (more than one receiver). In the former case, the user can generally almost freely choose the location of the station to be positioned whereas in relative positioning, one of the stations must be known and occupied. Access to the known station may in some cases be difficult and a time consuming task.

Point (absolute) positioning (§3.4) is commonly accomplished using only the code (pseudorange) observable. The navigation accuracy achievable with GPS is of the order of 10 to 15 m using the restricted Precise Positioning Service and 100 m (95% probability) under the freely available Standard Positioning Service (SPS). Even after several days of observation, the achievable absolute accuracy is no better than ± 5 m (Seeber, 1993). The high accuracy obtainable with GPS can therefore not be achieved with 'stand-alone' GPS, ie by point positioning.

To achieve a better positioning accuracy with GPS, the satellite signals collected by two or more receivers (§3.5) must be combined and differenced (relative positioning). This approach greatly reduces the systematic errors present in the GPS data. It should be pointed out that in relative positioning, any uncertainty in the base station position will transfer to the new stations. The use of the pseudorange observable in the differential approach is referred to as differential GPS (DGPS). In this case, one receiver is located at a known position providing the means to compute corrections in the observations or position. These corrections are then broadcast to remote users for application to their observations or positions. Relative navigational accuracy of approximately 2 to 3 m is successfully achieved (Seeber, 1993). This, however, is restricted to a relatively small area. A more sophisticated approach is the Wide Area Differential GPS (WADGPS) (Ochieng 1993), in which a sparse network of GPS reference stations can provide real-time network DGPS corrections to users over a large region, or even globally.

High accuracy GPS positioning (geodetic accuracy) is achieved in the relative positioning mode using the phase measurements. In the static mode, a relative accuracy of 10^{-8} to 10^{-6} of the baseline length has been achieved, depending on the time span of the observation, observable used, processing strategy

applied, and the reference system adopted. Results similar to those of Very Long Baseline Interferometry (VLBI) have been reported (Heflin *et al*, 1992b). Other powerful relative positioning techniques exploring the capability of GPS are the Rapid Methods (Seeber, 1993) providing accuracy levels of the order of 10 cm within a few minutes. The carrier phase data is used as the basic observable, and the code observable is sometimes used to aid in the resolution of the integer ambiguity. These techniques, where the distance from the base station does not exceed 30 km, are very suitable for detail surveying.

This short description of the GPS positioning shows the possibility of performing high accuracy surveying within a few minutes. Considering that the accuracy of the conventional geodetic networks (triangulation) is approximately 10 to 20 times worse (Hofman-Wellenhof *et al*, 1992) than that obtained by GPS, and that the stations are sometimes located on sites not easily accessible, the clear conclusion is that a new concept for the provision of geodetic networks should emerge. This should focus not only on the traditional users (surveying) but also on the new potential users (navigation, fleet managment, etc.). The next section describes the solutions to the provision of geodetic networks adopted by some countries.

6.3 GPS Control Networks

6.3.1 Conventional and GPS Control Networks

The conventional geodetic networks were generally surveyed by triangulation, traverse (or a combination of both) and by spirit levelling. The horizontal control network is normally separated from the vertical one. From the mid seventies, Doppler observations were used in the densification and control of these geodetic control networks. An example of network densification by Doppler observations, is the Brazilian Amazon network where the coordinates where first estimated in the satellite datum and then converted to the particular national datum (Godoy *et al*, 1991). In the United Kingdom and Republic of Ireland, distances derived from Doppler observations (translocation) were incorporated in the adjustment of the triangulation. This solution became known as OS(SN)80 (Ashkenazi *et al*, 1980). Similar solutions were adopted in other countries.

The conventional geodetic networks have been used to scale and orient maps to provide a unified reference frame for large scale projects and to provide a

common datum for property surveys. As already stated, these networks in addition to being less accurate than required by GPS users, their points are normally located on hilltops or church and water towers, and are often not easily occupied by GPS. Since almost all future geodetic surveys will be performed by GPS, the existing networks are inadequate.

The solution to the problems briefly outlined above was found by either establishing an array of new (passive) control points or by the so-called Active Control System (ACS).

It should be pointed out that GPS provides high precision solutions on a three-dimensional system. However, the height differences measured by GPS are referenced to an ellipsoid and not to the geoid as the conventional levelled heights. Therefore, the potential use of GPS as a levelling tool needs the provision a local or regional geoid model. The solution to this problem is out of the scope of this work and therefore it will not be discussed in detail.

6.3.2 Passive Control Network

The concept of a passive control network, involves the installation of a completely new network within a global geocentric reference datum, compatible with the World Geodetic System 84 (WGS84), which is defined with an absolute accuracy of about 1 to 2 m. As the station coordinates of the IERS Terrestrial Reference Frame (ITRF) sites are accurate to about 0.02 m, it is advisable to use the ITRF reference frame instead of the WGS84.

At a continental or sub-continental GPS network level, the fiducial concept is used (§4.7). The inter station distances should be between 300 and 500 Km, with about one week of observations carried out using dual frequency receivers. An example is the EUREF (EUropean REference Frame) project, with about 90 stations, performed with about 60 dual-frequency receivers in 1989. In 1990, 30 stations were added during the EUREF North Campaign. At a national GPS network level, the stations in the network are installed with a spacing of 25 to 100 Km, depending on the size of the country and objectives. In the processing of the national network, the stations of the continental level may be held fixed as fiducial points (Seeber, 1993).

In Great Britain, where six EUREF sites are located, an intermediate network between the continental and national networks has been installed, referred to as the Scientific Network. It consists of 27 stations spaced at approximately 100 to 150 km and includes the local EUREF stations (Wilson and Christie, 1992). The National GPS Network comprises 538 stations, spaced at 20 to 25 km around urban centres and more relaxed in rural areas. Many existing primary and secondary triangulation stations have been incorporated into the GPS network in order to provide transformation between the WGS84 and the UK national mapping datum (OSGB36). In order to provide vertical control, some stations of the National GPS network are being directly connected to the levelling network. This will provide control for the geoid model enabling height changes to be monitored by using GPS observations alone (Christie, 1992). The network stations were selected such that they will make ideal sites for GPS occupation. Thus, they should be accessible 24 hours a day by two wheel drive vehicles in all weather conditions.

In Germany, 109 stations with a mean spacing of 70 to 100 Km were observed with 83 dual frequency receivers. Some 20 stations are EUREF sites (Seeber, 1993). Another similar network is the Tennessee Geodetic Reference System Network (Zeigler, 1988), consisting of 60 control stations. It has been designed such that no location in the state would be farther than 25 km from a control station.

This new concept of a geodetic network will consist mainly of Continental and National networks and the division of geodetic networks into first to fourth order within a country will disappear.

A solution to the existing terrestrial network is the combination with new GPS observations. The existing network datum is maintained but the complete network is readjusted and strengthened with the inclusion of GPS measurements. New points can also be introduced into the existing network. The readjustment of the triangulation of the United Kingdom and the Republic of Ireland in 1980 used a similar approach, but with Transit-Doppler observations (Ashkenazi *et al*, 1980).

6.3.3 Active Control System

The main drawback of the passive control networks is that users have to occupy one or more stations in order to determine the position of the new ones. The user therefore has to have access to at least two receivers. An Active Control System (ACS) is a GPS-based system of fixed receivers continuously tracking all visible satellites and relaying the information via a communication link to a central Master Active Control Station (MACS). The GPS tracking stations are called Active Control Points (ACP), in which all operations should be performed automatically (Delikaraglou *et al*, 1986). Figure 6.1 illustrates the major components of an ACS. The user shown in Figure 6.1 can access the information from the ACP, either via a communication link (communication satellites) or off line via floppy disks. The former case refers to a real-time user (navigation) and the last to a static one, which essentially post processes the data. Information available from MACS can be accessed by the users using telephone and INTERNET links. The principal elements of each ACP are depicted in Figure 6.2. An ACP unit would mainly consist of one dual frequency receiver capable of tracking all satellites in view and a microcomputer to control the functions of the system. Meteorological sensors, communication interface and a continuous power supply are essential as well.

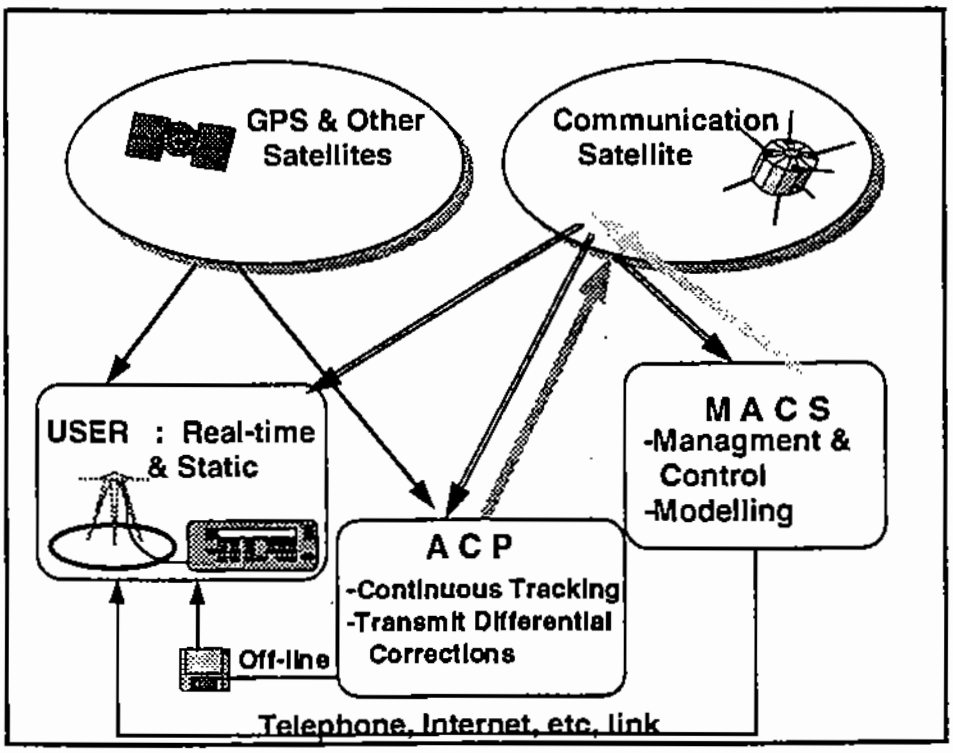

Figure 6.1: Active Control System Concept

The MACS controls the operation of the ACPs, processes the information obtained from the ACPs, performs data management and monitors the integrity of the GPS constellation. Besides this, it computes the satellite orbit and provides real-time and post mission GPS related information to the user community via a communication link.

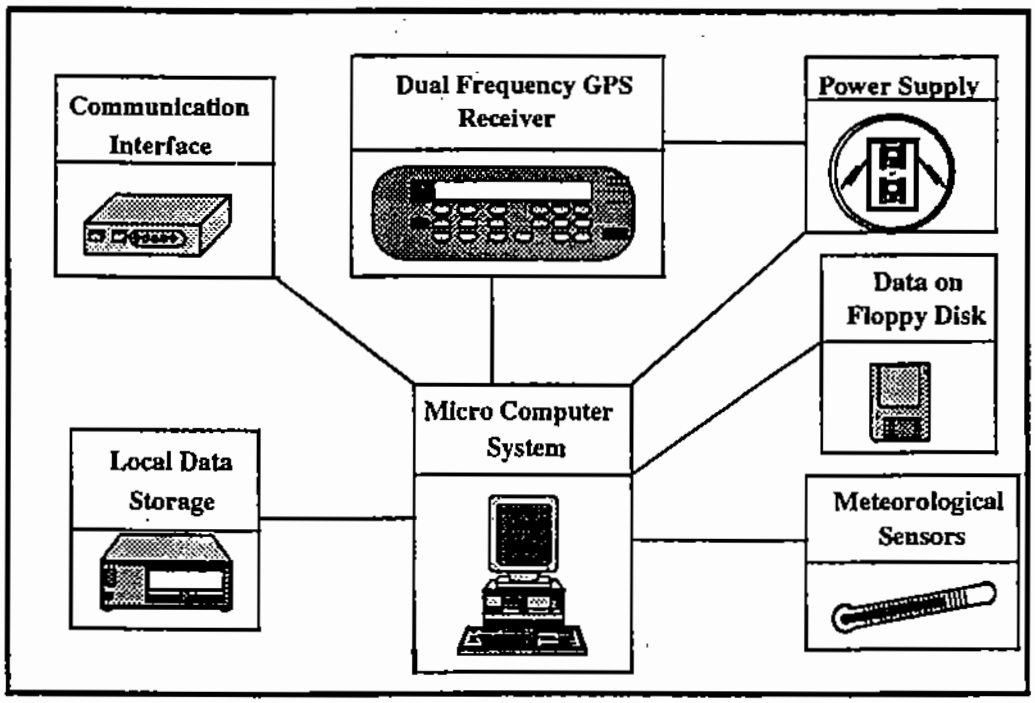

Figure 6.2 : Active Control Point Components

It is clear from the description of the system that a user with only one receiver can perform relative positioning and estimate the coordinates relative to the reference frame of the ACS. As such, there is no need to occupy an existing control point. The coordinates of the ACPs may be computed using the fiducial concept. The International GPS Service for Geodynamics (IGS) network may be thought of as a global ACS.

The Canadian ACS provides an example of a national ACS, the details of which have been reported by Delikaraoglou *et al* (1989). At the national level, the ACPs are spaced at about 500 Km (approximately 20 ACPs), providing the framework for the country. The provincial component will be more dense, with approximately 250 Km spacing. In British Columbia, the proposed ACS has an average station spacing of the order of 450 Km and is expected to satisfy all positioning requirements (Underhill *et al* ,1992).

6.4 The Brazilian Geodetic System

6.4.1 Present status

The Brazilian Geodetic System (SGB) has been developed and maintained by the Brazilian Institute of Geography and Statistics (IBGE). The levelling network of approximately 60,000 points has recently been readjusted. The horizontal network is composed of 6,209 points (3,498 triangulation points, 1,158 traverse points, 26 Hiran points, 384 Laplace points and 1,143 Doppler points) (Costa and Fortes, 1991).

The horizontal network is currently being readjusted using the software GHOST (Geodetic adjustment using Helmert blocking Of Space and Terrestrial data). This software is composed of a series of programs developed to adjust three-dimensional geodetic networks by the least-squares method, using the decomposition of the network into blocks (Helmert blocks). Measurements derived from GPS are planned to be introduced in the readjustment of the conventional horizontal network (Costa and Pereira, 1994). They will aid in the realisation of the Brazilian Geodetic System which is referenced to the South American Datum 1969 (SAD-69). This solution represents a preliminary answer to the Brazilian geodetic community.

The transformation from SAD-69 to the World Geodetic System of 1984 (WGS84) and vice-versa adopted in Brazil is realised only by 3 translation parameters (ΔX, ΔY and ΔZ). They were estimated from 24-days of Transit-Doppler data collected at the origin of the SAD-69 (Station CHUA) using precise ephemerides (Fortes *et al*, 1989). Recent assessment of the WGS84 coordinates of CHUA has shown an agreement of the order of 0.4 m with respect to the corresponding ITRF coordinates (Monico *et al*, 1994). This result is better than the expected accuracy of the WGS84, which is about 1 to 2 m. However, these translation parameters are expected to degrade as a function of distance from the origin of the reference frame. Considering that the conventional network provides a relative precision of the order of 10 ppm, the expected discrepancy at a point located for instance 1,000 Km away from the origin is about 10 m. An error of this order of magnitude in the absolute position of a station in the WGS84 may cause an error in the ellipsoid height difference of up to 2 ppm (see §2.7.4). Therefore, the Brazilian geodetic community should be aware and expect errors of this order or even worse when applying these transformation parameters at stations located far away

from the origin of the SAD-69. Once the readjustment of the SGB has been completed, better results might be obtained, depending on the precision of the realisation of the system.

6.4.2 Future Developments

The activities outlined in the previous section provided a short description of the current situation of the SGB. It is clear that for a more powerful use of GPS, additional solutions should take place. In terms of the passive control system, once the current adjustment is finished, a new readjustment is proposed by IBGE to be carried out around 1997. The adjustment will include GPS observations in areas of the network with weak geometry. A geocentric reference coordinate system, compatible with the recently created South American Geocentric Reference System (SIRGAS) will be used. The adjustment will include results of the GPS campaigns of the SIRGAS project in Brazil (Costa and Perreira, 1994; SIRGAS, 1994). The first SIRGAS campaign was held during May and June 1995.

Additionally, IBGE has proposed the establishment of a Brazilian Network for the continuous tracking of GPS satellites, referred to as RBMC (Rede Brasileira de Monitoramento Continuo). The proposed network, with some 9 tracking stations is illustrated in Figure 6.3. Details of the proposed network show that the network has some characteristics of an ACS (Fortes and Godoy, 1991; Fortes, 1991). From the configuration of the network, GPS users will place their receivers at a spacing of up to 500 km from the nearest station. Exceptions occur in the Amazon region and South of Brazil, where the separation can reach about 1,700 and 900 km respectively. This situation can be improved by the inclusion of some IGS stations located in South America, whose data are available at different IGS centres. In such cases, only static users can take advantage of this situation, because IGS data is not available in real-time. Figure 6.3 also shows the six IGS stations located in South America, besides those belonging to the proposed Brazilian GPS network. The station Fortaleza, which is located in the Brazilian territory, belongs to the Brazilian and IGS networks. The inclusion of stations Kourou, Arequipa, Bogota and La Plata may be useful because some regions of the Brazilian territory are closer to these stations than those of the Brazilian GPS network. In such a case, the maximum distance from the nearest station is about 900 km.

Considering the present situation and the future developments of the SGB, it is likely that a total support to the Brazilian GPS users can be reached. Once the Brazilian network becomes operational, it will represent the culmination of the Brazilian geodetic system. An ideal situation by that time would be to have the mapping system of Brazil and its National Grid transformed on the satellite datum (WGS84 or ITRF). This is a long term prospect, which requires all maps to be in digital form and then to carry out a massive transformation of all data involved. Therefore, the estimation of precise and reliable transformation parameters between the reference systems involved is essential to obtain the maximum benefits of this crucial task.

Figure 6.3 Proposed Brazilian GPS Network With Some IGS Stations

6.5 Assessment of the Expected Accuracy of the Brazilian GPS Network

The main aim of the Brazilian GPS network is to serve as a base and framework to support static relative positioning to an accuracy of the order of up to 0.1 ppm (Fortes and Gody 1991). Studies documented in GPS literature show relative accuracies even better than 0.1 ppm (Ashkenazi and Ffoulkes-Jones, 1990; Dong and Bock, 1989). To achieve this level of

accuracy, the fiducial GPS technique (§4.7) has to be used, which requires state-of-the-art software, such as GPS Analysis Software (GAS) developed at the Nottingham University (Stewart *et al*, 1994) and GPS Inferred Positioning System (GIPSY) of the Jet Propulsion Laboratory (JPL) (Blewitt, 1989).

Most users in Brazil will not have access to state-of-the-art software for data processing and will rely on the use of software supplied by the manufacturers. It was, therefore, necessary that some tests were carried out to try to simulate future scenarios in Brazil. The main objective was to assess the quality of the results obtainable by GPS users, with only one receiver, once the Brazilian GPS network becomes operational. The assumption is that the user will have access to GPS data of the (nearest) stations of the network, either via a communication link or off line via floppy disk. In both cases, only static positioning has been assessed.

6.5.1 Data Set and Processing Strategies

An ideal situation to perform the tests would require GPS data from Brazil. As this was not possible at the time of this research, data from Europe, available at Nottingham University was used. The data sets refer to the 1991 and 1992 GPS Campaign of the UK Tide Gauge GPS Project. It comprises 7 fiducial stations in Europe and 15 regional stations in the United Kingdom (Figure 6.4). Observations were taken during an 8-hour window, for 5 consecutive days with 20 dual frequency receivers. Tests have previously shown that these GPS data sets are of very high quality (Ashkenazi *et al*, 1993a).

The UK Tide Gauge 1991 data set was processed using the fiducial GPS technique and the results are described in Whitmore (1994). The ionospherically free (L0) observable was used and corrections applied for the tropospheric delay, antenna phase centre, earth body tides and ocean tide loading. The estimated coordinates of the stations were considered as the 'true' values. The result of this processing agrees quite well with the ITRF91N (Ashkenazi *et al*, 1993b).

In order to simulate the future scenarios in Brazil, tests were carried out for baselines ranging from 7 to 1,000 km. Such a range of baselines comprise most of the possible cases occurring in Brazil. It varies from an ideal condition (user close to the active control point) to the worst case, which involves a user

located approximately 1,000 km away from the nearest station. Table 6.1 gives the identification and lengths of the processed baselines. Whereas the fiducial network ('true' values) was processed using the 1991 campaign data, only data from the 1992 campaign was used in the processing of the baselines, providing a certain degree of independence between the two solutions.

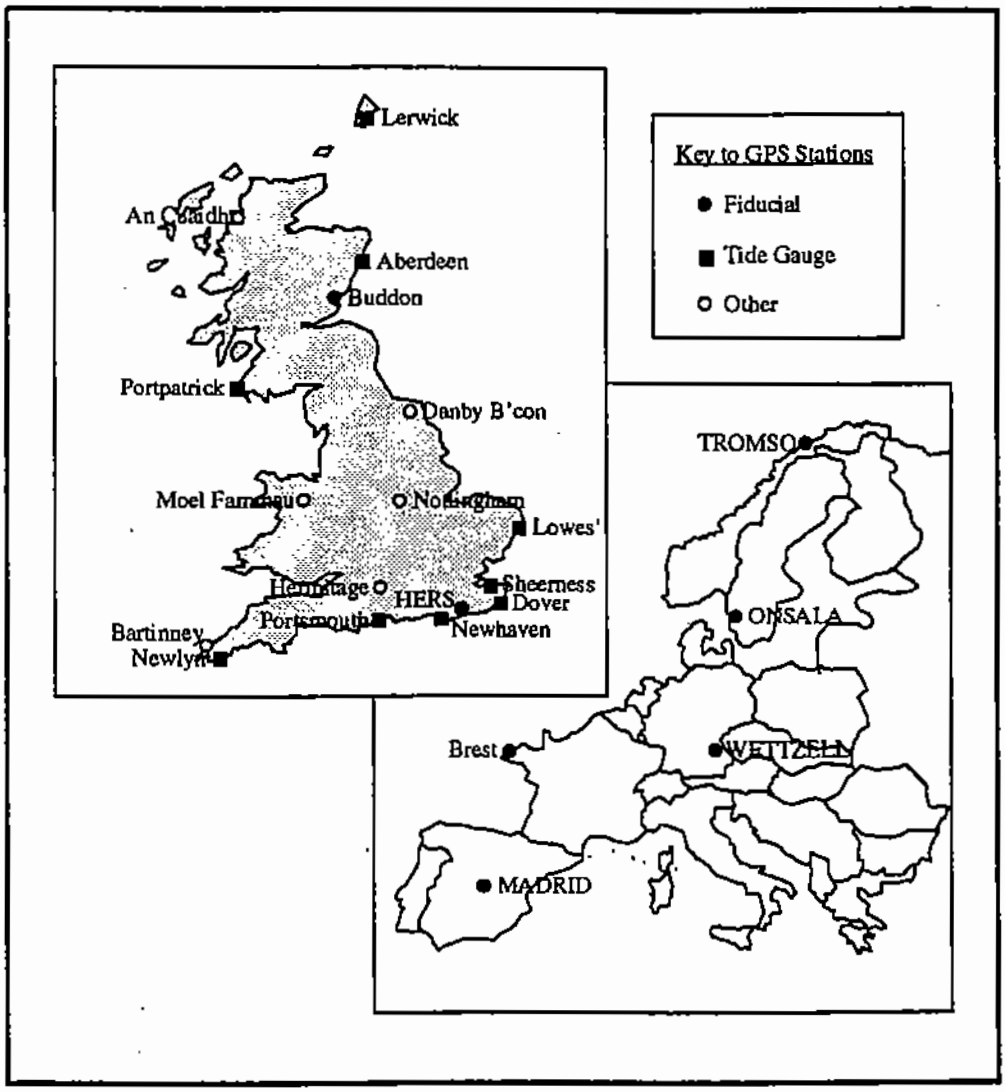

Figure 6.4: UK Tide Gauge GPS Network

The strategies were defined based on the fact that the users would be equipped with single or dual frequency receivers and accessing either broadcast or precise ephemerides. The results obtained from the baseline processing were compared with the assumed 'true' values, ie the results of fiducial network data processing. The differences between the 'true' and estimated values represent the strength of the recovery of each strategy. The processing was carried out

with the GPS Analysis Software (GAS) developed at the University Nottingham (§5.2).

Table 6.1: Lengths of the Baselines Processed

Baseline	Length (Km)
Newlyn-Bartinney	7
Newhaven-Hers	22
Dover-Sheerness	52
Buddon-Aberdeen	86
Sheerness-Lowestoft	133
Newlyn-Brest	203
Newlyn-Portsmouth	324
Dover-Danby Beacon	401
Dover-Newlyn	498
Dover-Portpatrick	598
Dover-Aberdeen	706
Newlyn-Aberdeen	815
Buddon-Onsala	898
Dover-Onsala	979

Table 6.2 gives the details of the scenarios tested. In the scenarios (a) and (b) the Jet Propulsion Laboratory (JPL) precise ephemerides were used. In the former case, the observable used was the ionospherically (Ion) free observable and in the latter, the L1 carrier phase observable. Scenarios (c) and (d) considered the ionospherically free and L1 carrier phase observables respectively, in conjunction with the broadcast ephemerides. For each test, data processing covering observation time spans of one, two and five hours was carried out. For all the tests, earth body tides and ocean tide loading corrections were not applied because of the assumption that most of the users will not have access to software providing these corrections.

Table 6.2: Scenarios Tested For the Proposed Brazilian GPS Network

Tests	Ephemerides	Observable
(a)	JPL precise	Ion-free
(b)	JPL precise	L1 carrier
(c)	broadcast	Ion-free
(d)	broadcast	L1 carrier

6.5.2 Results and Discussion

The baseline recoveries for the test using the JPL precise ephemerides and ionospherically free observable, which represents scenario (a) are illustrated in Figure 6.5. It can be seen (as expected) that better recoveries are obtained as more GPS data is involved in the data processing. The height component recoveries show the poorest results, followed by the east component.

The worst recoveries were of the order of 25 and 35 cm for the east and height baseline components respectively. In the former case such value was obtained with 2 hours of GPS data and in the latter, 1 hour of data was involved. With 2 and 5 hours of data, the recoveries of the height component were better than 15 cm for most of the baseline lengths. For all data span, the recoveries of the north component (better than 10 cm) were better than the east component (up to 25 cm). This is probably due to the fact that the GPS satellite provided a better geometry for the determination of the north component. The length component provided recoveries always better than 15 cm, for all data span and baseline lengths.

For the other tests carried out in order to try other user scenarios in Brazil, only the recoveries for the length and height components are presented. The former gives an indication of the quality in the three cartesians coordinates, and the latter generally represents the worst case of the three components. Therefore, if the recoveries derived from the tests taking into account these two components are acceptable, they are likely to be for the north and east components as well.

The recoveries for the processing with the JPL precise ephemerides and the L1 carrier phase observable (scenario (b)) are illustrated in Figure 6.6.

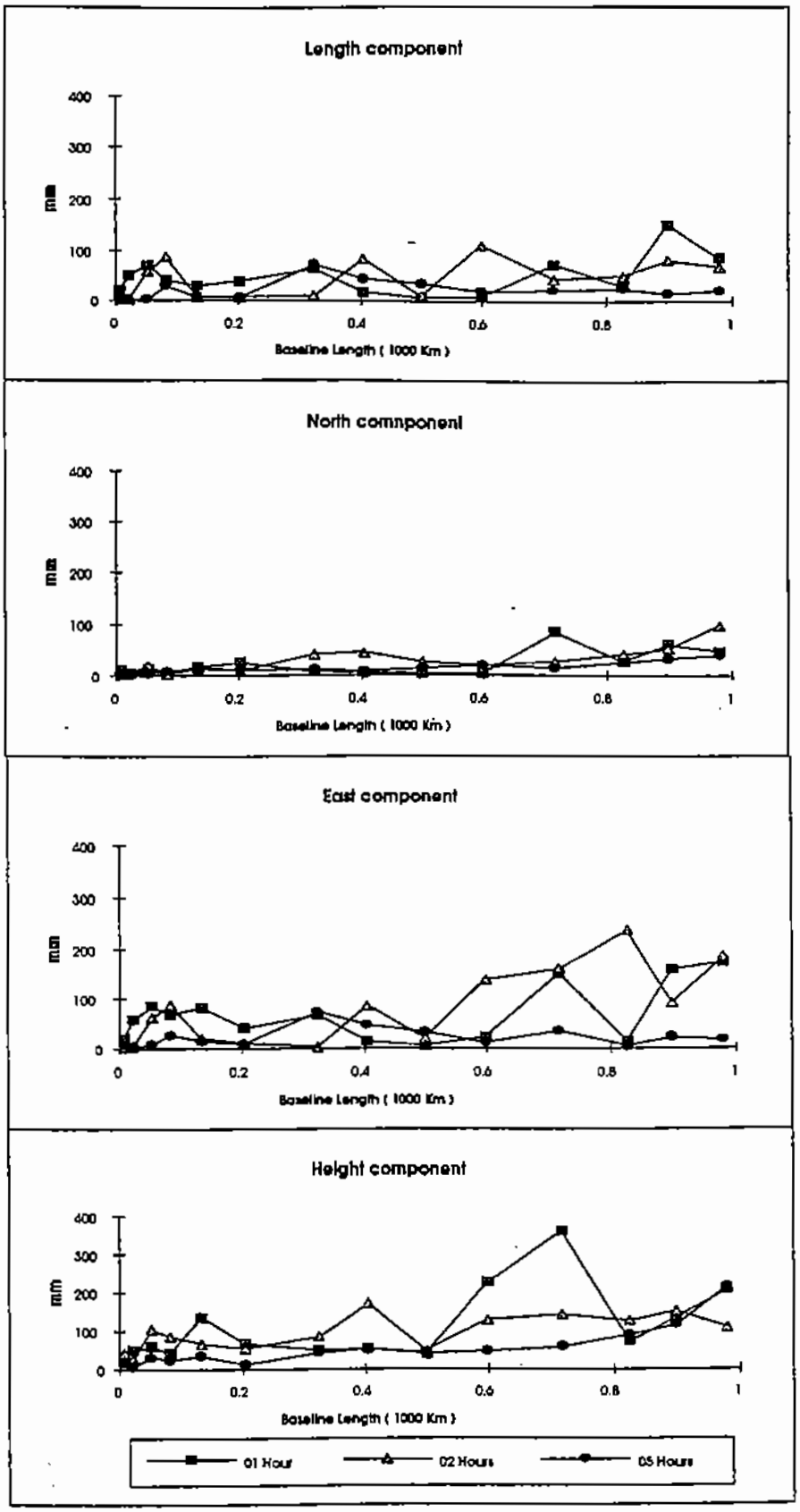

Figure 6.5: Recoveries for JPL Ephemerides and Ionospherically Free Observable

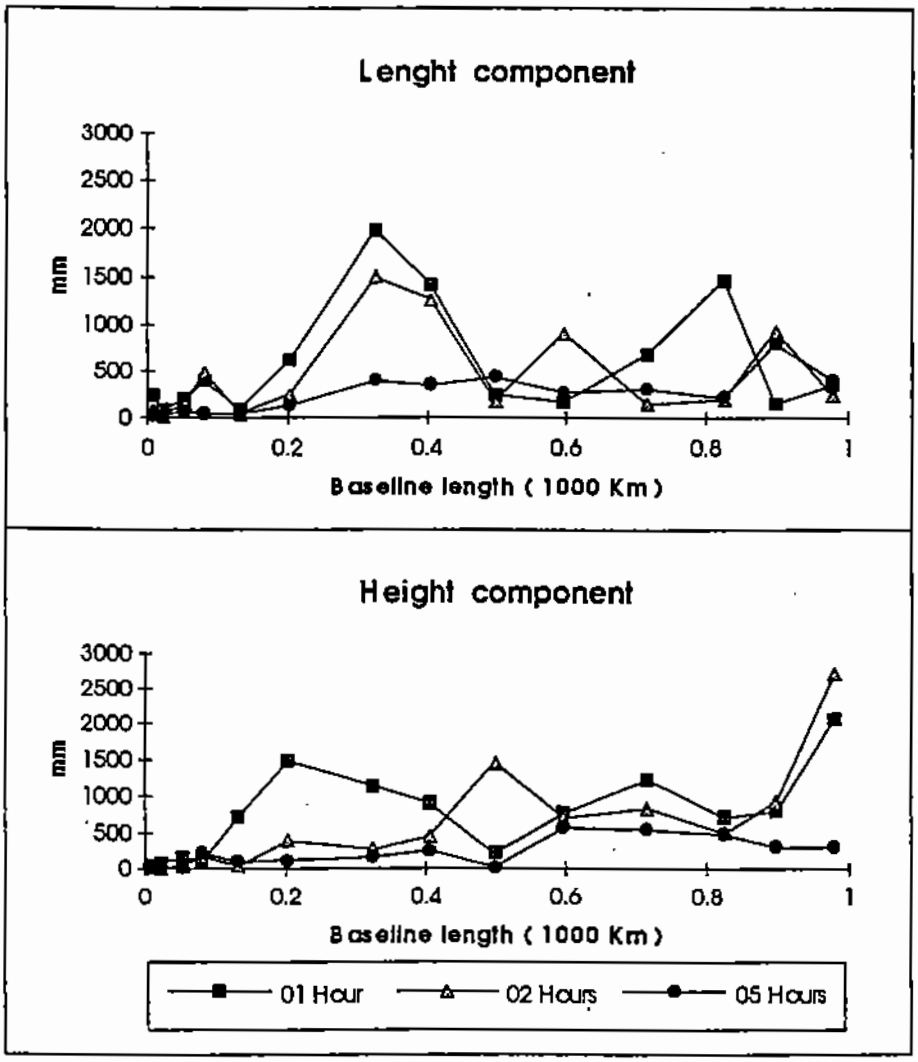

Figure 6.6 : Recoveries for JPL Ephemerides and L1 Observable

Considering scenario (b), which is illustrated by Figure 6.6, it can be seen that for shorter periods of observation, the recoveries for baselines longer than 50 km deteriorate. For longer baselines, the recoveries for one and two hours of data are very inconsistent. It is due to the effects of the ionosphere which were not taken into account and do not cancel out over long baselines, neither they average out over short period of observations. For a longer period of observation (5 hours), the height component recoveries reduce from 2.5 m to about 50 cm and from 2.0 m to about 80 cm for the length component. The recoveries of the latter were on average 40 cm.

The recoveries of the tests carried out with broadcast ephemerides and ionospherically free (scenario (c)) and L1 carrier phase observables (scenario (d)) are illustrated in Figures 6.7 and 6.8, respectively.

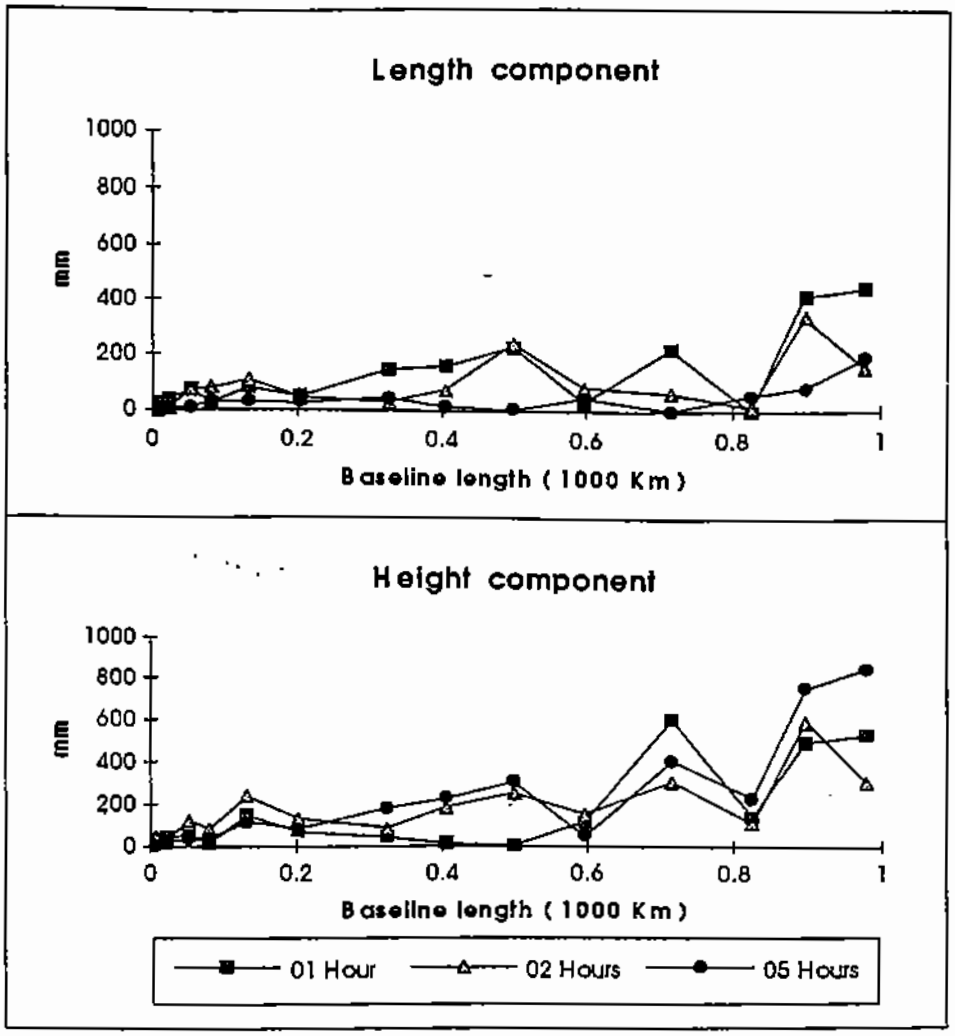

Figure 6.7: Recoveries for Broadcast Ephemerides and Ionospherically Free Observable

As expected, the recoveries of the tests with broadcast ephemerides, illustrated by Figure 6.7 and 6.8, are worse than those with the precise ephemerides, since the same observable is taken into account. The effects on the recoveries are more significant for baselines longer than 100 Km, in which the errors of the broadcast ephemerides are not cancelled out. The height component recoveries for scenario (c), (see Figure 6.7) reach about 80 cm in the data processing with 5 hours of data. The length component recoveries reach at maximum 20 cm. One can observe that with data span of 1 and 2 hours, the height component recoveries are generally better than those of 5 hours. It is due to the fact that the broadcast ephemerides were used beyond the 'valid' interval (2 hours) in the longer data span.

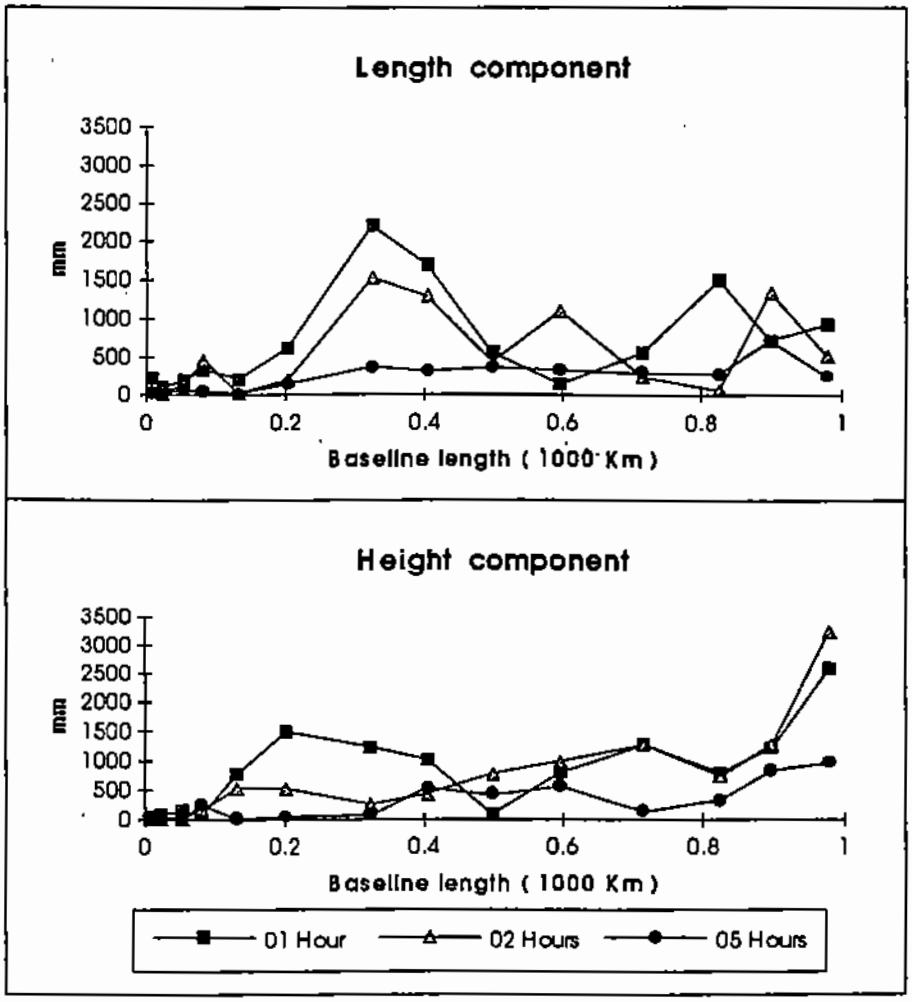

Figure 6.8: Recoveries for Broadcast Ephemerides and L1 Observable

The test of scenario (d), ie broadcast ephemerides and the L1 carrier phase (Figure 6.8) demonstrated that considering 1 hour of data the recoveries of the height component can reach, for the longer baselines, almost 3 m. They reduce to better than 1 m for data span of 5 hours. The recoveries of the height components for the shorter intervals do not behave as in the previous scenario (ie shorter interval with better recoveries than those of longer intervals), because the ionospheric effects, which where not taking into account in this scenario, are more significant than the errors of the broadcast ephemerides beyond the 'valid' interval. The ionospheric effects do not average out over short intervals. For the length component, the recoveries reach 2 m for 1 hour of data and reduce to better than 1.50 m and 50 cm for 2 and 5 hours respectively.

In order to obtain a more convenient description of the results, a linear fit through the recoveries of length and height components obtained from all the

tests was carried out. The resulting values, which are given in Table 6.3, provide an average value of the repeatabilities as function of the baseline length.

Table 6.3 : Linear Fit of the Baseline Recoveries for the Different Scenarios

	Length Component			Height Component		
Scenarios	1 Hour	2 Hours	5 Hours	1 Hour	2 Hours	5 Hours
ION-FREE and Precise Ephem.	0.1 ppm	0.1 ppm	0.08 ppm	0.22 ppm	0.17 ppm	0.13 ppm
L1 and Precise Ephem.	1.0 ppm	0.8 ppm	0.6 ppm	1.5 ppm	1.5 ppm	0.5 ppm
ION-FREE and Broad. Ephem	0.3 ppm	0.2 ppm	0.1 ppm	0.4 ppm	0.4 ppm	0.6 ppm
L1 and Broad. Ephem.	1.3 ppm	1.0 ppm	0.5 ppm	1.8 ppm	1.9 ppm	0.7 ppm

The values given in Table 6.3 show recoveries, for 1 hour of data, in the range of 1.3 to 0.1 ppm and 2 to 0.1 ppm for the length and height components respectively. With a single frequency receiver collecting 1 hour of data, precision better than 2 ppm is expected for height, and 1.3 ppm for length, independently of using either broadcast or precise ephemerides. With 5 hours of data, such values reduce to about 1 ppm. Once 1 hour of data of a dual frequency receiver is used in conjunction with the precise ephemerides, precision better than 0.2 ppm for the length and height components has been demonstrated. Both components do not improve significantly by increasing the interval of data collection. Dual frequency receiver, broadcast ephemerides and 1 hour of data collection have shown results better than 0.4 ppm for the length and height components. The latter became worse for longer intervals due to the fact that the broadcast ephemerides were being used beyond the valid interval.

The values given in Table 6.3 show the expected accuracies that can be obtained by a GPS user equipped with only one receiver in a region with an ACS, taking into account four different scenarios. Once the Brazilian GPS network becomes operational, relative positioning accuracies at these levels are expected for baseline data processing. However, as the tests were carried out using data from Europe, it would be advisable to repeat some of these tests

using data from Brazil, once they are available. The data collected during the recent SIRGAS campaign (May-June 1995) may be used (§6.4.2) and all factors that are position dependent (ionosphere, troposphere, etc.) have to be taken into account.

It has to be pointed out that although the results of the data processing using only a single baseline have provided very high precision, they are not very reliable. Therefore, the concept of reliability within the context of an ACS must be further investigated.

6.6 Summary

The solutions adopted by some countries in the provision of geodetic networks for supporting GPS activities have been described. It has been found that the general tendency is the establishment of new passive networks, retaining some stations of the conventional network, in order to provide a set of parameters to realise the transformation between the two systems. However, the state-of-the-art geodetic network is the so-called Active Control System (ACS). The ACS provides users equipped with only one receiver with the capability of relative positioning without occupying any control point. The proposed Brazilian GPS network has some characteristics of an ACS

Tests have been carried out to assess the expected accuracy that can be obtained by a user of the Brazilian GPS network (RBMC) equipped with only one receiver and accessing GPS data from the nearest station. Four scenarios were tested, taking into account the ephemerides accessed (broadcast or precise) and the receivers used (single or dual frequency). Furthermore, the period of data collection was also considered, but restricted to 1, 2 and 5 hours. The expected accuracies, computed from a linear fit through the recoveries of all the tests are given in Table 6.3.

Chapter 7

ANALYSIS OF THE IGS EPOCH '92 CAMPAIGN IN BRAZIL

7.1 Introduction

The permanent GPS network of the International GPS Geodynamics Service (IGS) provides a global data set of GPS measurements. The 1992 IGS Test Campaign was held from 21 June to 23 September 1992 and the intensive observation campaign, referred to as Epoch '92 from 27 July to 9 August 1992. The Brazilian participation in the IGS Epoch '92 campaign was as a Regional Centre (Bergamini, 1993). The aim was to cooperate with the international scientific community, and to provide GPS data to the geodetic community in Brazil in order to establish new GPS control stations into a global reference frame.

Three stations belonging to the proposed Brazilian GPS network for continuous tracking of GPS satellites (§6.4.2) were continuously occupied for 14 days of the IGS Epoch '92 campaign. An initial realisation of the new Brazilian reference frame can therefore be performed, which can be integrated into a global reference frame. Additionally, four stations located in São Paulo State collected GPS data for a local project. Each of these four stations was occupied for a period of 3 hours, for each of 2 days. The station CHUA, origin of the South American Datum 1969 (SAD-69), was occupied for a whole day.

In order to integrate the Brazilian stations into a global reference frame, such as the IERS (International Earth Rotation Service) Terrestrial Reference Frame (ITRF), the collected GPS data was processed jointly with GPS data from IGS stations which form part of the ITRF. These stations included Santiago in Chile, and Goldstone and Richmond in the United States. The results obtained will enable the assessment of the quality of the World Geodetic System 1984 (WGS84) coordinates of the station CHUA, which is the base station for most of the GPS activities in Brazil.

The processing and analysis of the IGS Epoch '92 in Brazil is the main topic of this Chapter. The quality of the results has been assessed by the repeatabilities of the baseline components and the recoveries of known station coordinates, which were estimated in the adjustment. Analysis of the estimated variance factor ($\hat{\sigma}_0^2$) of the network adjustment has been used to assess the mathematical models applied. Such investigation was carried out in order to achieve the highest accuracy for the Brazilian stations.

At the beginning of the author's research, the software available at Nottingham (GPS Analysis Software - GAS) did not allow the processing of very large networks (§5.3). At that stage, the processing of the Brazilian GPS network had to be carried out as two sub-networks, which is referred to as 'Quasi-Network' processing. Once the capability of GAS was enhanced to process global GPS networks (§5.4.2), the processing was repeated for the full network. The results of these two approaches are described in this Chapter.

The effects of earth body tides (EBT) were investigated by considering their influence on the repeatabilities and recoveries of the solutions, when processing different periods of data. Over long baselines, such effects should be significant but may be reduced over a certain period of observation. Otherwise, a model should be used to apply such corrections to the observations. The EBT effects, if not corrected may be absorbed by some other parameters in the model. The zenithal scale factor for tropospheric delay has been modelled by using a polynomial of first and second order, in order to investigate the absorption of EBT effects by these models.

Some stations involved in this processing are located near the ocean. It is well known that ocean tide loading (OTL) effects are more significant at stations located near the ocean than on continental ones. In order to investigate the OTL effects on the results, the network was processed by applying or not applying OTL corrections.

7.2 The International GPS Geodynamics Service (IGS)

The IGS is a permanent international service established in 1990 by the International Association of Geodesy (IAG). The primary goals of the IGS are (Mueller, 1993) :

(i) to provide the scientific community with high quality GPS orbits,
(ii) to provide earth rotation parameters of high resolution,
(iii) to expand geographically, the current ITRF maintained by the IERS and
(iv) to monitor the global deformations of the earth's crust.

The IGS accomplishes its mission through a set of functional components, which are shown in Figure 7.1.

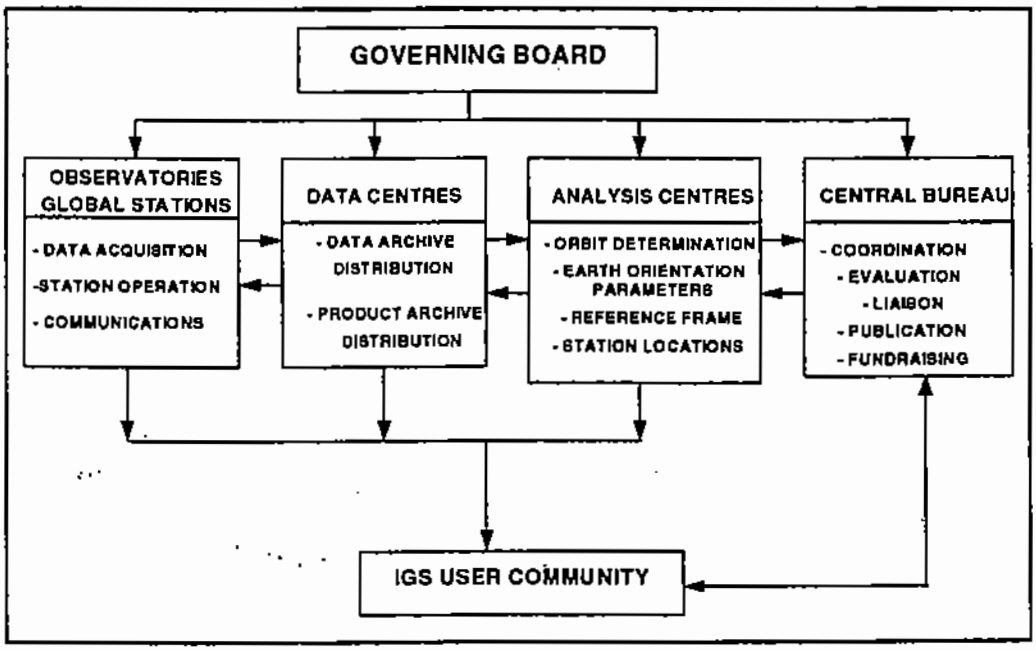

Figure 7.1 : Organisation of the IGS

The data centres are divided into three categories: operational, regional and global. The operational data centres are in direct contact with the tracking stations and provide quality control of observation sites, besides transmitting the data to regional or global data centres. A regional data centre collects data from several operational data centres, maintains a local archive of the data received and transmits the data to the global data centres. The main interfaces to the analysis centres and the user community are the global data centres. They relay global data to the analysis centres and provide archive functions.

The analysis centres receive and process tracking data from one or more data centres (core and fiducial stations) for the purpose of producing IGS products such as GPS ephemerides, earth rotation parameters and site coordinates. The products are delivered to the global data centres and to the IERS.

The Central Bureau (CB) coordinates and manages the services of the IGS consistent with the directives and policies set by the Governing Board (GB). Major responsibilities include liaison with external organisations, product distribution, and information dissemination. The GB exercises general control over the activities of the service.

The network of tracking stations consists of about 42 core stations (Figure 7.2) and 150 - 200 fiducial stations[7.1] . A core station is equipped with a P-code receiver, which complies with the IGS standards and is capable of delivering data within a specific time period to the data centres (normally 24 hours). The fiducial stations are occupied at certain epochs for the purposes of extending the terrestrial reference frame all over the globe and to monitor deformations.

In order to evaluate the concept of the service, a test campaign was carried out, which is referred to as 1992 IGS Test Campaign. Within this campaign, the intensive Epoch '92 campaign was conducted. The main purpose of 1992 IGS Test Campaign was to check the ability of participating institutions to produce orbits regularly. Observations were collected from 21 June to 23 September 1992 with a design network of about 30 globally distributed core stations (Beutler, 1993). During this period the IGS Epoch '92 Campaign was conducted from 27 July to 9 August 1992, with about 100 fiducial stations distributed all over the world.

7.3 IGS Epoch '92 Campaign in Brazil

The Brazilian participation in the IGS Epoch '92 campaign involved a Regional Centre (Bergamini, 1993). It included several institutions, notably the Federal University of Paraná (UFPr), the Brazilian Institute of Geography and Statistics (IBGE), the University of São Paulo (USP), the Paulista State University (UNESP) and the National Institute for Space Research (INPE). The main objectives of the participation were to cooperate with the international scientific community, and to provide GPS data to the geodetic community in Brazil, for the establishment of new GPS control stations. The stations occupied during the campaign can be integrated into a global reference frame.

[7.1] Fiducial stations in the sense that they are tied to the global network and the resulting reference frame an coordinate system

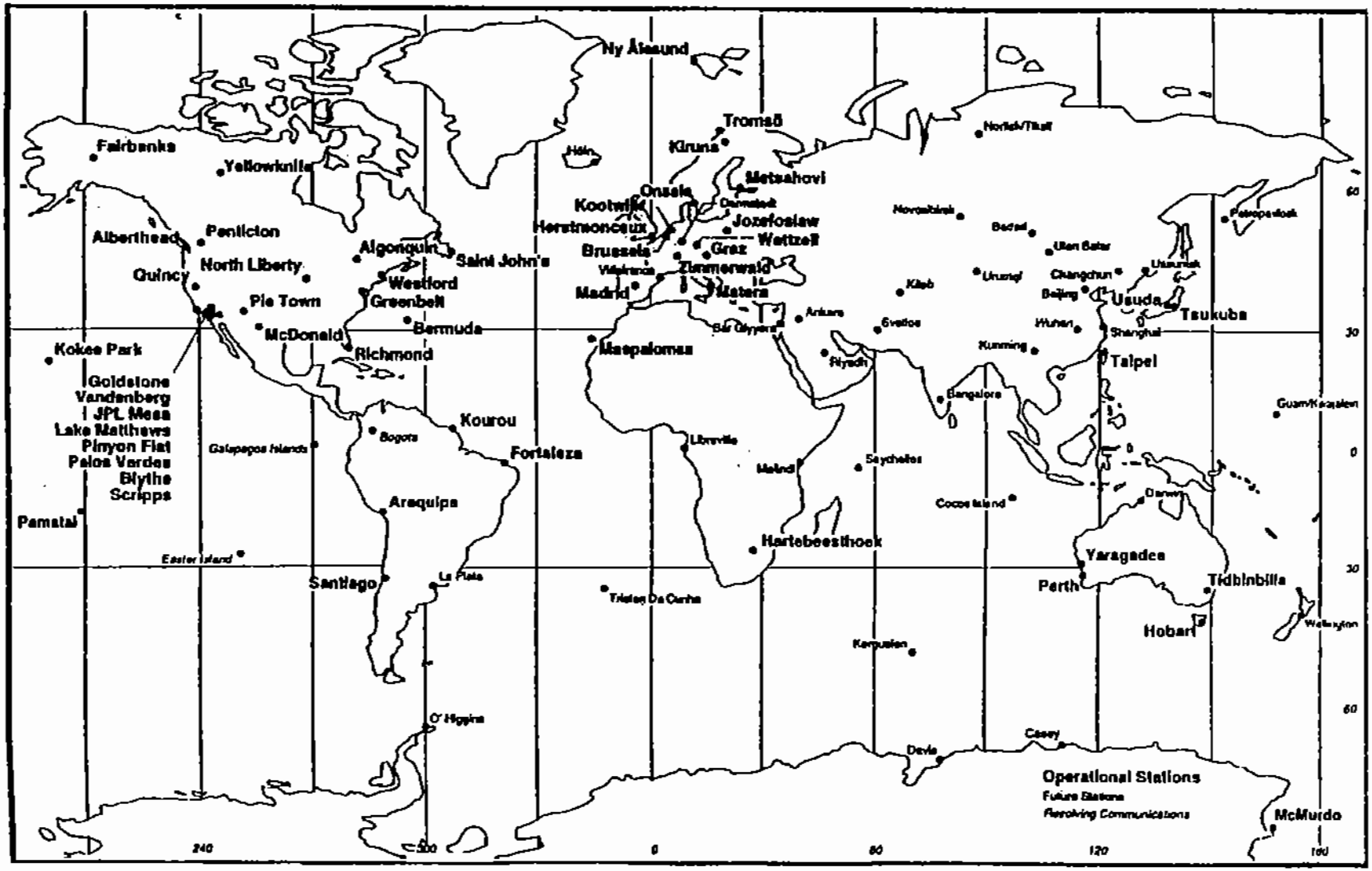

Figure 7.2 : IGS Network Core Stations

Three stations (Paraná, Presidente Prudente and Brasilia) were continuously occupied during the 14 days of the IGS Epoch '92 campaign. These stations belong to the proposed Brazilian GPS network for continuous tracking of GPS satellites (RBMC). A further four stations in the state of São Paulo (Taquarussu, Ilha Solteira, Avanhandava and Salto Grande) were also occupied for a local project. Each of these four stations was occupied for a period of 3 hours, for each of 2 days. The station CHUA, origin of SAD-69, was also occupied, but for a whole day.

In order to integrate the stations occupied in Brazil during this campaign into an a global reference frame, the collected GPS data was processed jointly with GPS data from IGS stations outside Brazil, which form part of the ITRF. These stations included Santiago in Chile, and Goldstone and Richmond in the United States. Figure 7.3 shows the locations of the stations that were involved in the processing of the IGS Epoch '92 campaign in Brazil.

Figure 7.3: Brazilian Epoch '92 Campaign

7.3.1 GPS Data Sets

Although the IGS Epoch' 92 campaign involved 14 days of tracking data, no more than 7 days for each of the Brazilian stations were included in the

processing. This was based on the typical periods of occupation used for large regional campaigns designed to monitor deformation (Ashkenazi *et al*, 1994; Blewitt *et al*, 1994). It was also thought to be an amount of data that could be processed and analysed within the period of the author's research. The stations and the amount of data used to define a Brazilian High Precision Network (Brazilian HPN) are listed in Table 7.1. The receiver at station PARA was a Trimble 4000 SST (L1 and L2 carrier-phase with P-code). All of the other receivers of the Brazilian stations were Trimble 4000 SLD with C/A-code (squaring type). The stations outside Brazil (SANT, RCM2, GOLD), were equipped with Rogue receivers (RN8). All measurements were recorded at an interval of 30 seconds.

Table 7.1 Stations and Data Sets in the Brazilian HPN

Name	Site location	Data Processed (Julian Day)	Receiver
BRAS	Brasilia - DF, BR	208-213 and 218 24 hours/day	Trimble
PARA	Curitiba - PR, BR	208-213 and 218 24 hours/day	Trimble
UEPP	P.Prudente-SP, BR	208-213 and 218 24 hours/day	Trimble
AVAN	Avanhandava-SP, BR	210 and 209 3 hours/day	Trimble
ILHA	Ilha Solteira -SP BR	210 and 211 3 hours/day	Trimble
TAQU	Taquarussu- SP, BR	208 and 211 3 hours/day	Trimble
SALT	Salto Grande-SP, BR	208 and 209 3 hours/day	Trimble
CHUA	Minas Gerais, BR	218 - 24 hours	Trimble
SANT	Santiago -Chile	208-213 24 hours/day	Rogue
RCM2	Richmond - USA	208-213 24 hours/day	Rogue
GOLD	Goldstone - USA	208-213 24 hours/day	Rogue

A sample of 12 independent baselines and their corresponding lengths in km are listed in Table 7.2. They give an indication of the spread of the baseline lengths involved in this processing.

Only three of the stations, all outside Brazil (SANT, RCM2 and GOLD), had known ITRF coordinates. Although two of these three stations are a very long distance away from the Brazilian stations, they were nevertheless used as fiducial stations, because of a lack of better alternatives. In such a case, however, there are a reduced number of satellites (about 2 or 3) being simultaneously tracked by both stations on a long baseline (about 8000 km). The baseline components may be poorly estimated because the number of

double differences will also be reduced. Besides this, the effects of the satellite orbit errors on the baseline components increase with baseline length.

Table 7.2 - Length of the Processed Baselines

Baselines	Length (km)	Baselines	Length (km)
SANT-PARA	2,234	UEPP-SALT	168
PARA-UEPP	430	CHUA-UEPP	432
UEPP-BRAS	777	CHUA-PARA	640
UEPP-ILHA	193	CHUA-BRAS	423
UEPP-AVAN	166	BRAS-RCM2	5,593
UEPP-TAQU	77	BRAS-GOLD	8,438

At the time of the campaign, the GPS constellation consisted of 18 operational satellites (3 Block I and 15 Block II satellites), and Anti-Spoofing (AS) was turned off during the days included in the processing.

7.3.2 Reference Frame and Precise Ephemeris

For the connection to a global reference frame, the coordinates of IGS stations (SANT, RCM2 and GOLD) had to be constrained to their known values, once they had been transformed to the epoch of the campaign. These coordinates were taken from a global fiducial-free GPS processing of data for the periods: January to February 1991, and June 1992 to September 1993. The epoch of the solution refers to 1 July 1992 (Blewitt *et al*, 1993a). This solution is hereafter referred to as the IGS solution. It agrees with the ITRF92 (IERS Terrestrial Reference Frame of 1992) to within 12 millimetres after applying a 14-parameter transformation[7.2]. The coordinates of these three stations were also taken from the ITRF93 at epoch 1993.0 and mapped to the epoch of the campaign (1 July 1992) by using the ITRF93 velocity field (Boucher *et al*, 1994). Table 7.3 lists the station coordinates at both reference frames and the antenna heights. The antenna height of station GOLD refers to the top of the choke ring (TCR) in the IGS solution and to the bottom (BCR) in the ITRF.

The precise ephemerides used in this processing were derived by the Jet Propulsion Laboratory (JPL) in Pasadena, CA, using GPS data from the core stations observed during the IGS Epoch '92 campaign.

[7.2] A 14-parameter transformation involves the usual 7 parameters and their rates.

Table 7.3: IGS and ITRF93 Coordinates of the IGS Stations on 1 July 1992

Station	X (m)	Y (m)	Z (m)	Antenna Heights (m)
	IGS Solution			
SANT	1 769 693,271	-5 044 574,138	-3 468 321,143	0.143
RCM2	961 318,983	-5 674 090,965	2 740 489,584	0.142
GOLD	-2 353 614,110	-4 461 385,476	3 676 976,518	-0.021
	ITRF 93			
SANT	1 769 693,221	-5 044 574,121	-3 468 321, 112	0.143
RCM2	961 318,955	-5 674 090,992	2 740 489,606	0.142
GOLD	-2 353 614,121	-4 461 385,404	3 676 976,485	0.049

7.4 Processing Strategies

The GPS Analysis Software (GAS) (§5.2) was used to process the data collected during the IGS Epoch '92 campaign in Brazil. At the preliminary stage of the author's research, the complete processing of the network was not possible with the version of the GAS software available at that time. The concept of base satellite (§3.3.3) was a unique option available in the software for the formation of double difference observable, and the same base satellite had to be applied to all baselines. However, over the Brazilian HPN (Figure 7.3), the satellite constellations were different at both extreme ends of the network. This concept therefore, was not valid in this case.

The initial solution was to process the network as two sub-networks. Sub-network (a) consisted of stations SANT, PARA, UEPP and BRAS (24 hours of data) and those stations with only 3 hours of data (SALT, ILHA, TAQU, AVAN). Sub-network (b) is composed of stations BRAS, GOLD and RCM2. This is referred to as 'Quasi-network' solution.

Once the capability of processing global GPS networks was implemented in GAS (§5.4.2), the complete network was processed simultaneously. This is referred to as the 'Full network' solution. This has provided the opportunity to compare the differences between the two approaches in this thesis.

The JPL precise ephemeris used in the processing did not contain the satellite clock errors. Therefore, the first stage of the pre-processing was to insert the

ephemeris clock values, given in the broadcast ephemerides into the precise ephemeris by using the CON2SP3 (CONvert to SP3 format) program (§5.2.1). In the next stage, the FILTER program (§5.2.1) was used to convert GPS data in RINEX format to the Nottingham (NOT) format used in GAS. During the data conversion, FILTER was also used to detect and approximately correct large cycle slips in the carrier phase by comparing the change in the phase and pseudorange measurements at adjacent epochs. In addition, a point positioning pseudorange solution was performed for all the stations, which provides a preliminary indication of the quality of the data sets and receiver clock offsets. Furthermore, each 24 hour of data was converted into two sessions of 12 hours, for easy manipulation of data.

Once the data was converted to the NOT format and the independent baselines defined, the detection of cycle slips and outliers was performed by using the PANIC program (Program for the Adjustment of Network using Interferometric Carrier phase) in the cleaning cycle slip mode. The ionospherically free (L0) and widelane (L3) observables were used for this purpose. A tropospheric model was also applied. The Magnet model was used and a zenithal scale factor per station (first order polynomial) was included as an unknown in the adjustment. This is essential during the pre-processing of long baselines because the tropospheric effects are significantly different at each station and do not cancel out in the baseline processing, making the detection of cycle slips and outliers difficult.

With the baselines cleaned of cycle slips, the PANIC program was run to perform the network adjustment. The satellite positions were fixed to values given by the JPL precise ephemeris. The reference frame was defined by constraining the coordinates of the selected IGS stations to the known (IGS or ITRF93) coordinates, with corresponding standard errors. At this stage, several options and models can be selected for data processing using GAS. This allows for the analysis of the relative merits and demerits of different models.

For all of the tests carried out, the observable was the linear combination (L0) of L1 and L2 carrier phases (§3.3.1) referred to as the ionospherically free observable, which greatly reduces the part of the dispersive delay due to the ionosphere. The tropospheric refraction was modelled by using the Magnet model (§2.7.2). Within Magnet, a zenithal scale factor per station was generally modelled as a first order polynomial, and estimated as unknown parameters in

the network adjustment. Whenever applied, earth body tides (EBT) and ocean tide loading (OTL) corrections followed the IERS standards (McCarthy, 1992).

The processing of each session led to a coordinate solution with its respective covariance matrix. These solutions were combined together using the CARNET (CARtesian NETwork adjustment) program(§5.2.3), producing a set of weighted mean values. The repeatabilities of the results, which give an indication of the consistency of the results (precision) was computed by using the REPDIF (vector REPeatability DIFerences) program (§5.2.3).

7.5 Data Pre-Processing

At the pre-processing stage, a high drift in the oscillators of the C/A-code Trimble receivers stationed at São Paulo State stations, CHUA and BRAS was detected. The clock drift for a period of approximately 24 hours of each of the four receivers used is illustrated in Figure 7.4 as a function of the GPS time of week (ToW). The oscillator drift of the C/A-code Trimble receiver at station UEPP was beyond 0.1 seconds after 24 hours. At station BRAS, the drift was slightly lower than that at station UEPP. This behaviour was similar during the other days, at both stations. With such a level of drift, the pseudorange observation values were unusual, and sometimes negative in value. The performance of the oscillator of the P-code Trimble receiver, (station PARA), was much better. The drift of the Rogue receiver oscillator was similar for all the three stations equipped with this kind of receiver (GOLD, SANT and RCM2). Figure 7.4 illustrates the drift of the Rogue receiver oscillator at station SANT, and reflects the behaviour of a very stable oscillator.

The double difference observable eliminates the effects of the receiver clock. However it should be pointed out that to compute the satellite positions at the instant of transmission of the signal, the receiver clock error is used in GAS. The high drift of the Trimble C/A-code receiver oscillators is not a problem if the clock correction is computed with a precision of the order of 10^{-6} seconds or better. This precision is normally obtained with pseudorange observation, in which the receiver clock error is estimated in the solution.

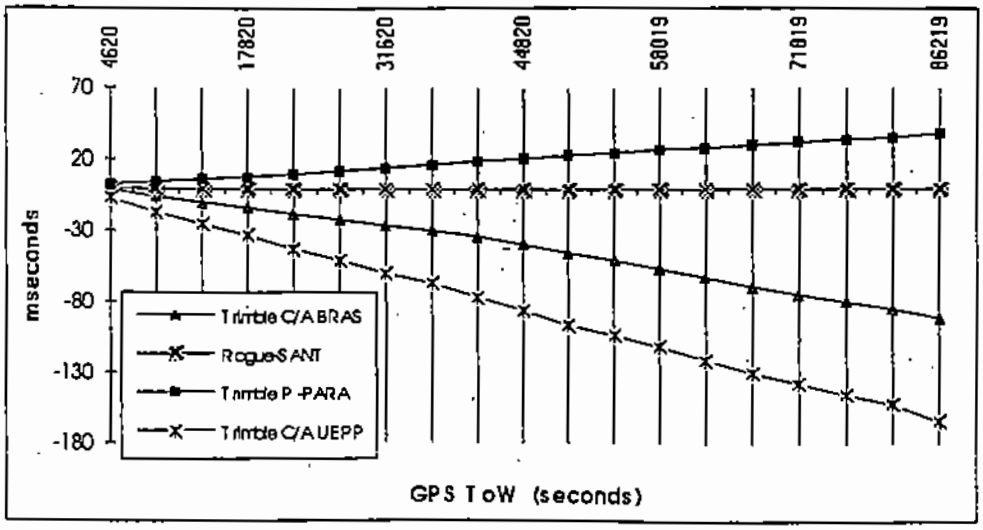

Figure 7.4: Clock Drift From Pseudorange Point Positioning

In sub-network (a), the conversion of RINEX to NOT format adopted a 60 seconds interval whilst in sub-network (b), the original interval (30 seconds) was maintained. The main reason for doing this was to reduce the quantity of data in sub-network (a) and to maintain all of the data in sub-network (b), which comprises the two longest baselines and therefore, with not so many simultaneous measurements. However, for the complete adjustment of the full network, the data interval had to be the same for all baselines. In this case, it was advisable to use the original 30 seconds interval.

Increasing the sampling rate improves the precision of the baseline components, but the main factor is related to the satellite geometry during the period of data collection. During a period of observation, the geometry dependent factor will be approximately the same, for different sampling intervals, since they are not very long. It has been shown that the effects of increasing the sampling rate on the precision of the baseline components are 12/k (Teunissen and Van der Marel, 1992), where k is the number of epochs with at least two satellites being simultaneously tracked at both ends of a baseline. For short periods of observation or long baselines (few double differences), it is therefore important to include all observations in the processing.

The number of double difference observations involved in the processing of the Julian day 208 is listed in Table 7.4. They refer to the processing involving the two sub-networks and only baselines with 24-hour of GPS data are listed. For the other days, the number of observations is quite similar. It is important to

note that the two longest baselines (BRAS-GOLD and BRAS-RCM2), were processed using the original data collection interval (30 seconds) whereas the other baselines were processed with 60 seconds interval. The reduction of the number of observations in the two longest baselines (BRAS-GOLD and BRAS-RCM2) is very significant. The components of these two baselines should, therefore, be poorer estimated than the others.

Table 7.4: Number of Double Difference Observations at the Julian Day 208

Baseline	Number of DD	Baseline	Number of DD
SANT-PARA	3, 232	PARA-UEPP	3, 903
UEPP-BRAS	3, 771	BRAS-RCM2	2, 128
BRAS-GOLD	732		

The baselines given in Table 7.2 were pre-processed in order to detect and repair cycle slips. High precision GPS-based geodesy requires reliable detection of and, where possible, correction of integer discontinuities of the carrier phase. This is therefore one of the most important part of the whole processing. The detection and repair of cycle slips on baselines involving Trimble C/A-code receivers was very time consuming. This was due to the fact that the squaring technique is used in these receivers, producing half wavelength on the L2 carrier phase (§2:4.2). Furthermore, the ionosphere effects may also have contributed to this problem. In the equatorial region, where most of the stations of the network are located, the ionosphere effects on GPS measurements are worse than in the mid-latitude region (Warninger, 1993). Additionally, during the IGS Epoch '92 campaign, the solar cycle was in a period of maximum solar activity, making the correction of the cycle slips even more difficult.

Figure 7.5 illustrates the effects of the ionosphere during this campaign on a specific (cleaned) baseline and day (Julian day 208) by the double difference residuals of the widelane (L3) observable. Maximum residuals amount to 1.5 cycles of L3 (129 cm). On the basis of the results obtained by Warninger (1993), even larger values were expected. In his example, the L3 residuals exceeded 0.5 (43 cm) cycles for six out 24 hours, for a 10 km baseline in southern Brazil. The magnitude of double difference residuals caused by ionospheric refraction is, in the first approximation, proportional to the baseline length. The baseline length illustrated in Figure 7.5 is 777 km.

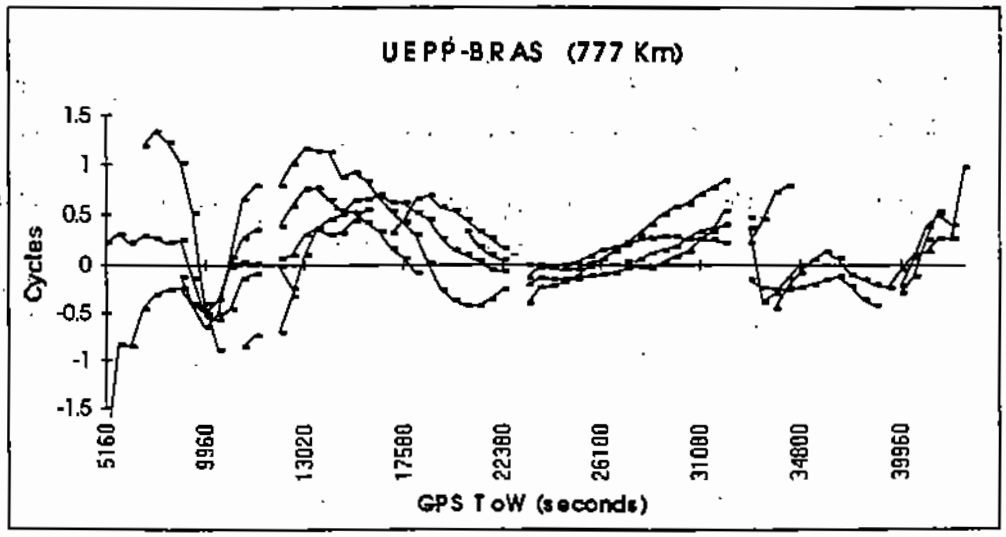

Figure 7.5: Widelane Double Difference Residuals

The ionospherically free double difference (L0) residuals, illustrated in Figure 7.6 reach a maximum of 0.2 cycles (4 cm) and do not show any systematic effect. This implies that the second order effects of the ionosphere, not eliminated in the ionospherically free observable, do not appear to have any significant effects on this baseline. Nevertheless, the pre-processing of this baseline was very time consuming.

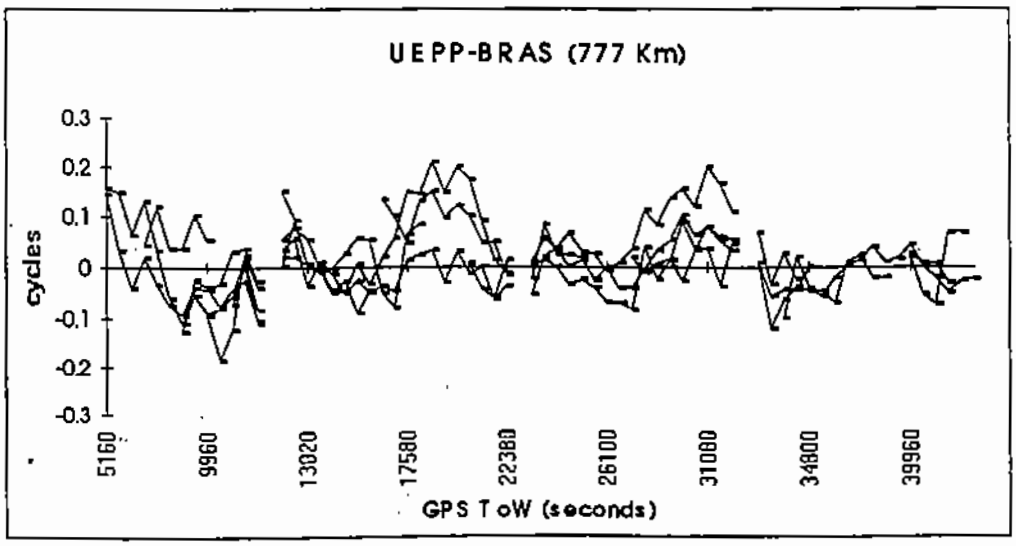

Figure 7.6: Ionospherically Free Double Difference Residuals

7.6 Data Processing: Results and Discussion

Two different approaches were used to adjust the network. The first was to process the network as two sub-networks, (a) and (b), by using the options available in the GAS software at the beginning of the author's research. The two sub-networks were then combined using the CARNET program. This is referred to as the 'Quasi-network' solution. Once the capability of processing global GPS networks was implemented in the GAS software, the second procedure involved the adjustment of the complete network, hereafter referred to as the 'Full-network' solution.

The undifferenced phase observables were assumed to be uncorrelated and of equal unknown variance. The correlation resulting from the double difference approach and baseline combination (mathematical correlation) was properly introduced into the covariance matrix of the observables. The *a posteriori* variance ($\hat{\sigma}_0^2$) was estimated in the adjustment (§3.2.4).

7.6.1 Quasi-Network Solution

Sub-networks (a) and (b) were processed independently. In the former case the IGS coordinates of station SANT were held fixed in the adjustment. In the latter, the coordinates of station BRAS, estimated from sub-network (a) were held fixed. In sub-network (a), each of the six days was processed as two independent 12 hour sessions, providing a total of twelve 12-hour solutions. Sub-network (b) was processed on a daily basis because of the reduced number of simultaneous observations at each baseline, providing a total of six 24-hour solutions.

The effects of earth body tide (EBT) are not only a function of time, but also of position. Over longer baselines, such effects are different at both stations and do not cancel out in the differential processing. In order to investigate the effect of EBT on the solution, the processing was carried out with and without such corrections.

(a) Solution Without Earth Body Tide Corrections

In order to detect any mis-specification of the mathematical model, an analysis of the estimated variance factor was carried out. Table 7.4 gives the degrees of

freedom (df) and the estimated square root of the *a posteriori* variance ($\hat{\sigma}_0$) of each sub- network solution.

Assuming that the carrier phase observable ϕ_1 and ϕ_2 are uncorrelated with equal standard deviation (σ_ϕ) of 0.01 cycles, (Hofmann-Wellenhof *et al*, 1992), and applying the covariance propagation law to the ionospherically free double difference observable, its resulting standard deviation (σ_{if}) is approximately 12 mm. A comparison of this value with those presented in Table 7.5 shows that the results of the processing of sub-network (a) do not appear to have any significant problems. At a level of significance α = 5%, all sessions are accepted based on the *global test statistic* (§3.2.4). On the other hand, Julian days 210, 211, 212 and 213 of sub-network (b) are rejected by this test. The reason for the rejection may be the result of mis-specifications in the mathematical model used, either functional or stochastic. One of the possible sources of this error is the EBT. Further investigations, mainly of the effects of EBT corrections were, therefore, carried out in order to test this theory.

Table 7.5: Estimated $\hat{\sigma}_0$ and Degrees of Freedom of Sub-networks (a) and (b) Without EBT Corrections

Julian day	Session	Sub-network (a)		Sub-network (b)	
		df	$\hat{\sigma}_0$	df	$\hat{\sigma}_0$
	1	7,433	8.98		
208	2	4,689	8.17	2,819	10.41
	1	7,119	9.76		
209	2	5,109	8.20	2,809	11.76
	1	6,556	9.89		
210	2	4,924	9.28	2,772	13.59
	1	7,417	10.30		
211	2	4,873	8.46	3.083	17.98
	1	5,925	9.94		
212	2	4,538	8.64	2,861	15.34
	1	6,293	10.38		
213	2	4,616	8.55	2,245	15.83

An additional analysis of the network adjustment concentrated on the repeatabilities (§5.2.3) of the baseline components. The repeatability provides

an indication of the internal consistency of the network (precision). For the purpose of this analysis, only the repeatabilities of the baseline components related to those stations with at least six-days of processing were computed. Figure 7.7 illustrates the repeatabilities of the solutions without applying EBT corrections. The length component shows precisions of the order of 20 ppb (parts per billion). The repeatabilities of the east component were worse than the height component for the two longest baselines. Results reported in others literature have shown the height component to have the worst repeatabilities (Blewitt, 1989; Dong and Bock, 1989), a result obtained for the shortest baselines. This could be due to the reduced number of observations in the two longest baselines and the effects of EBT, which were not included in the processing at this stage. The two longest baselines belong to sub-network (b), in which the *global test statistic* rejected four out of six days of processing. Therefore, it is likely that the main mis-specification in the mathematical model may be related to EBT, whose effects were not taken into account in this processing.

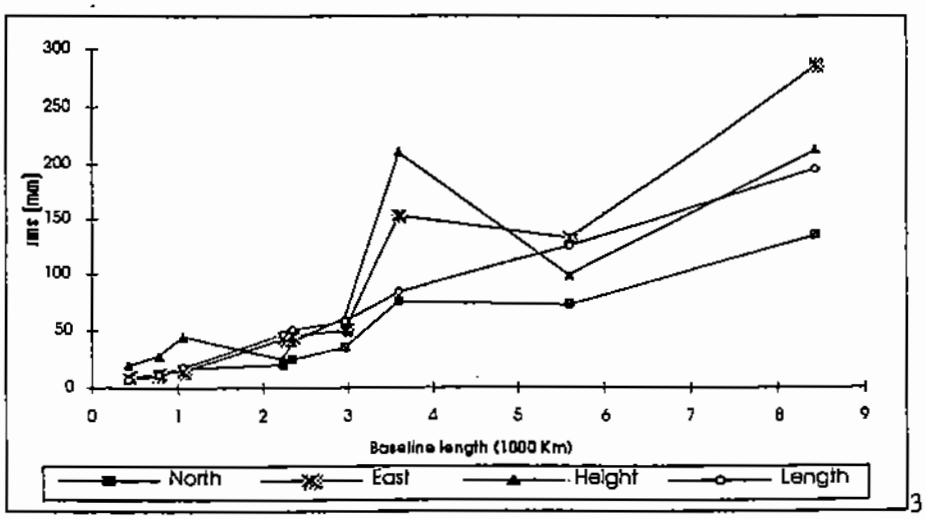

Figure 7.7: Repeatabilities Without EBT Corrections

The accuracy of the network adjustment without EBT corrections was assessed by analysing the recoveries of known high accuracy station coordinates. Stations GOLD and RCM2 were held fixed and all baselines components (ΔX, ΔY and ΔZ) with the respective covariance matrix were introduced as observables in the adjustment carried out by CARNET. The coordinates of all the other stations were estimated. Figure 7.8 shows the recoveries of station SANT, ie the assumed 'true' coordinates (Table 7.3, IGS solution) subtracted from those estimated in the adjustment.

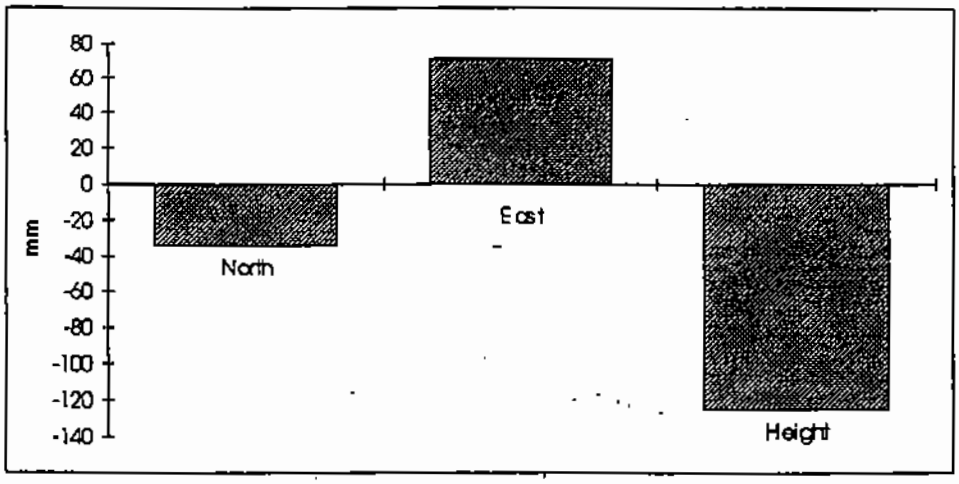

Figure 7.8: Recoveries of Station SANT Without EBT Corrections: IGS Solution minus GAS (IGS Reference Frame)

Considering the errors resulting in not applying EBT corrections, and the fact that some other errors are not completely modelled or cancelled out during the processing, and taking into account the dimension of the network (GOLD-SANT is approximately 8,200 km), one can conclude that the results obtained are quite satisfactory. The worst coordinate component recovery (height accuracy) agrees with the assumed 'true' value at the level of 15 ppb (120 mm over 8200 km). This result is better than the repeatability of the height component (Figure 7.7), which gives an indication of the network precision. Similar behaviour was observed for the north and east components.

(b) Solution With Earth Body Tides Corrections

Although the processing described so far had provided good results, it was clear that the mathematical model was likely to have been mis-specified. The network was re-processed including EBT corrections, suspected of being the main reason of the problems outlined before. The estimated sigma ($\hat{\sigma}_0$) and degrees of freedom (df) of this processing are given in Table 7.6.

From this table one can see that the estimated square root of the variance factors, ($\hat{\sigma}_0$), have improved with respect to those given in Table 7.5. This improvement is more significant in the case of sub-network (b), which comprises the two longest baselines. Such a result was expected because the effect of EBT is a function of station position. For long baselines, the effect should be significantly different at both stations and will not cancel out in the

differencing approach. The results of all the adjustments carried out with EBT corrections are therefore, accepted based on the *global test statistic* at a level of significance, $\alpha = 5\%$.

Table 7.6: Estimated σ and Degrees of Freedom of Sub-Networks (a) and (b) With EBT Corrections

Julian	Session	Sub-network (a)		Sub-network (b)	
Day		df	$\hat{\sigma}_0$	df	$\hat{\sigma}_0$
	1	7,433	8.14		
208	2	4,689	7.92	2,819	9.40
	1	7,119	8.55		
209	2	5,109	7.16	2,809	9.79
	1	6,556	7.89		
210	2	4,924	8.25	2,772	10.54
	1	7,417	8.41		
211	2	4,873	7.26	3,083	11.32
	1	5,925	8.54		
212	2	4,538	6.54	2,861	10.30
	1	6,293	8.10		
213	2	4,616	7.22	2,245	9.78

Figure 7.9 illustrates the repeatabilities of the baseline components with the introduction of EBT corrections. All the baseline components seem to have improved. For the two longest baselines, the repeatabilities of the east component, although better than before, are still worse than the height component. From Figure 7.9, one can see that this situation occurs beyond a certain baseline length. This may be due to the geometry of the network and the reduced number of simultaneous observations at both stations over such long baselines.

In order to assess the accuracy of the results, the recoveries of the coordinates of the IGS station SANT were computed. As before, stations GOLD and RCM2 were held fixed in the adjustment and all baseline components were introduced as observables in the CARNET program. Figure 7.10 shows the recoveries of station SANT. Comparing Figure 7.10 with 7.8, one can see that the introduction of the EBT corrections produces worse results. Notice that the recovery of the height component has approximately the same absolute value at

both processings (with and without EBT), but opposite sign. On the other hand, the recovery of the east component with EBT corrections is better than that without EBT, and has the same sign. The recovery of the north component, which was about -40 mm in the solution without EBT, reached 200 mm in the solution with EBT corrections applied. The north component repeatabilities were of about 70 mm, which is quite better than the recovery. In summary, the repeatabilities of the solution with EBT corrections improved relatively compared to the solution without EBT, whereas the recoveries deteriorated. This is an unexpected result, which could be due to the effect of using the 'Quasi-Network' approach.

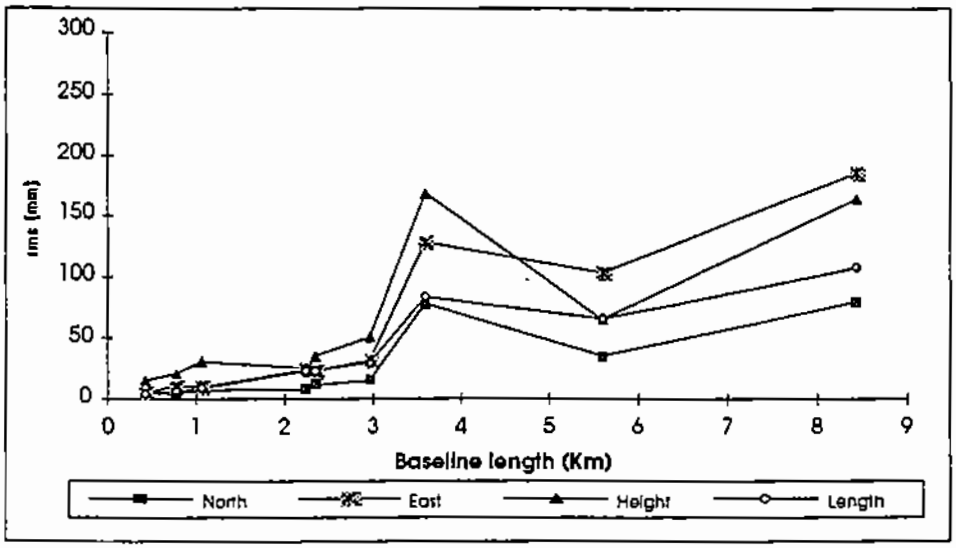

Figure 7.9: Repeatabilities With EBT Corrections

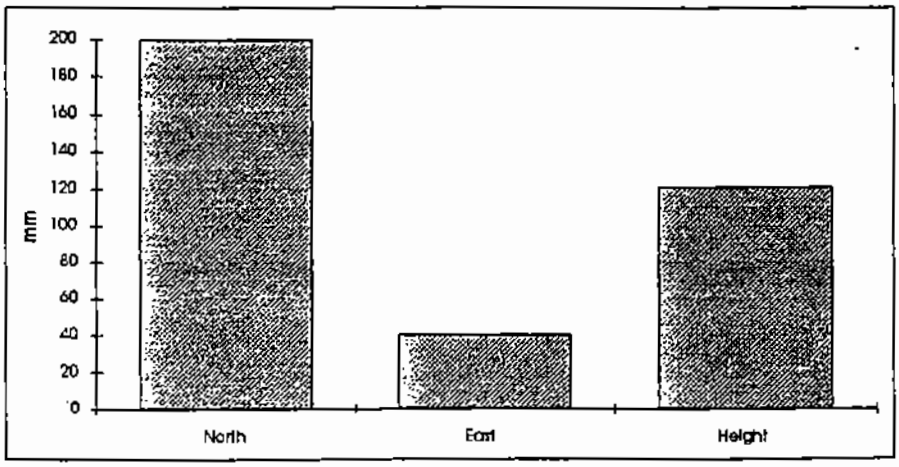

Figure 7.10: Recoveries of Station SANT With EBT Corrections: IGS Solution minus GAS (IGS Reference Frame)

Considering the results given in Figure 7.10 and the spread of the network, the accuracy of the worst component (north) is of the order of 24 ppb (200 mm over 8200 km).

7.6.2 Full Network Solution

The 'Quasi-Network' processing described in the previous section does not represent a rigorous adjustment of the network, as the correlation between the two sub-networks was not properly taken into account. Once the *base satellite per baseline* option was implemented in the GAS software (§5.4.2), a rigorous adjustment of the network was carried out. In order to assess the differences between 'Quasi-network' and 'Full network', solutions with and without EBT corrections were also carried out for the latter case.

(a) Solution Without Earth Body Tides Corrections

Each of the six days was processed as a full 24-hour session, or as two consecutive 12-hour sessions. Therefore, six and twelve solutions were obtained for the former and latter case respectively. The IGS coordinates of the three reference stations (GOLD, RCM2 and SANT) were constrained to their known coordinates (Table 7.4) with a standard deviation of 02 cm.

Figure 7.11(a) illustrates the repeatabilities of the twelve 12-hour session solutions. Comparing the repeatabilities illustrated in Figure 7.11 with that of Figure 7.7 one can conclude that the result improved by a factor of 4 over the longer baselines. A slight improvement can also be seen over the shorter baselines. As expected, the worst coordinate component repeatability refers to the height. In Figure 7.11(b), which illustrates the 24-hour solution, the repeatabilities further improved by about 20 millimetres. Neither Figure 7.11(a) nor 7.11(b) includes earth body tide corrections. The significant improvement of the repeatabilities derived from the use of 24-hour session may be mainly attributed to earth body tide effects, partially averaging and cancelling out during this period. The 24-hour data set includes the two main periods of EBT, the semi diurnal and the diurnal with approximately 12 and 24 hours respectively.

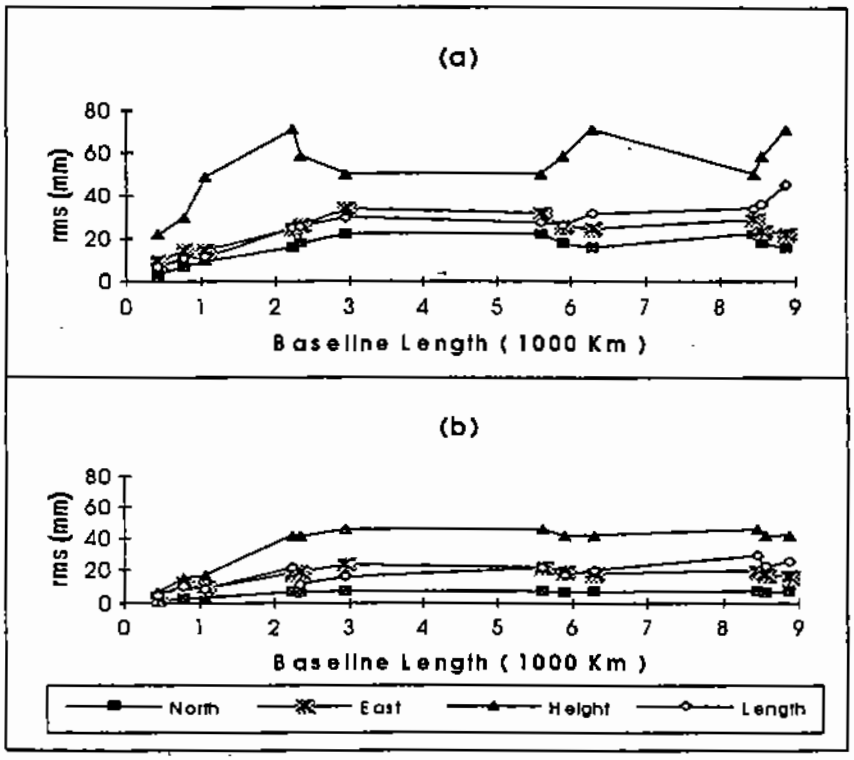

Figure 7.11: Repeatabilities Without EBT Corrections
(a) 12-hour Sessions (b) 24-hour Sessions

Figure 7.12 illustrates the recoveries of station SANT obtained from the six 24-hour sessions. Stations GOLD and RCM2 were constrained to their known values with standard deviations of 2 cm. The six 24-hour solutions where then combined together in the CARNET program. As one can see, the recoveries are about 3 times worse than the repeatabilities (height component) and also worse than the solution carried out with two sub-networks (Figure 7.8). Such result suggests that systematic errors may be present in the model.

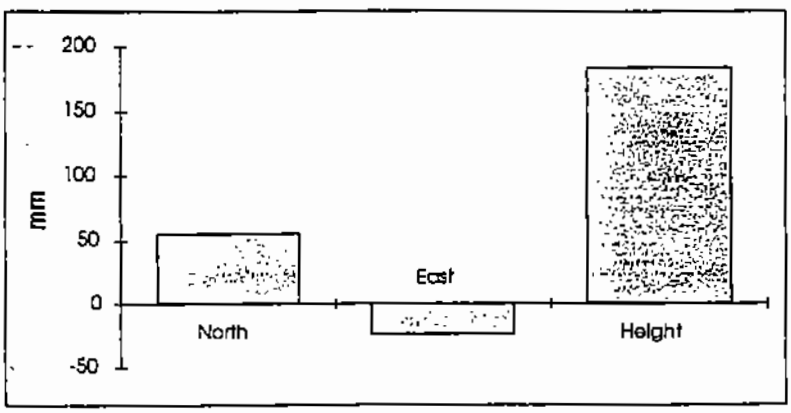

Figure 7.12: Recoveries of Station SANT Without EBT Corrections:
IGS Solution minus GAS (IGS Reference Frame)

(b) Solution With Earth Body Tide Corrections

The processing was carried out as before, but applying EBT corrections. Figure 7.13(a) shows the repeatabilities of the twelve 12-hour sessions. By comparing with the similar solution of the previous section, illustrated in Figure 7.9, a significant improvement can be seen, mainly over the longer baselines. Figure 7.13(b) illustrates the repeatabilities of the six 24-hour sessions. The root mean square error (RMS) for height reduces to only 20 mm. This constitutes an improvement with respect to the 12-hour solution (Figure 7.13(a)) of the order of 10 mm for most of the baselines. This improvement is probably due to the averaging out and the cancelling of long term (24 hours) bias terms, such as ocean tide loading (OTL) which has not been corrected for.

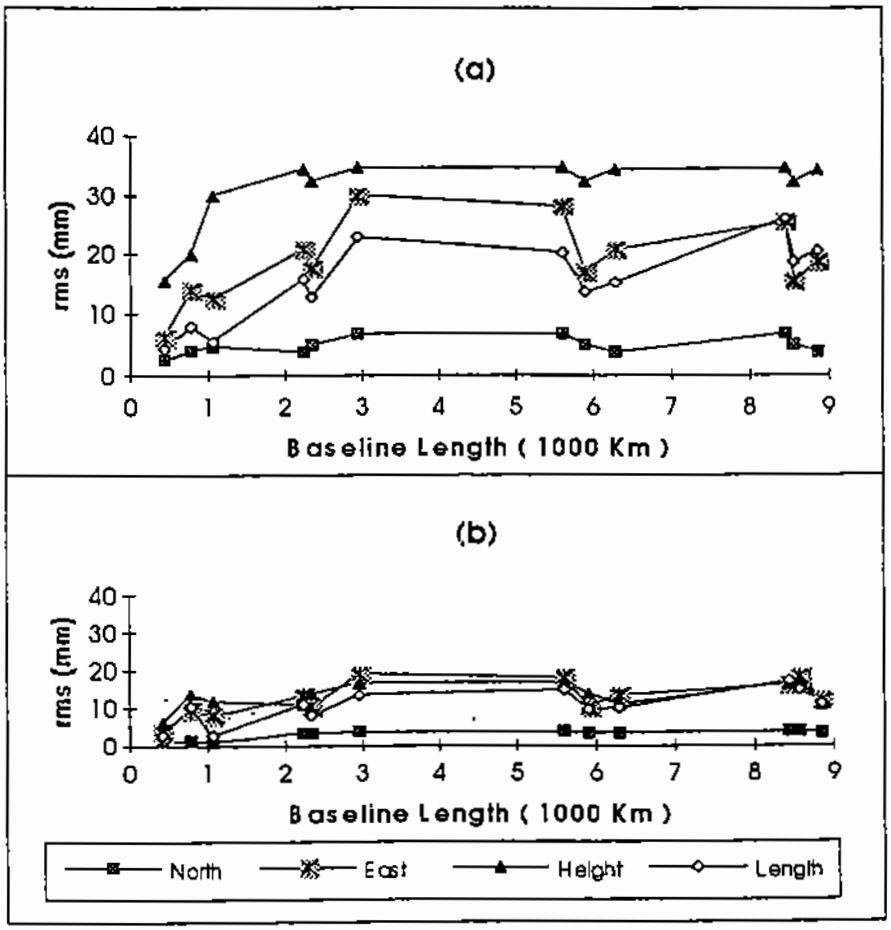

Figure 7.13: Repeatabilities With EBT Corrections
(a) 12-hour Sessions (b) 24-hour Sessions

The solution involving the six 24-hour sessions with EBT corrections applied (Figure 7.13 (a)) provides a RMS the order of 8 ppb (parts per billion) for the worst coordinate component (height). The repeatabilities of the length

component are better than that of height by a factor of 2, ie an RMS for lengths of the order of 4 ppb.

Figure 7.14 illustrates the recoveries of station SANT estimated from six 24-hour sessions with EBT corrections. This has improved by a factor of 2, if compared with the recoveries without EBT corrections (Figure 7.12) and is much better than the solution provided by the so called 'Quasi-Network' approach (Figure 7.10).

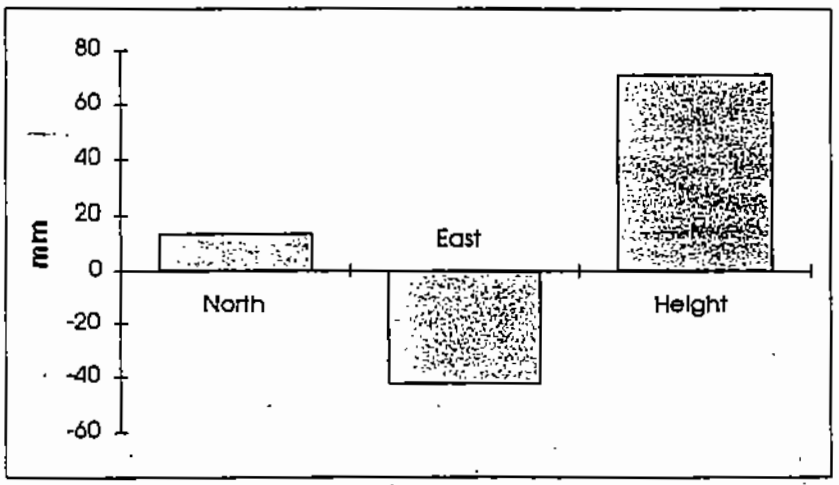

Figure 7.14: Recoveries of Station SANT With EBT Corrections: IGS Solution minus GAS (IGS Reference Frame)

It is clear from the results presented so far, the advantage of the new module (base satellite per baseline) implemented in GAS, for the processing of large GPS networks.

(c) Statistical Analysis of the Models With and Without EBT Corrections

The square root of the estimated variance factor, ($\hat{\sigma}_0$), and degrees of freedom, (df), of the twelve 12-hour and six 24-hour sessions, both with and without EBT corrections, are given in Table 7.7 and Table 7.8 respectively. For the 12-hour sessions, each day was sub-divided into two sessions, identified as 1 and 2. Session 1 corresponds to the interval 00:00 to 12:00 hours and session 2 from 12:00 to 24:00 hours, both in universal time (UT).

Assuming the square root of the *a priori* variance factor of the ionospheric free observable to be equal to 12 mm (§7.6.1) and applying the *global test statistic*

(§3.2.4), all the solutions with EBT corrections are accepted at a level of significance $\alpha = 5\%$. Solutions without applying EBT corrections for sessions 210-1, 211-1, 212-1 and 213-1 are rejected. Clearly, the reason for rejecting these solutions was not only due to not applying EBT corrections, otherwise, all the sessions should have been rejected. Additional effects of some other residual errors, due to mis-modelling, are also present. The effect of including EBT corrections in the adjustment is however, clearly demonstrated by the results.

Table 7.7: Estimated $\hat{\sigma}_0$ and Degrees of Freedom for the Twelve 12-hour Sessions

day-session	DF	$(\hat{\sigma}_0)$ no EBT	$(\hat{\sigma}_0)$ with EBT
208-1	6,275	9.33	9.02
208-2	5,140	8.35	8.35
209-1	6,273	10.40	9.16
209-2	5,801	8.42	7.68
210-1	6,042	12.15	8.38
210-2	5,487	9.63	8.37
211-1	6,639	13.12	9.19
211-2	5,399	8.84	8.23
212-1	6,384	13.76	9.33
212-2	5,179	9.07	7.23
213-1	7,119	13.70	9.54
213-2	4,883	8.99	7.67

A further analysis of Table 7.7 indicates that the rejected solutions (210-1, 211-1, 212-1, 213-1) refer to the first session of the corresponding days (00:00 to 12:00 hours UT). Furthermore, one can also observe that the estimated variance factor, $(\hat{\sigma}_0^2)$, of session 1 is always higher than that of session 2. It has been reported (Wanninger, 1992) that in the equatorial region, during the maximum of solar cycle 22 (1989-1992), the worst effects of the ionosphere on GPS data occur between 18:00 and 02:00 hours local time, ie 22:00 and 06:00 UT . The data processed in this experiment was collected during the period of maximum of solar cycle, and all first sessions (with higher estimated variance factor) comprise most of the period of the day with worst

ionospheric effects. Therefore, the estimated variance factor, which gives an indication of the validity of the model, is likely to be showing such expected effects.

A statistical analysis was also carried out to investigate the effects of applying ocean tide loading (OTL) corrections. The square root of the estimated variance factor of solutions with EBT, and EBT and OTL corrections are listed in Table 7.8. Only the six 24-hour sessions have been used, since they have produced the best results so far. The OTL corrections were applied for the three known stations (SANT, RCM2 and GOLD) following the IERS standards (McCarthy ,1992). For the Brazilian stations, the loading parameters required to compute OTL corrections were unavailable.

Table 7.8: Estimated $\hat{\sigma}_0$ and Degrees of Freedom for the Six 24-hour Sessions

Day	DF	$(\hat{\sigma}_0)$ with EBT	$(\hat{\sigma}_0)$ with EBT & OTL
208	11,433	8.87	8.85
209	12,090	8.60	8.59
210	11,541	8.60	8.90
211	12,055	8.94	8.60
212	11,577	8.56	8.58
213	12,097	8.90	8.84

From the results listed in Table 7.8 there is no clear evidence of significant improvement in the results due to the introduction of OTL corrections at the three known stations. Although not described in this work, the same conclusion could be derived from the analysis of the repeatabilities and recoveries of results in which OTL corrections were applied. This is most likely due to the fact that the OTL effects have averaged out over the 24 hour observation period without corrections applied. Furthermore, the maximal amplitude of M2, the principal lunar tidal harmonic, is 9 mm in the radial component of station RCM2, well below the network precision (about 20 mm).

(d) EBT Corrections and Tropospheric Delay Modelling

The effects of modelling the zenithal scale factor for tropospheric delay as a second order polynomial, instead of the usual first order one, considering the

cases with and without applying EBT corrections, were investigated. This was carried out based on the estimated variance factor of the solutions and repeatabilities of the results. The square root of the estimated variance factor, ($\hat{\sigma}_0$), and degrees of freedom, (df), for each of these solutions are given in Table 7.9. Notice that although the degrees of freedom of a solution with a first order polynomial are different from a solution with a second order one, the same values are listed in Table 7.9. Within the scope of this analysis, the derived conclusions would not change because of the high number of degrees of freedom.

Analysis of the values listed in Table 7.9 shows that with respect to the solutions without EBT corrections, a second order polynomial provided a smaller value for the estimated variance factor, an indication of a better fitting mathematical model. All daily solutions would be accepted by the *global test statistic* with level of significance $\alpha = 5\%$, whilst two would be rejected in the solution with a first order polynomial (212 and 213). This may be due to EBT and some other effects being absorbed in the higher order polynomial applied to model the tropospheric delay. Although less significant, improvement can also be seen in the solution in which EBT corrections were applied. It seems that some un-modelled and residual effects, have also been absorbed by the higher order polynomial.

Table 7.9: Estimated $\hat{\sigma}_0$ and Degrees of Freedom for Solutions with First and Second Order Tropospheric Scale Factors Polynomial

[illegible]	DF	1st without EBT	2nd without EBT	1st with EBT	2nd with EBT
208	11,422	9.71	9.19	8.87	8.32
209	12,078	10.48	9.75	8.60	8.14
210	11,530	11.35	10.64	8.60	8.20
211	12,043	11.76	11.10	8.94	8.50
212	11,565	12.13	11.28	8.56	8.26
213	12,085	12.27	11.15	8.90	8.69

The day-to-day repeatabilities of the baseline components (dN, dE, dh and dL) for different solutions are listed in Table 7.9. For the six 24-hour sessions the zenithal scale factor for tropospheric delay was modelled as a first (1) or a

second (2) order polynomial per station, for every 12 hour. Furthermore, for each of these two alternatives, the effects of applying or not applying EBT corrections were also considered.

It is important to note that the order of the polynomial cannot be increased indefinitely, as this may result in problems such as instability of the normal equations. It has been reported (Shardlow, 1994) that the choice of polynomial for a GPS campaign has to be made on purely a subjective basis. From the results listed in Table 7.9 and 7.10, it seems reasonable to model the tropospheric zenithal scale factor as a polynomial of order 2 for each 12-hour session. The estimated variance factors (Table 7.9) and the repeatabilities (Table 7.10) of the solution without EBT and second order polynomial are better than that with a first order polynomial. In such a case, the polynomial besides taking into account the tropospheric delay, also absorbs some un-modelled effects, such as EBT. The solution with EBT corrections also showed that the results provided by including a second order polynomial is better than a first order one. The day-to-day repeatabilities improved by 4 and 2 mm for the east and height components respectively.

Table 7.10: Average RMS of the Six 24-hour Sessions

Polynomial Order	EBT applied ?	dN (mm)	dE (mm)	dh (mm)	dL (mm)
1	no	5	22	42	19
2	no	4	17	29	18
1	yes	3	17	14	12
2	yes	3	13	12	11

7.7 Integration of the Brazilian GPS Network into a Global Reference Frame (ITRF93)

The results presented so far have been carried out in the IGS reference frame. Conclusions similar to those presented in the previous sections could be obtained, if the ITRF93 coordinates were used instead. So, in order to produce a solution consistent with the ITRF, the final solution was estimated using ITRF93 coordinates. This realises the integration of the Brazilian stations into a global reference frame.

In the final solution, a further stage in the processing was to include the data collected during Julian day 218. On this day, stations PARA, UEPP, BRAS and CHUA recorded GPS data for 24 hours. The baselines CHUA-BRAS, CHUA-UEPP and CHUA-PARA were processed as a network. This solution provided means of integrating station CHUA, the origin of the SAD-69 (South American Datum 1969) to the global reference frame.

The final stage of the processing involved all baselines components (ΔX, ΔY and ΔZ) processed on the different days with their respective covariance matrices. They were combined together by using the CARNET program. Stations GOLD, RCM2 and SANT were held fixed to their known coordinate values of the date of the campaign (1 July 1992). The resulting estimated coordinates are listed in Table 7.11.

Table 7.11: Estimated Coordinates Referenced to the ITRF93 on 1 July 1992

STATION	X(m)	$\hat{\sigma}_X$ (mm)	Y(m)	$\hat{\sigma}_Y$ (mm)	Z(m)	$\hat{\sigma}_Z$ (mm)
SANT	1 769 693.221	FIXED	-5 044 574.121	FIXED	-3 468 321.112	FIXED
PARA	3 763 751.694	20	-4 365 113.807	24	-2 724 404.826	15
UEPP	3 687 624.341	21	-4 620 818.589	25	-2 386 880.455	14
BRAS	4 114 500.478	24	-4 551 173.098	26	-1 741 210.638	13
ILHA	3 732 193.628	95	-4 674 886.685	102	-2 206 380.873	43
AVAN	3 810 097.072	92	-4 573 380.840	99	-2 284 127.728	41
TAQU	3 628 144.889	87	-4 644 484.387	98	-2 431 011.407	42
SALT	3 778 535 627	88	-4 503 386.815	100	-2 467 128.351	43
CHUA	4 010 548.056	44	-4 470 077.052	47	-2 143 178.822	26
RCM2	961 318.955	FIXED	-5 674 090.992	FIXED	2 740 489.606	FIXED
GOLD	-2 353 614.108	FIXED	-4 641 385.404	FIXED	3 676 976.485	FIXED

The standard errors of the stations occupied during seven days (PARA, UEPP, BRAS) are of the order of 2.6 cm. Such a value is optimistic and has same level of precision as the ITRF coordinates. On the basis of the accuracies (Figure 7.14) and repeatabilities of the results (Table 7.10), it is likely that the coordinates of stations UEPP, PARA and BRAS have an absolute accuracy better than 8 cm. Such value also corresponds to approximately 3σ (99.99%

probability that the 'true' value lies within 3σ). The accuracy of the other stations should be slightly worse, because of the reduced amount of data.

7.8 Assessment of CHUA WGS84 Coordinates

It has been claimed that the use of precise ephemeris for the reduction of Transit-Doppler measurements provides absolute accuracy of the WGS84 coordinates of a (single) station of about 1 to 2 m (Seeber 1993). Therefore, this is the expected accuracy of the WGS84 coordinates of CHUA, the origin of the SAD-69. These coordinates were estimated from 24 days of Doppler measurements, using precise TRANSIT ephemeris (Fortes *et al*, 1989). They have been used to support most of the GPS activities in Brazil but have never been assessed by a more accurate positioning system.

The coordinates of CHUA determined during the IGS Epoch '92 campaign in Brazil have been compared with the WGS84 coordinates. The differences between these two are given in Table 7.12: These values are remarkable since they are well below the 2 m level, ie the accuracy of the absolute WGS84 coordinates obtained using the Transit-Doppler system.

Table 7.12: ITRF93 minus WGS84 Coordinates (m) for Station CHUA

ΔX	ΔY	ΔZ
-0.379	-0.425	0.192

7.9 Summary

The high drift detected in the oscillators of C/A-code Trimble receivers, did not cause any major problems for the purpose of this work. The same can be concluded from the ionospheric effects, which were probably the main causes of the difficulties with cycle slip detection and repair.

Analysing the results obtained from the 'Quasi-network' and the 'Full network' processing, it can be concluded from the repeatabilities and recoveries tests that the results improved significantly in the latter approach, justifying the development and inclusion of the *base satellite per baseline* approach in GAS.

Within the processing using the new module implemented in GAS, it has been made clear that, for large networks, EBT corrections should be applied for highest accuracies. The application of ocean tide loading corrections did not have any significant improvement over the network analysed. Furthermore, the use of tropospheric delay zenithal scale factors per station, modelled as a second order polynomial, showed better results than with a first order polynomial, suggesting that some un-modelled errors were still present, such as Atmospheric Pressure Loading, multipath, etc.

The Brazilian stations occupied during the IGS Epoch '92 Campaign have been integrated into a global reference frame (ITRF93). The repeatabilities of the worst component, height, was of about 20 mm for baselines of up 8200 km. The recoveries, which give an indication of the accuracy was about three times worse than the repeatabilities. Such tests suggest that the coordinates of the Brazilian stations have been determined with an accuracy better than 8 cm. The coordinates of these stations can be used in future GPS activities in Brazil.

The International GPS Geodynamic Service (IGS) has provided an effective way of conncecting the Brazilain GPS network into a global reference frame (ITRF93).

The newly computed ITRF93 coordinates of station CHUA, the origin of SAD-69, differ from the currently used WGS84 values by -0.340, -0.421, 0.171 in X, Y and Z geocentric coordinates respectively. These differences are remarkable as they are well below the 2 m level, the accuracy of the Transit-Doppler derived absolute position of station CHUA.

Chapter 8

ANALYSIS OF AN INTER-CONTINENTAL GPS NETWORK

8.1 Introduction

This chapter addresses the processing of an inter-continental network, which is an extension of the network presented in the previous chapter. The main purposes are to perform comparisons between the fiducial network approach and the ordinary network adjustment, and to investigate aspects of the free network adjustment or non-fiducial approach applied to GPS. The non-fiducial approach allows the establishment of a global reference frame by using GPS to be investigated. Furthermore, the capability of processing very large networks, or even a global one is a new module available in the GPS Analysis Software (GAS), and needs be tested in order to evaluate its performance.

In the case of ordinary network adjustment, the investigation has been focused on the results obtained either by fixing the reference stations during the main processing or by performing a transformation at the last stage of the processing. The disadvantage of the former case is the fact that if the reference stations have to be changed, all the main steps of the processing must be repeated. Such a procedure is very time consuming. Alternatively, by leaving all of the stations free, a transformation can be performed at the last stage of the data processing. One obvious advantage of this procedure is that any change of reference stations can be easily adapted by applying a transformation to the original (free) solution. The aspects described above have also been investigated within the context of the non-fiducial and fiducial approaches.

To investigate the capability of GPS for realising a geocentric reference frame independent of other positioning systems, solutions without fixing any station, ie the so-called free or non-fiducial network approach have been carried out. In this approach, all the station coordinates and satellite state-vectors, as well as the bias parameters, are estimated during the processing.

The station coordinates estimated in the non-fiducial approach are mapped to the International Terrestrial Reference Frame (ITRF93) via a seven-parameter transformation. Since the ITRF stations are claimed as having absolute precision of the order of 2 cm (Blewitt *et al*, 1992), the transformation parameters can provide a means to assess the quality of the reference frame established by GPS. Similar investigations have been carried out by Blewitt *et al* (1992) and Mur *et al* (1993). Their conclusions are different, probably due to using different strategies. In this study several strategies have been tested in order to get an insight into the problem. A detailed discussion of these tests is included in this chapter.

It should be pointed out that the results of these investigations provide an additional set of coordinates for the Brazilian stations, estimated using strategies different from those used in the previous chapter. This therefore provides an extra means of assessing the quality of the Brazilian stations.

8.2 The Tested Network

The network tested during this investigation is comprised of stations at which data were collected during the IGS Epoch '92 Campaign. The sample data comprises 6 days of the campaign (Julian day 208 to 213 or 26 July 1992 to 31 July 1992) collected at 16 tracking stations, which are illustrated in Figure 8.1.

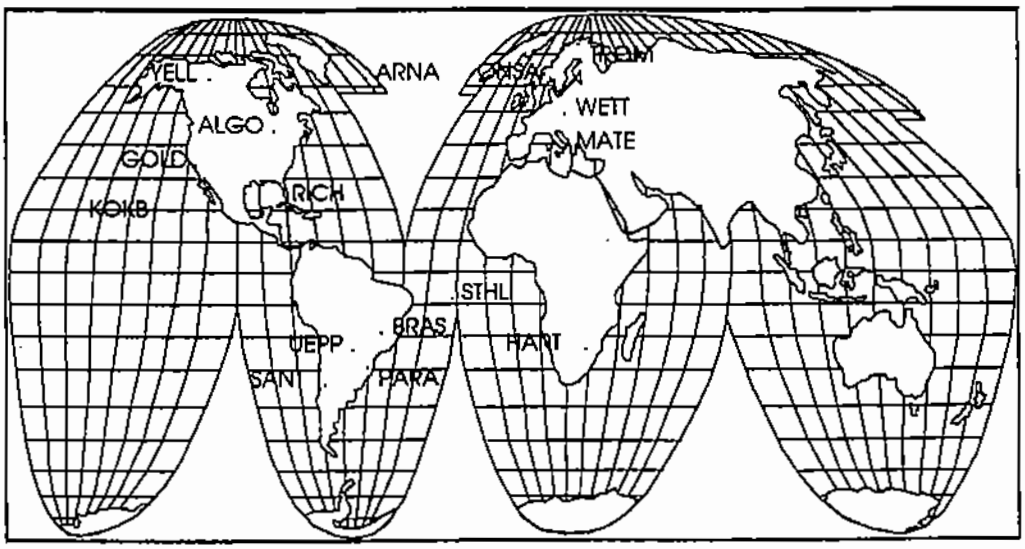

Figure 8.1 : The Inter-Continental GPS Network

8.2.1 GPS Data Sets

Although the IGS Epoch '92 campaign involved 14 days of tracking data, no more than 6 days of data were used for each of the stations. This sample is larger than the typical 3-5 days normally used for large regional campaigns designed to monitor regional deformation (Ashkenazi *et al*, 1994). Furthermore, as stated in Chapter 7, it was thought to be an amount of data that could be processed and analysed within the period of the author's research.

Each daily station data set was divided into two sessions (1 and 2) of 12 hours. The data, originally recorded at an interval of 30 seconds, was processed as a 60 seconds interval for ease of data management. Session 1 started at 00:00 UT and stopped at 12:00 UT. Session 2 completed the day data set. The data available at each station and the receivers used are listed in Table 8.1.

Table 8.1 : Stations and Data Sets in the Inter-Continental GPS Network

Name	Site Location	Julian Days / Sessions												Receiver
		208		209		210		211		212		213		
		1	2	1	2	1	2	1	2	1	2	1	2	
BRAS	Brasilia-DF, BR	x	x	x	x	x	x	x	x	x	x	x	x	Trimble
PARA	Curitiba-PR. BR	x	x	x	x	x	x	x	x	x	x	x	x	Trimble
UEPP	P.Prudente-SP. BR	x	x	x	x	x	x	x	x	x	x	x	x	Trimble
SANT	Santiago-Chile	x	x	x	x	x	x	x	x	x	x	x	x	Rogue
GOLD	Goldstone-USA	x	x	x	x	x	x	x	x	x	x	x	x	Rogue
RCM2	Richmond-USA	x	x	x	x	x	x	x	x	x	x	x	x	Rogue
STHL	St. Helena-UK	x	x	x	x	x	x	x	x	x	x	x	x	Ashtech
ARNA	Island		x	x	x	x	x	x	x	x	x	x	x	Trimble
WETT	Wettzell-Germany	x	x	x	x	x					x	x	x	Rogue
MATE	Matera- Italy	x	x	x	x	x	x	x	x	x	x	x	x	Rogue
ONSA	Onsala-Sweden	x	x	x	x	x	x	x	x	x	x	x	x	Rogue
YELL	Yellowknife-Canada	x	x	x	x	x	x	x	x	x	x	x	x	Rogue
KOKB	Kokee Park- USA	x	x	x	x	x	x	x	x	x	x	x	x	Rogue
ALGO	Algonquin-Canada	x	x	x	x	x	x	x	x	x	x	x	x	Rogue
HART	Hartebeesthoek- S.Afr	x	x	x	x	x	x	x	x	x	x	x	x	Rogue
TROM	Tromso-Norway	x	x	x	x	x	x	x	x	x	x	x	x	Rogue

The 15 independent baselines included in the processing and their corresponding lengths in km are listed in Table 8.2. They give an indication of the range of the baseline lengths involved in this study. The receivers at stations WETT and ARNA failed to collect data during four and one sessions respectively. In the former case, the baseline ONSA-MATE was included in the data processing to replace the baselines ONSA-WETT and WETT-MATE. In the latter, the baseline ALGO-ONSA replaced the baselines ALGO-ARNA, ARNA-ONSA.

Table 8.2: Sample Lengths of Processed Baselines

Baselines	Length (km)	Baselines	Lengths (km)
SANT-PARA	2,234	GOLD-KOKB	4,305
PARA-UEPP	430	RMC2-ALGO	2,254
UEPP-BRAS	777	ALGO-ARNA	3,877
BRAS-STHL	4,419	ARNA-ONSA	1,956
STHL-HART	3,582	ONSA-TROM	1,406
BRAS-RCM2	5,594	ONSA-WETT	919
RCM2-GOLD	3,596	WETT-MATE	990
GOLD-YELL	2,986	ONSA-MATE	1,887
		ALGO-ONSA	5,676

8.2.2 Reference Stations and Precise Ephemeris

Eleven of the sixteen stations defining the inter-continental GPS network are stations included in the realisation of the ITRF. For the purpose of this research, the coordinates of these stations given in the ITRF93 were used. They were mapped to the epoch of the campaign (1 July 1992) by using the ITRF93 velocity field (Boucher *et al*, 1994) and are listed in Table 8.3.

Some of these stations have been used either as fiducial stations or as supposedly 'true' values in some of the experiments carried out. The accuracy of the coordinates of these stations is about 2 cm (Blewitt *et al*, 1992).

The precise ephemeris used in the ordinary network adjustment was derived by the Jet Propulsion Laboratory (JPL) in Pasadena, California, using GPS data from the core stations observed during the IGS Epoch '92 campaign (Zumberge *et al*, 1993).

Table 8.3: ITRF93 Coordinates mapped to 1 July 1992

STATIONS	X (m)	Y (m)	Z (m)
TROM	2 102 940.423	721 569.358	5 858 192.076
ONSA	3 370 658.724	711 876.970	5 349 786.823
WETT	4 075 578.656	931 852.614	4 801 569.989
MATE	4 641 949.802	1 393 045.192	4 133 287.264
HART	5 084 625.445	2 670 366.499	-2 768 494.044
ALGO	918 129.564	-4 346 071.223	4 561 977.830
YELL	-1 224 452.415	-2 689 216.071	5 633 638.289
GOLD	-2 353 614.121	-4 641 385.404	3 676 976.485
GOLD-PEQ[8.1]	-2 353 614.108	-4 641 385.401	3 676 976.498
KOKB	-5 543 838.094	-2 054 587.519	2 387 809.569
RCM2	961 318.955	-5 674 090.992	2 740 489.606
SANT	1 769 693.221	-5 044 574.121	-3 468 321.112

8.3 Processing Strategies

The data processing of the inter-continental GPS network was carried out using the following three strategies:

- Ordinary Network Adjustment (Precise Ephemeris) (§3.5.1)
- Fiducial Network Adjustment (§4.7)
- Free Network Adjustment (§4.8).

A set of common options was applied to each of these strategies. A summary is given in Table 8.4. Wherever the fiducial network adjustment was applied, the fiducial stations used are those listed in Table 8.4. For all the tests, each daily data set was processed as a full 24-hour period (2 sessions of 12 hours) using the GAS (GPS Analysis Software) software (§5.1). The final solution of each test was obtained as a combination of the six day solutions using the CARNET (CARtesian NETwork adjustment) program (§5.2.3). The repeatabilities and recoveries of the tests were obtained by using the REPDIF (vector REPeatability DIFfrences) program (§5.2.3).

[8.1] (PEQ) Post EarthQuake : Landers earthquake of 28 June 1992

Table 8.4 : Common Options Applied to the Different Processing Strategies

Models Applied	
Ionospheric Delay	Ionospherically free observable
Tropospheric Delay	Magnet Model, with standard atmosphere
Antenna Phase Centre	Elevation angle dependent model (Schupler and Clark, 1991)
Ocean Tide Loading	Corrected according to IERS standards (McCarthy, 1992)
Earth Body Tides	Corrected according to IERS standards (McCarthy, 1992)
Adjusted Parameters	
Tropospheric Delay	1 Zenithal scale factor per session (1st order polynomial)
Ambiguities	Estimated as real values (not integer fixed)
Fiducial Stations	SANT, HART, YELL, KOKB, TROM, MATE

8.3.1 Ordinary Network Adjustment

Three different solutions have been investigated using the ordinary network adjustment. A description of each of these solutions follows:

1- The satellite positions were computed from the JPL precise ephemeris and fixed in the adjustment as known quantities. All stations were left free during the adjustment. Fixing the satellite coordinates, even without fixing any stations, provides a realisation of the datum during the observation period. The uncertainties of such a realisation are mainly due to the ephemeris errors. Therefore, it is possible to approximately evaluate the quality of the precise ephemeris, if a set of highly accurate (known) coordinates is estimated in the network adjustment where the datum realisation is provided only by the precise ephemeris. The differences between the known and estimated coordinates (recoveries) provide an indication of the precise ephemeris' quality.

2- In addition to fixing the satellite positions computed from the precise ephemeris, the coordinates of six fiducial stations (Table 8.4) were constrained to their ITRF93 values (Table 8.3), with 2 cm standard error. In such a case, the reference frame is realised not only with respect to the satellite ephemeris, but also with respect to the fiducial stations constrained in the adjustment. The remaining five ITRF stations were

estimated in the adjustment, providing a means of evaluating the accuracy of the solution.

3- The coordinates of the stations estimated in the adjustment carried out using only the precise ephemeris, without fixing any station (see 1 above), were transformed using a seven-parameter transformation (§4.8.1) via the known coordinates of the six fiducial stations (Table 8.4) of the network. In this case, the complete realisation of the reference frame is taken from the known stations, since the satellite information is eliminated in the transformation process. Again, the remaining five fiducial stations provide a means of assessing the accuracy of the solution.

For the purposes of this study, these three strategies have been identified as follows: 1-) 'Free Precise Ephemeris', 2-) 'Precise Ephemeris with Fiducial Stations' and 3-) 'Free Precise Ephemeris Transformed to Fiducial'.

8.3.2 Fiducial Network Adjustment

In the fiducial network technique the coordinates of a minimum of three accurately known stations are constrained to values previously known, and the coordinates of the new stations, satellite state-vectors and some biases are estimated in the adjustment (§4.7). The reference frame is defined by the adopted coordinate values of the fiducial stations constrained in the network adjustment (Ashkenazi *et al*, 1990).

For the fiducial network, two solutions were carried out during this research. A brief summary of each one is given below.

1- The fiducial stations used are those listed in Table 8.4, whose coordinates (Table 8.3) were constrained with standard errors of 2 cm. Throughout this work this technique is identified as 'Full Fiducial'.

2- This was not strictly a fiducial solution, but fiducial constraints were introduced to the free network adjustment solution by performing a transformation. Firstly, a free solution was carried out and the estimated coordinates were transformed to the reference frame defined by the fiducial stations used in the 'Full Fiducial' approach (see 1 above) via a

seven-parameter transformation (§4.8.1). This solution is referred to as 'Free Network Transformed to Fiducial'.

These two solutions, although using different approaches, should provide similar results since the same stations were used in the realisation of the reference frame. As already outlined, a free solution can be transformed to the reference frame defined by the fiducial stations, in the last step of the processing. If for any reason the reference frame has to be changed, only a transformation is required in the free network solution to provide a 'Free Network Transformed to Fiducial' solution, which is different from the 'Full Fiducial' approach, in which all main steps have to be repeated. Therefore, if the 'Free Network Transformed to Fiducial' approach provides results at the same level as the 'Full Fiducial' one, the former would be the most advantageous to use for cases in which the reference frame has to be tested.

8.3.3 Free Network Adjustment or Non-Fiducial Approach

In a free network solution it is attempted to solve for all stations coordinates, satellite orbits and even some bias parameters. In such a case, no fiducial sites are used, meaning that no station coordinates are held fixed. This solution has been referred to as the free network or non-fiducial approach. At a first analysis, such solution may appear impossible because of the lack of information in the mathematical model.

It was outlined that a three-dimensional terrestrial network requires a minimum of seven constraints, which represent the origin, orientation and scale. However, for a global GPS network, fiducial stations are not necessary to provide these minimal constraints (Heflin *et al*, 1992b). An origin at the earth's centre of mass is implicit in the force model, which together with the GPS data imply a scale as well. The model has deficiency in orientation, but the Z-axis direction is further constrained by the earth's daily rotation.

It has been suggested that very loose constraints to the stations coordinates referenced to the ITRF and initial satellite state-vector position components should be applied (Blewitt *et al*, 1992; Blewitt *et al*, 1993b; Heflin *et al*, 1992b). Such an approach should solve the problem related to the rank deficiency of the model.

Applying loose constraints to some (or all) of the parameters involved in the adjustment can be interpreted as the "problem with a priori knowledge about the parameters" reported by Vanicek and Krakiwisky (1986) and Monico (1988). Considering the papers reported in the GPS literature, the assumed *a priori* knowledge about the parameters has been subjectively chosen. Heflin *et al* (1992b) have chosen 10 km for each coordinate of the stations and satellite state-vectors, whereas Heflin *et al* (1993) report 10 m to 1 km. Hering *et al* (1991) apply weak constraints on the station position of 10 m and allow the satellite state vector to vary as a random walk process with constraints of 10 m. Brockmann *et al* (1993) use values from 0.02 to 0.10 m for the station positions, and identify the solution as being a free one. Such a case does not represent a strictly free network solution, since the constraints applied to the station coordinates may have effects similar to the case in which the stations are held fixed.

Applying weak constraints to the parameters prompts a strategy to investigate the amount of geodetic information that GPS can provide without using fiducial sites.

8.4 Ordinary and Fiducial Network Data Processing: Results and Discussion

In this section, the discussion has been restricted to the results of the data processing carried out using the ordinary network adjustment, which involves the solutions using the precise ephemerides, and the fiducial network adjustment. In the latter case the 'Free Network Transformed to Fiducial' and 'Full Fiducial' approaches have been included.

8.4.1 Precise Ephemeris Solutions

Three distinct solutions have been carried out by using the precise ephemeris. As outlined before, they are referred to as:

- 1) Free Precise Ephemeris,
- 2) Precise Ephemeris with Fiducial Stations,
- 3) Free Precise Ephemeris Transformed to Fiducial.

(a) The 'Free Precise Ephemeris' Solution

The results obtained in terms of repeatabilities are listed in Table 8.5. They are given for the cartesian (X, Y, and Z) and North (N), East (E) and height (h) coordinates as well as for the baseline components (dN, dE, dh and dL). The RMS's of the baseline components are represented in mm and parts per million (ppm). The recoveries of the known stations were also computed. The RMS's of the recoveries for the eleven known stations are given in Table 8.6 for the daily solutions (Julian Day 208 to 213) and the combined (final) solution.

Table 8.5: Repeatabilities for the 'Free Precise Ephemeris' Solution

Coordinates (mm)						Baseline components (mm ppm)			
X	Y	Z	N	E	h	dN	dE	dh	dL
106	99	51	64	111	86	79 0.013	137 0.021	121 0.019	82 0.010

Table 8.6: Recoveries (mm) for the 'Free Precise Ephemeris' Solution

Solution	X	Y	Z	N	E	h
208	212	124	85	98	160	180
209	113	256	106	105	189	207
210	112	216	72	100	170	160
211	91	189	88	82	135	162
212	39	147	102	87	78	140
213	185	62	49	108	124	115
Final	94	140	64	71	106	128

The values shown in Table 8.5 and Table 8.6 give an indication of the precise ephemeris' quality, because the reference frame (datum) was completely defined by the precise ephemeris. By considering the results given in Table 8.6, it can be seen that they are better than the expected error of 50 cm for the precise ephemeris (Goad, 1993). The worst resulting recovery refers to the Julian Day 209 and is about 30 cm. Precise ephemeris with such level of precision (30 to 50 cm) can support geodetic activities requiring a relative precision of the order of 0.03 ppm of the baseline length.

The repeatabilities of the north and the east coordinate components (64 and 111 mm respectively) are approximately equal to the corresponding recoveries (71 and 106 mm). For height, the repeatability is better than the recovery, ie 86 mm versus 128 mm. Considering that only a precise ephemeris was used to define the reference frame, these results not only show the high quality of the ephemeris, but also the high quality of the data collected during this campaign.

(b) The 'Precise Ephemeris with Fiducial Stations' Solution

The 'Precise Ephemeris with Fiducial Stations' is the strategy normally used at the University of Nottingham when precise ephemeris is used in the data processing. The six fiducial stations used in this data processing were those listed in Table 8.4. Their coordinates were constrained to the ITRF93 values with 2 cm standard error. The repeatabilities of the baseline components are illustrated in Figure 8.2.

The precision illustrated in Figure 8.2 corresponds to 10 to 50 mm in all three coordinate components, for baselines of up to 12,000 km in length. From these results, there is no clear evidence of correlation between precision and baseline lengths. The east and height components showed results with a similar level of precision. The north component provides the most precise results, which are about twice as precise as the east and height components. This may be due to the satellite geometry, which is more favourable to the determination of the north component. The precision related to the length component ranges from 10 to 40 mm.

The day-to-day repeatabilities (precision) of the processing shown in Figure 8.2 are summarised in Table 8.7. The repeatabilities of all the station coordinates (except for the fiducial stations) are also included. For the baseline components, the RMS is given in terms of mm and ppm.

Table 8.7: Repeatabilities for the 'Precise Ephemeris with Fiducial Stations' Solution

Coordinates (mm)						Baseline components (mm ppm)			
X	Y	Z	N	E	h	dN	dE	dh	dL
17	23	15	8	20	24	10 0.003	25 0.006	30 0.006	23 0.005

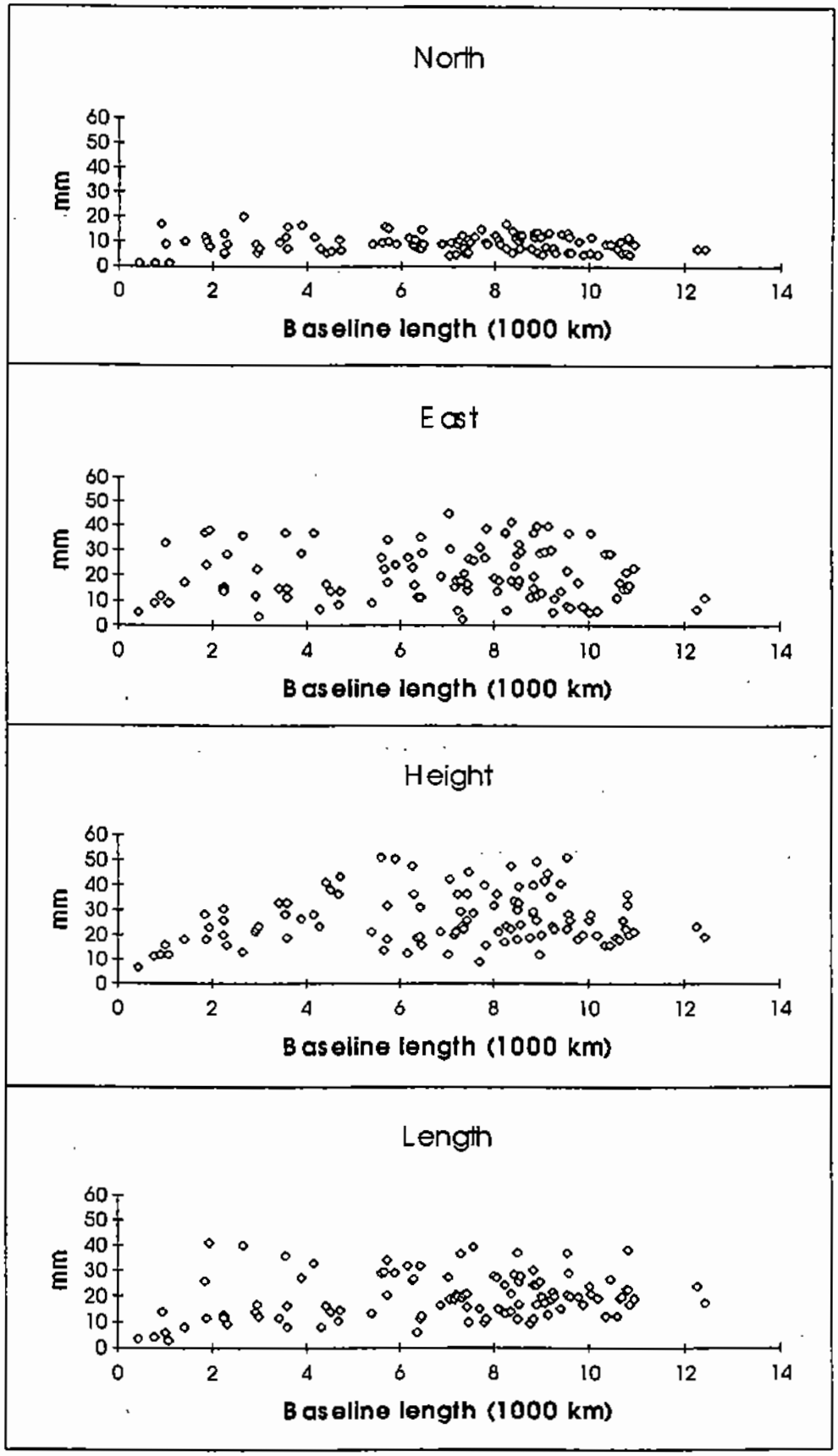

Figure 8.2: Precision for the 'Precise Ephemeris With Fiducial Stations' Solution

The day-to-day repeatabilities given in Table 8.7 again indicate the high quality of the data collected during these six days of the IGS Epoch 92 Campaign. The RMS plan coordinate repeatabilities are better than 20 mm and the RMS height repeatabilities are better than 24 mm. These are equivalent to RMS vector repeatabilities better than 25 ppb (parts per billion) in the plan components, 23 ppb in the baseline length and 30 ppb in the height component.

The coordinates of five ITRF stations were estimated in the network adjustment and used to evaluate the accuracy of the solution. This enables the recoveries of these stations to be obtained. The RMS of the recoveries of these 5 stations are given in Table 8.8 for the final solution (combination of six-daily solutions).

Table 8.8: Recoveries (mm) for the 'Precise Ephemeris with Fiducial Stations' Solution

X	Y	Z	N	E	h
49	46	31	31	40	54

The recoveries provide a good indication of the accuracies of the results. The results given in Table 8.8 show that the repeatabilities (Table 8.7) are about twice as good as the recoveries. It can also be seen that the height component recovery is worse than those of the two horizontal components. The coordinate accuracies of the final solution (combination of six-daily solutions) resulting from this processing are 31, 40 and 54 mm for the north, east and height components respectively.

The fact that the repeatabilities (precision) are about twice as good as the recoveries (accuracy) suggests that some systematic effects exist in the model used in the data processing. Considering, however, that the repeatabilities give an indication of the precision of the solution (approximately 3 cm) and that the accuracy of the ITRF stations is of the order of 2 cm, the resulting recoveries are approximately what could be expected.

(c) **The 'Free Precise Ephemeris Transformed to Fiducial' Solution**

The results of the network adjustment referred to as 'Free Precise Ephemeris' were transformed, via a seven-parameter transformation, to the reference frame defined by the six fiducial stations used in the 'Precise Ephemeris with Fiducial

Stations' approach. Therefore, the results of these two strategies should be similar, since they were referenced to the same framework. The transformation was applied for each daily solution, providing a set of coordinates referenced to the framework realised by the six fiducial stations. The six transformed solutions were then combined together, providing the final solution. The repeatabilities and recoveries of the 'Free Precise Ephemeris Transformed to Fiducial' approach are given in Table 8.9 and Table 8.10 respectively. The RMS's of the residuals of the fiducial stations after the transformation are also included in Table 8.10. They give an indication of the quality of the transformation.

Table 8.9: Repeatabilities for the 'Free Precise Ephemeris Transformed to Fiducial' Solution

Coordinates (mm)						Baseline components (mm ppm)			
X	Y	Z	N	E	h	dN	dE	dh	dL
22	28	23	10	23	34	11 0.003	26 0.007	38 0.008	27 0.005

Table 8.10: Recoveries and RMS's (mm) After Transformation of the 'Free Precise Ephemeris Transformed to Fiducial' Solution

X	RMS X	Y	RMS Y	Z	RMS Z	N	E	h
20	51	17	93	22	57	10	17	28

The worst repeatabilities and recoveries resulting from this solution also refer to the height component. The precisions (repeatability) and accuracies (recovery) of the three coordinate components of this particular solution show good agreement.

The RMS's of the residuals of each coordinate components for the fiducial stations, after applying the transformation, are 51, 93 and 57 mm for the X, Y and Z coordinates respectively. These values give an indication of the quality of the transformation, since they show the level of recoveries of the fiducial stations after the transformation. They absorb some of the errors in the model, which in this case are likely to be mainly due to ephemeris errors. Such errors were therefore eliminated by the transformation process. Notice that they are worse than the recoveries of the final solution, which were remarkable good, ie 20, 17 and 22 mm in X, Y and Z respectively (see Table 8.10).

8.4.2 The Fiducial Network Solutions

(a) 'Full Fiducial' Solution

The aim of performing this solution was to test the GAS software in the processing of a large network and to compare the results of the 'Full Fiducial' approach with that of the ordinary network adjustment, in which a precise ephemeris is used in conjunction with fiducial stations, and with the 'Free Precise Ephemeris Transformed to Fiducial' approach. Such analysis may provide a base for future projects.

In the 'Full Fiducial' approach the position and velocity of the satellites (state-vector) and a solar radiation pressure parameter for each satellite were estimated in the adjustment (§4.4.2). Six of the eleven available fiducial stations were used as fiducial stations, which are listed in Table 8.4. The coordinates of the other five ITRF stations were estimated in the fiducial network adjustment, providing a means of evaluating the accuracy of the solution.

The day-to-day repeatabilities of the solution are listed in Table 8.11. The recoveries of the solution are listed in Table 8.12.

Table 8.11: Repeatabilities for the 'Full Fiducial' Solution

Coordinates (mm)						Baseline components (mm ppm)			
X	Y	Z	N	E	h	dN	dE	dh	dL
25	38	19	14	28	38	14 0.004	28 0.007	43 0.009	31 0.006

The precision of this solution is of the order of 43 mm (9 ppb) for the worst case, the baseline height component. The plan baseline components are about twice as good as that of the height component. The length component provides precision of the order of 31 mm (6 ppb). One can also observe that the repeatabilities (Table 8.11) are better than the recoveries (Table 8.12). Whereas the precision of the height component is about 38 mm (Table 8.11), the recovery is 64 mm (Table 8.12). For the plan coordinate components (north and east), it can be seen that the repeatabilities and recoveries are quite similar.

Table 8.12: Recoveries (mm) for the 'Full Fiducial' Solution

X	Y	Z	N	E	h
35	43	46	18	28	64

The better repeatability of the height component compared with its accuracy again suggests the presence of some systematic effects in the data processing. However, as stated before, such a level of accuracy is approximately as expected if one considers the precision of the solution obtained (38 mm) and the claimed accuracy of the ITRF stations (20 mm).

(b) 'Free Network Transformed to Fiducial' Solution

Although a more detailed discussion on free network adjustment is outlined within the context of a global reference frame (§8.5), one of the results presented there is used in this section in order to compare the results of the different strategies.

The results of the free adjustment were transformed to the same reference frame defined by the fiducial stations, using the 'Full Fiducial' approach. Such a solution is referred to as 'Free Network Transformed to Fiducial'. The fiducial and transformed solutions are referenced to the same framework and may therefore be directly compared.

In this strategy, the free network solution involved the application of loose constraints to the approximate coordinates of the stations. The ITRF stations were constrained to 1000 m and the new stations to 100 000 m. Before performing the transformation from the free solution, to the reference frame defined by the six fiducial stations (Table 8.4), internal constraints (§4.8.2) were applied to the covariance matrix of the daily and combined solutions (see §8.5.2).

In order to analyse the results of this solution, the repeatabilities and recoveries are given in Tables 8.13 and 8.14 respectively. Table 8.14 also gives the RMS's of the residuals of the fiducial stations after the transformation.

Table 8.13: Repeatabilities for the 'Free Network Transformed to Fiducial' Solution

Coordinates (mm)						Baseline components (mm ppm)			
X	Y	Z	N	E	h	dN	dE	dh	dL
31	40	28	18	30	47	17 0.004	27 0.007	49 0.011	39 0.007

Table 8.14: Recoveries and RMS's (mm) After the Transformation of the 'Free Network Transformed to Fiducial' Solution

X	RMS X	Y	RMS Y	Z	RMS Z	N	E	h
24	36	17	50	15	44	14	25	17

The results obtained from this solution show that the accuracies are better than the repeatabilities, differing from all previous solutions. The better recoveries should be due to errors eliminated during the transformation process. These errors are represented by the residuals of the coordinates of the stations used in the transformation, whose RMS's are given in Table 8.14.

The RMS's of the residuals of the fiducial stations after the transformation are 36, 50 and 44 mm for X, Y and Z respectively. The recoveries of the same components, ie X, Y and Z are 24, 17 and 15 mm respectively.

8.4.3 Comparisons of the Results

In order to analyse the agreement of the solutions, comparisons have been carried out by taking into account the repeatabilities and recoveries of the cartesian coordinate components for similar solutions. In the ordinary network adjustment, a comparison has been carried out between the 'Precise Ephemeris with Fiducial Stations' and 'Free Precise Ephemeris Transformed to Fiducial' solution. The 'Full Fiducial' approach has been compared with the 'Precise Ephemeris with Fiducial Stations' and 'Free Network Transformed to Fiducial' approaches.

(a) 'Precise Ephemeris with Fiducial Stations' versus 'Free Precise Ephemeris Transformed to Fiducial'

This comparison is to evaluate the results obtained from the approach in which the fiducial stations were fixed during the processing and that where a

transformation was performed to the fiducial stations as the last step of the processing.

The solution (1) represents the 'Precise Ephemeris With Fiducial Stations' and solution (2) the 'Free Precise Ephemeris Transformed to Fiducial'. A summary of the repeatabilities and the recoveries of each solution is listed in Table 8.15.

Table 8.15: Repeatabilities and Recoveries of the Solutions

(1) 'Precise Ephemeris With Fiducial Stations '

(2) 'Free Precise Ephemeris Transformed to Fiducial'

Baseline components	day-to-day repeatability		Recoveries Final Solution	
	Sol. (1)	Sol. (2)	Sol. (1)	Sol. (2)
X (mm)	17	22	49	20
Y (mm)	23	28	46	17
Z (mm)	15	23	31	22

By analysing the values in Table 8.15, it can be seen that whereas the repeatabilities of the solution 'Precise Ephemeris with Fiducial Stations' (solution (1)) are slightly better than those of the 'Free Precise Ephemeris Transformed to Fiducial' (solution (2)), the recoveries of solution (2) are much better than those of solution (1). The maximum discrepancy between the repeatabilities of both approaches was 8 mm in the Z component. The better recoveries of the transformed solution are due to the fact that some errors (e.g. ephemeris errors) were eliminated in the transformation process. The RMS's of the residuals of the fiducial station coordinates after the transformation, which were 51, 93 and 57 mm for X, Y and Z respectively (see Table 8.10), give an indication of the errors involved.

It can be seen clearly from this analysis that, in terms of accuracy, the 'Free Precise Ephemeris Transformed to Fiducial' approach is superior to the traditional one (solution (1)). Furthermore, this approach has the advantage of providing a means of changing the reference stations, by simply performing a transformation from the 'Free Precise Ephemeris' solution to the chosen reference stations, as the last step in the processing.

(b) 'Precise Ephemeris With Fiducial Stations' versus 'Full Fiducial'

The 'Precise Ephemeris with Fiducial Stations' approach (solution (1)) has also been compared with the 'Full Fiducial' approach (solution (3)). The aim was to test the latter in the context of a very large network. The repeatabilities and recoveries of these solutions are listed in Table 8.16.

Table 8.16 : Repeatabilities and Recoveries of the Solutions

(1) 'Precise Ephemeris With Fiducial Stations' (3) 'Full Fiducial'

Baseline components	day-to-day repeatabilities		Recoveries Final Solution	
	Sol. (1)	Sol. (3)	Sol. (1)	Sol. (3)
X (mm)	17	25	49	35
Y (mm)	23	38	46	43
Z (mm)	15	19	31	46

From the results shown in Table 8.16, it can be seen that the repeatabilities of solution (1) are better than those of solution (3) for the three coordinate components. The recoveries of solution (3) for X and Y components are better than solution (1). For the Z component, however, the recoveries of solution (1) are better than solution (3). Considering the resulting recoveries of the three coordinate components $[(X^2 + Y^2 + Z^2)^{1/2}]$ for both solutions, they are quite similar, ie 74 and 72 mm for solution (1) and (3) respectively.

From a global point of view the 'Precise Ephemeris with Fiducial Stations' approach provided slightly better results than those of the 'Full Fiducial' approach. This may be due to a better quality of the ephemerides used in the former approach. The 'Full Fiducial' approach tested in this experiment involved a network of 16 stations, but only six were used as fiducial stations. The JPL approach to estimate the precise ephemerides involved all 30 IGS core stations, with eight of them as fiducial sites (Zumberge *et al*, 1993).

(c) 'Full Fiducial' versus 'Free Network Transformed to Fiducial'

In this section, the 'Full Fiducial' approach (solution (3)) has been compared with the 'Free Network Transformed to Fiducial' approach, identified as solution (4). As the fiducial stations involved in each of these approaches are the same (Table 8.4), the results are referenced to the same framework and are therefore suitable for a direct comparison. The repeatabilities and recoveries of these solutions are listed in Table 8.17.

Table 8.17: Repeatabilities and Recoveries of the Solutions

(3) 'Full Fiducial' (4) 'Free Network Transformed to Fiducial'

Baseline components	day-to-day-repeatability		Recoveries Final Solution	
	Sol.(3)	Sol.(4)	Sol.(3)	Sol.(4)
X (mm)	24	31	35	24
Y (mm)	38	40	43	17
Z (mm)	19	28	46	15

The results presented in Table 8.17 show reasonable agreement between solution (3) and solution (4) in terms of repeatabilities. Solution (4), however, provided much better recoveries than those of solution (3). This reflects the errors eliminated in the transformation process. Taking into account such errors, represented by the RMS's of the residuals of the fiducial station coordinates after the transformation, which are 36, 50 and 44 mm for X, Y and Z respectively (see Table 8.14), it can be seen that they are quite similar to the recoveries of the 'Full Fiducial' approach.

(d) Summary

The 'Precise Ephemeris with Fiducial Stations' approach (solution (1) provided similar results to the 'Full Fiducial' approach (solution (3)), the latter being slightly worse.

The 'Free Precise Ephemeris Transformed to Fiducial' (solution (2)) and the 'Free Network Transformed to Fiducial' (solution (4)) approaches provided the best recoveries, which are quite similar in both approaches (see Tables 8.15 and 8.17). However, the RMS's of the residuals after the transformation for solution (4) are much better than solution (2) (see Tables 8.10 and 8.14), suggesting that the former solution provided better results than the latter.

8.5 Establishment of a Global Reference Frame Using GPS

In order to investigate the establishment of a global reference frame by GPS, solutions adopting the free network approach have been carried out. Firstly, an investigation on the effects of applying weak constraints to some of the parameters (coordinate positions) involved in the adjustment, was carried out.

8.5.1 The Effects of Applying Weak Constraints to the Parameters

Some tests were carried out to investigate the effects on the results by imposing different values to the so called loose (weak) constraints. Such tests can also provide a means to interpret the information contained in the GPS observations and in the dynamic model describing the satellite orbits.

The position and velocity (state-vector) of the satellites were held free for all tests carried out as well as an additional solar radiation pressure parameter (§4.2.2) per satellite. The tests were as follows:

Test 1: All stations were held free,
Test 2: The coordinates of the ITRF stations were constrained to 1000 m and the new stations to 100 000 m,
Test 3: The coordinates of all stations were constrained to 1000 m,
Test 4: One ITRF station (RCM2) was constrained with 2 cm standard error for each coordinate and all other stations were held free,
Test 5: The coordinates of the ITRF stations were constrained to 10 m and the new stations to 1000 m
Test 6: The coordinates of all stations were constrained to 10 m.

The approximate station positions, wherever possible were taken from the ITRF93 and mapped to the epoch of the campaign by using the corresponding velocity field (Table 8.3). Otherwise, they were taken from the results estimated in the baseline pre-processing. Such cases involved the new stations, ie the Brazilian stations (PARA, UEPP and BRAS) and STLH and ARNA (see Table 8.1).

The average standard errors (from the covariance matrix) of all the estimated station coordinates for each of these tests are listed in Table 8.18. These values give an indication of the GPS formal precision, without fixing any fiducial stations (apart from test 4). The square root of the variance factor, ($\hat{\sigma}_0$), is also included to aid the interpretation of the results. They refer to the Julian day 212, and are similar in the other days.

Table 8.18: Average Standard Errors (mm) of the Free Network Solutions

Coordinate	Test 1	Test 2	Test 3	Test 4	Test 5	Test 6
X (mm)	12 000	31	25	13	2	2
Y (mm)	14 000	34	27	12	2	2
Z (mm)	30	28	24	5	2	2
$\hat{\sigma}_0$	9.4	9.75	9.75	9.80	10.59	15.23

As expected (§8.3.3), the Z component provides the best precision due to the fact that it is implicitly constrained by the earth's daily rotation. It is remarkable how the precision of the coordinates improves from test 1 to test 2 by simply applying very loose constraints of 1000 and 100 000 m to the ITRF and new stations respectively, instead of holding all stations free. The improvement is about 3 orders of magnitude for the X and Y components and the Z component maintains the same level of precision. The results of test 3 have provided further improvement with respect to test 2. The precision provided by test 4 (only one station is constrained) is more than two times better than that of test 3, in which all stations were constrained to 1000 m. Test 5 provided precision at the mm level, but the *a posteriori* variance factor increased slightly compared with the previous tests. The precision resulting from test 6 is at the same level of test 5, but the *a posteriori* variance factor differs significantly from all the previous tests.

A further analysis of Table 8.18 also shows that the rank deficiency in the model is not a real one, but a *quasi* rank defect. Otherwise, the solution in which all stations were held free (test 1) could not be obtained by using conventional least squares, since the normal equation matrix would be singular. It means that the model also provides information relating to the orientation of the network.

Analysing the estimated variance factor or unit variance, ($\hat{\sigma}_0^2$), all the adjustment tests except for test 6 would be accepted by the *global test statistic* (§3.2.2) at the 5% significance level. The problem relating to test 6 could be due to the fact that constraints were applied to the new stations at the same level as the ITRF stations, an inappropriate strategy.

It should be pointed out that each of these solutions provides its own realisation of a global reference frame and is (almost) independent of any other positioning system.

A direct comparison between the coordinates estimated in each of these tests and the ITRF93 coordinates was carried out in order to perform a further analysis of the deficiency of the different models. The RMS's of the discrepancies are listed in Table 8.19.

Table 8.19: RMS's of the Discrepancies Between the Coordinates Estimated in the Free Network Solutions and the ITRF93 Values

Solution	dN (m)	dE (m)	dh (m)
Test 1	0.240	1089.500	0.216
Test 2	0.172	0.269	0.184
Test 3	0.143	0.265	0.155
Test 4	0.071	0.189	0.115
Test 5	0.009	0.007	0.009
Test 6	0.066	-0.018	0.011

From the first solution it is clear that the predominant deficiency is orientation, implicitly given by the E component. Although less clear, such a deficiency is also present in tests 2, 3 and 4. The results of test 5 are compatible with the ITRF93, since the discrepancies are better than the expected precision of the ITRF coordinates (2 cm). The conclusion derived from test 5 is that constraining the coordinates to the ITRF at the 10 m level, has effects 'almost' similar to fixing these coordinates. The results of test 6, compared with test 5, are much worse, since the new stations were constrained at the same level as the ITRF ones.

The improvement of the precision of the station coordinates (e.g. from 1000 m to the decimetre level) should be due to the good geometry provide by the GPS satellites within a global network, to the strength of the observations and also to the model of force used. Such initial results suggest that GPS is able to provide highly accurate results independent of other positioning systems.

8.5.2 Global Coordinates Using GPS

In the further investigations related to the free network solutions, the conditions applied in test 6 were not applied again since they were already proved inappropriate. The conditions involved in test 3, although accepted by the *global test statistic*, were also not applied again. Notice that the constraints applied in test 3 did not take into account the fact that more about the ITRF stations was known than the new ones. It was accepted by the test statistic probably due to the fact that the constraints were very weak and that they did not affect the observations involved in the model.

The next stage in this investigation involved the processing of the six-day data. For each of the tests which was thought to provide suitable results after the initial investigation (Test 1, Test 2, Test 4 and Test 5), three different solutions were performed:

1) The combined solution (§8.3) of the free and very loose constrained approaches (X and Σ_X) were mapped to the ITRF93 via a seven-parameter transformation (§4.8.1)

2) Internal constraints (§4.8.2) were applied only to the covariance matrix of the combined solution (Σ_X) by using the program CONSCOV3 (CONStraints COVariance with 3 internal constraints) (§5.4.3). From the new covariance matrix, only the 3x3 blocks related to the 3 coordinates of each station were taken into account, since the full covariance matrix is singular (§4.8.2). It means that the correlation between stations was not considered. One possible solution would be to make use of the pseudo inverse of the matrix (Monico, 1988; Blewitt, 1995). The combined solution with the new covariance matrix was mapped to the ITRF93 via a seven-parameter transformation (§4.8.1).

3) Internal constraints were applied to the covariance matrix of each daily solution in the same way as solution 2. The daily solutions (with the covariance matrix constrained) were mapped to the ITRF93 via a seven-parameter transformation. From these seven parameters, only the orientation parameters were applied to each corresponding constrained daily solution. Such a strategy provided an orientation to the network. The 'oriented' solutions were then combined together to provide a final

solution. It was then transformed to the ITRF93, but using only a four-parameter transformation (translations and scale).

The orientation parameters used in strategy 3 were computed using the seven-parameter transformation, because they were correlated with the translations. If the GPS solution's location of the geocentre disagrees with the reference solution, the estimate of 3 angles alone will absorb some of the translation offset, thus giving erroneous orientation (Blewitt *et al*, 1993b).

In order to perform solutions 2 and 3 above, some options of CARNET program were essential (§5.2.3). The main stages involved in solutions 2 and 3 are illustrated in Figure 8.3. The GAS POSITION/COVARIANCE file, obtained from PANIC program is the input for both solutions.

From Figure 8.3 it can be seen that besides using the CARNET program, two other programs were also involved in the strategies. They were CONSCOV3 and DEGRADE. The former was developed to apply internal constraints to the covariance matrix (§5.4.3) and the latter (§5.2.3) provides options of neglecting the correlation among all or part of the parameters involved in the covariance matrix. For this case, only correlation between stations was neglected.

Some tests were also carried out using the program CONSCOV7 (§5.4.3), in which seven internal constraints were involved (§4.8.2). As the network deficiency is in orientation, such a strategy was considered inappropriate, though the improvement of the covariance matrix was more significant than that using CONSCOV3. Blewitt *et al* (1992) have made use of the seven internal constraints.

Some information for the three solutions, applied to the tests 1, 2, 4 and 5 is listed in Table 8.20. Included is the seven-parameter transformation for solutions (1) and (2), four-parameter transformation (3 translation and 1 scale factor) for solution 3 and the RMS's of the residuals after the transformation for all the solutions.

PANIC	
GAS POSITION/COVARIANCE FILE	
Solution 2	Solution 3
1	1. Apply internal constraints to the DAILY COVARIANCE MATRICES, using the CONSCOV3 program.
2.	2. Degrade each CONSTRAINED DAILY COVARIANCE MATRIX to blocks of 3x3 (banded), using the DEGRADE program.
3.	3. Estimate a 7-parameter transformation for each daily solution (with CONSTRAINED DAILY COVARIANCE MATRIX) with respect to ITRF93, using CARNET program.
4.	4. Apply the 3 parameters (rotations) estimated in 3.3 to transform each daily solution, using the CARNET program, invoking a NEW DAILY COVARIANCE MATRIX as output.
5..	5. Create a new GAS POSITION/ COVARIANCE file for each daily solution using the output from 3.4
6. Compute a combined solution, using CARNET program, invoking a COMBINED COVARIANCE MATRIX as output	6. Compute a combined solution, using the CARNET program, invoking a CONSTRAINED COVARIANCE MATRIX as output.
7.	7. Create a new GAS POSITION/ COVARIANCE file for the combined solution using the output from 3.6
8. Apply internal constraints to the COMBINED COVARIANCE MATRIX using CONSCOV3 program.	8.
9. Degrade the CONSTRAINED COMBINED COVARIANCE MATRIX to blocks of 3x3 (banded), using the DEGRADE program.	9.
10. Estimate a 7-parameter transformation for the combined solution (with CONSTRAINED COMBINED COVARIANCE MATRIX) with respect to ITRF93, using CARNET program.	10 Estimate a 4-parameter transformation for the combined solution (with CONSTRAINED COMBINED COVARIANCE MATRIX) with respect to ITRF93, using CARNET program.
11. Apply the 7 parameters estimated in 2.10 to transform the combined solution (with CONSTRAINED COMBINED COVARIANCE MATRIX) to the ITRF93 using CARNET program	11. Apply the 4 parameters (translations and scale) estimated in 3.10 to transform the combined solution (with CONSTRAINED COMBINED COVARIANCE MATRIX) to the ITRF93, using the CARNET program.

Figure 8.3: Main Stages Involved in Solutions 2 and 3

Table 8.20: Transformation Parameters and RMS's of the Residuals After the Transformation From Individual Solutions to ITRF93

	Test 1			Test 2			Test 4			Test 5		
Para-meter	Solution 1	Solution 2	Solution 3	Solution 1	Solution 2	Solution 3	Solution 1	Solution 2	Solution 3	Solution 1	Solution 2	Solution 3
Tx (cm)	0.69	-8.8	4.4	2.47	-10.09	-1.52	4.17	-8.41	-1.49	-0.07	-0.16	-0.05
±	15.45	4.6	3.9	11.83	2.17	2.14	11.54	2.78	0.29	0.38	0.31	0.21
Ty (cm)	16.24	14.52	12.56	15.34	13.77	12.67	10.43	5.36	8.79	0.01	0.07	0.09
±	14.75	'4.2	3.66	11.26	2.02	1.97	3.73	1.43	1.71	0.37	0.30	0.21
Tz (cm)	-14.78	-33.04	-10.28	-10.41	-16.18	-1.88	6.47	-11.46	-4.24	-0.21	-0.06	-0.11
±	39.30	3.33	3.56	25.70	1.57	1.95	2.91	1.0	0.82	0.36	0.26	0.20
Rx (.001")	.67	.34	-	.58	1.64	-	0.58	2.64	-	0.06	0.02	-
±	1.32	1.42	-	1.03	.68	-	1.03	0.38	-	0.14	0.10	-
Ry (.001")	-0.04	-3.29	-	-0.04	-1.85	-	-0.06	-1.10	-	-0.02	-0.06	-
±	1.24	1.44	-	0.98	.68	-	0.98	0.62	-	0.14	0.10	-
Rz (.001")	540.98	32 633.9	-	2.44	-0.03	-	2.17	-1.93	-	0.00	-0.00	-
±	8269.7	1.56	-	19.88	0.74	-	3.94	0.84	-	0.14	0.11	-
S (ppm)	0.0204	0.0412	0.0401	0.0186	0.0183	0.0187	0.0179	0.0172	0.0155	0.0006	0.0005	0.0005
±	0.01	0.00	0.00	0.01	0.00	0.00	0.01	0.00	0.00	0.00	0.00	0.00
RMS X (cm)	49 600.0	4.96	9.6	10.00	3.4	6.6	11.28	4.3	7.8	0.42	0.44	0.42
RMS Y (cm)	51 800.0	6.20	7.7	6.0	3.8	4.7	7.2	3.5	5.1	0.46	0.47	0.48
RMS Z (cm)	13.8	9.4	13.2	7.0	3.4	8.1	6.0	3.6	7.3	0.62	0.60	0.64

Test 1: All Stations Free

Test 2: ITRF stations constrained to 1000 m and NEW to 100 000 m

Test 4 : 1 Station (RCM2) constrained to 2 cm

Test 5: ITRF stations constrained to 10 m and NEW to 1000 m.

The results presented in Table 8.20 do not rely on fixing any fiducial station coordinates, except in test 4 where the coordinates of one station were constrained to the ITRF93 values with 2 cm standard error. From Table 8.20, except solution 1 of test 1, it can be seen that GPS provides very accurate results. The maximum RMS after the transformation was 13.2 cm (Z component) in solution 3 of test 1.

From test 1, the deficiency of the network in orientation can be clearly seen again. In the free solution (solution 1 of test 1), the precision of the rotation about Z was poorly estimated (540.98 ± 8269.7 *mas*[8.1]). Once internal constraints were applied to the covariance matrix of the combined solution, (solution 2 of test 1), the orientation about the Z-axis was estimated with a precision of 1.56 *mas*, and the estimated rotation was about 33 ".

The results of test 2 and test 4, concerning the transformation parameters, were quite similar if one takes into account the precision of the estimated parameters. One can also confirm from test 4 that the main network deficiency is in orientation. This can be explained by the fact that constraining one station in this test (RCM2) did not significantly change the translation parameters relative to test 1 (free solution), but the rotation parameters changed.

Results from Table 8.20, concerning solution 2 of tests 1, 2 and 4, show that the RMS's of these solutions were always better than the solutions 1 and 3. One can also assess that solution 2 of tests 2 and 4 agrees with ITRF after the transformation by better than 4.3 cm. Clearly, solution type 2 has provided the best results.

In the solution 2 of test 2, the RMS's after the transformation were better than 3.8 cm for all three components. This result was obtained with the inclusion of all ITRF stations in the transformation. Excluding the station with the worst RMS (SANT) from the transformation, the RMS's of the X and Y coordinates were slightly better than those reported by Blewitt *et al* (1992) (see Table 8.21) and the RMS of the Z component reduced to 3.0 cm.

Finally, test 5, in which the ITRF stations were constrained to 10 m and the new stations to 1000 m, provided the best results, which were compatible with

[8.2] 1 mas = 0.001"

the precision of the ITRF. The maximum RMS was 6.4 mm in the Z component. Concerning the transformation parameters, the maximum absolute value was 2.1 mm, taking into account solutions 1, 2 and 3. This is a remarkable result, since no fiducial constraints were used.

It can be seen from Table 8.20 that the estimated transformation parameters for test 5 are smaller than the corresponding standard deviations. Therefore, such parameters have no meaning of being estimated. This shows that applying constraints at the 10 m level has effects almost similar to the case in which the stations are fixed. Therefore, at such a case, no internal constraints need be applied.

The transformation parameters from test 5 (solution 1) to ITRF93 were also computed considering only translation. They were 0.01, 0.03 and 0.00 cm for Tx, Ty and Tz respectively. The RMS's of the three components were 0.44, 0.50 and 0.66 cm for X, Y and Z respectively, which indeed agree with solutions 1, 2 and 3.

Some of the solutions presented in Table 8.20 have been compared with results reported by other researchers in order to have a further assessment of the results obtained. Mur *et al*, (1993) describe a free network solution (all stations free) for three periods of about 10 days of data and for a total of 33 days (Epoch '92 campaign) involving a total of 30 stations. The seven-parameter transformation for one of these solutions (with the smallest RMS) with respect to the IERS/IGS (Boucher and Altamini (1993b)) set of coordinates are listed in Table 8.21. The standard errors are not given, since they were not described in the original solution. This solution is referred to as the *Mur solution*. The results obtained by Blewitt *et al*, (1992) are also listed in Table 8.21 and referred to as the *Blewitt solution*. It involves 21 days of GPS data from 21 globally distributed receivers operating during early 1991. No fiducial stations were held fixed, but the ITRF90 stations and satellite state-vector coordinates were constrained with 10 km standard deviations. The transformation parameters are related to the ITRF90.

The experiments described in this research involved only 6 days of data and 16 stations occupied during the IGS Epoch '92 Campaign. Therefore, this data set represents a different situation compared with the two experiments cited above. Nevertheless, a comparison between these solutions has been performed. The

solution 2 of test 1, referred to as *Sol. 1-2*, and solution 2 of test 2, referred to as *Sol. 2-2* have been listed in Table 8.21 for comparison. The parameters of the transformation of these two solutions have been computed with respect to the ITRF93.

Table 8.21: Transformation Parameters and RMS's of the Residuals After Transformation of Each Solution to a Global Reference Frame

Solu -tion	Tx (cm)	Ty (cm)	Tz (cm)	Rx (.001")	Ry (.001")	Rz (.001")	S (ppm)	RMS (cm)		
								X	Y	Z
Mur	-3.0	14.1	-187.7	-2.19	-4.39	-87.77	0.006	7.5	8.2	13.5
Blewitt	-7.5	13.0	-14.8	1.23	0.08	-61.77	-0.004	2.0	2.3	1.8
Sol 1-2	-8.8	14.5	-33.0	0.34	-3.29	32633.9	0.041	5.0	6.2	9.4
Sol. 2-2	-10.9	13.8	-16.2	1.64	-1.85	-0.03	0.018	3.4	3.8	3.4

Notice that each solution has its own parameters of transformation computed with respect to a particular reference frame. For the purpose of this analysis, no distinction is made about these reference frames, since they have approximately the same level of precision. Furthermore, the aim of this comparison was only to further assess the quality of the results obtained.

Taking into account the RMS's of the residuals after the transformation, the best results of these four solutions is the *Blewitt solution*. It is not a strictly free solution unlike the *Mur Solution* and *Sol. 1-2*, since the coordinates of the stations and satellite state-vectors were constrained to 10 km. The translation parameters of the *Blewitt solution* and *Sol. 2-2* agree quite well. The RMS's of the latter are, nevertheless, slightly worse.

The most significant discrepancies between these four solutions are the translation Tz of the *Mur solution* and the rotation Rz of the *Sol.1-2* . It should be pointed out that an uncertainty of about 33" in rotation about the Z axis, corresponds to an uncertainty of about 1000 m in the East (longitude) component. It is approximately the value listed in Table 8.19 for test 1. Notice that once the free coordinates were constrained (*Sol. 2-2*), the uncertainty in rotation about the Z axis was almost irrelevant (-0.03 *mas*).

An additional solution was carried out in order to investigate further the fact that there was a very large orientation parameter compared with the other two

solutions. Therefore, a solution in which only the satellite state-vector positions were loosely constrained to 10 km was carried out, as in the *Blewitt solution*, but all stations were left free. The orientation parameter about the Z-axis reduced to 5.38 ±18.74 *mas* in the solution without internal constraints (type solution 1) and to 3.97 ± 0.75 *mas* once internal constraints were applied (type solution 2). Such results, besides showing that the global solutions obtained appear to be reliable, also point out the remarkable effects produced by simply constraining the satellite-state vector positions to 10 km.

Since ITRF errors are expected to be at the 10^{-9} level (Blewitt *et al*, 1992), the scale differences do appear to be significant. The results listed in Table 8.20, except those of Test 5, are at the 10^{-8} level. Notice that the *Mur* and the *Blewitt* solutions listed in Table 8.21 agree with the ITRF level of precision. In the latter solution (Blewitt *et al*, 1992), the model of the earth's gravity field used was the GEM-T2, including coefficients of up to the order and degree 12. In GAS, this is currently represented by the WGS84 earth gravity model, with coefficients of up to the order and degree 8 (§4.4.1). Further investigation should be carried out but one reason to explain the scale differences may be due to the use of a different earth gravity model.

Most of the results presented so far have shown that GPS can provide results of high accuracy. Notice that no stations were fixed in the processing. Although limited tests were carried out concerning this topic, there is evidence that GPS alone can provide a highly accurate global reference frame. The deficiency in orientation is also present in the systems capable of providing the geocentre, such as SLR and LLR. The estimated translation parameters from the GPS solution to the ITRF represent geocentric offsets, which are at the decimetre level, therefore, deviating significantly from zero. This may illustrate one aspect of orbit mis-modelling, requiring further investigation.

8.6 Comparison Between the Brazilian Stations Estimated in the Inter-Continental Network and in the Brazilian HPN

Some of the stations involved in the processing of the IGS Epoch '92 Campaign in Brazil, described in Chapter 7 and referred to as Brazilian HPN (High Precision Network), were also included in the inter-continental network processing described in this chapter. As these two solutions were referenced to the ITRF93, a direct comparison was carried out between the

Brazilian stations belonging to both networks. The discrepancies between these two solutions are listed in Table 8.22. For the inter-continental network, a type solution 1 of test 5 (see Table 8.20) was used after transforming to the ITRF93, but only translations were considered.

Table 8.22: Discrepancies (mm) Between the Inter-Continental and the Brazilian IGS Epoch '92 GPS Networks

Stations	dX	dY	dZ	dN	dE	dh
PARA	-37	59	19	-12	10	-70
UEPP	-28	55	11	-12	12	-60
BRAS	-18	53	6	-13	22	-50
RMS	28	55	12	12	16	60

The RMS's of the discrepancies between both solutions are at a maximum of 60 mm in height component and 12 and 16 mm for north and east respectively. These values correspond approximately to the expected accuracy of the Brazilian HPN solution (8 cm). Clearly, it can be seen that there are biases between both solution, which reflect the level of precision of the solution presented in Chapter 7.

The coordinates of the Brazilian stations plus the stations ARNA and STHL are listed in Table 8.23. These values, together with those coordinates given in Table 8.3, represent one of the final solutions of the inter-continental network. The estimated standard deviations of the coordinates of the Brazilian stations are of the order of 2 cm.

Table 8.23: Estimated Coordinates Referenced to the ITRF93 on 1 July 1992

STATION	X(m)	$\hat{\sigma}_X$ (mm)	Y(m)	$\hat{\sigma}_Y$ (mm)	Z(m)	$\hat{\sigma}_Z$ (mm)
PARA	3 763 751.731	19	-4 365 113.865	19	-2 724 404.845	11
UEPP	3 687 624.362	20	-4 620 818.644	20	-2 386 880.466	11
BRAS	4 114 500.496	23	-4 551 173.150	21	-1 741 210.639	10
STHL	6 104 823.994	34	-605 863.070	22	-1 740 699.634	15
ARNA	2 587 441.591	14	-1 042 831.292	9	5 716 573.554	22

The repeatabilities of the stations listed in Table 8.23 are given in Table 8.24.

Table 8:24 Coordinate Repeatabilities(mm) for the Inter-Continental GPS Network

X	Y	Z	N	E	h
25	35	14	7	35	29

It is important to notice that the repeatabilities (Table 8.24) and the coordinate standard errors (Table 8.23) agree quite well. The repeatabilities give an indication of the precision of the coordinates of these stations. The coordinates of the Brazilian stations are therefore estimated with a precision better than 3.5 cm.

8.7 Summary

The processing of an inter-continental GPS network has been described in this chapter. Several strategies have been applied, which include ordinary network adjustment, fiducial network adjustment and free (or non-fiducial) network adjustment.

Considering the several results obtained from the different tests carried out, it can be concluded that the GAS software has been extensively tested for the processing of very large GPS networks, even a global one and has provided satisfactory results.

For the ordinary network adjustment approach applied to the inter-continental network, three solutions have been tested, namely 'Free Precise Ephemeris', 'Precise Ephemeris with Fiducial Stations', and 'Free Precise Ephemeris Transformed to Fiducial'. As expected, the worst results in terms of repeatabilities and recoveries were obtained using the 'Free Precise Ephemeris' solution, in which only the satellite positions were fixed. The recoveries obtained using this solution provided an approximate indication of the accuracy of the precise ephemeris used in the processing. The ephemeris errors are directly transferred to the stations coordinates, since no stations are fixed in the adjustment. The results showed accuracies compatible with the values claimed in the literature, ie better than 30 cm.

The 'Free Precise Ephemeris' solution was transformed to the same reference frame defined by the stations which were used as fiducial stations in the 'Precise Ephemeris with Fiducial Stations'. The transformed solution, referred to as 'Free Precise Ephemeris Transformed to Fiducial' solution, provided the best accuracies, which were 20, 17 and 22 mm for X, Y and Z respectively, compared with 49, 46 and 31 mm of the 'Precise Ephemeris with Fiducial Stations' approach. The precision, however, was slightly worse than that of the 'Precise Ephemerides with Fiducial Stations'. The maximum discrepancy between the repeatabilities of both approaches was 8 mm in the Z component. The better recoveries of the transformed solution are due to the fact that some errors (eg ephemeris errors) were eliminated in the transformation process.

The comparison between the approaches 'Full Fiducial' and 'Precise Ephemeris with Fiducial Stations' demonstrated that from a global point of view in terms of repeatabilities and recoveries, the latter provided slightly better results. The repeatabilities of the 'Full Fiducial' approach were 25, 38 and 19 mm in X, Y and Z respectively and 17, 23 and 15 mm in the 'Precise Ephemeris with Fiducial Stations'. The resulting recoveries of the three components were slightly better in the 'Full Fiducial' approach, ie 72 mm opposed to 74 mm in the latter. Such results show that the precise ephemeris used in the data processing (JPL precise ephemeris) was better determined than in the 'Full Fiducial' approach used in this test, in which only six fiducial stations were used. The precise ephemerides determined by JPL for the IGS Epoch' 92 involved the 30 IGS core stations, with eight of them fixed as fiducial.

The free (or non-fiducial) approach solution was transformed to the reference frame defined by the fiducial stations used in the 'Full Fiducial'. This approach is referred to as 'Free Network Transformed to Fiducial'. The recoveries and repeatabilities of both approaches have been compared. In terms of repeatabilities they are quite similar, but the recoveries in the 'Full Fiducial' approach were much worse. They were 35, 43 and 46 mm for X, Y and Z respectively as opposed to 24, 17 and 15 mm for the 'Free Network Transformed to Fiducial' approach. However, analysing the RMS's of the residuals of the fiducial stations after the transformation, ie 36, 50 and 44 mm for X, Y and Z respectively (see Table 8.14), it can be seen that they are quite similar to the recoveries of the 'Full Fiducial' approach. Such results, as expected, show a good agreement between these two approaches.

The benefits involved in the 'Free Network Transformed to Fiducial' and 'Free Precise Ephemeris Transformed to Fiducial' refer to the definition of the reference frame, which is involved in the last stage of the processing. Therefore, any change of the reference frame is easily adapted in this processing method. The conventional 'Full Fiducial' and 'Precise Ephemeris with Fiducial' approaches, however, require all the main steps of the processing to be repeated.

A complete free network adjustment (without loose constraints) was carried out with the inter-continental GPS network and the results have shown that the network has a *quasi* rank defect. In this solution, the deficiency of the network orientation about the Z axis is clearly illustrated by a very high orientation parameter (approximately 33") estimated in the transformation between the free network solution and the ITRF framework. When very loose constraints were applied to the station coordinates (1000 m to the ITRF stations), the orientation parameter reduced to 0.0024".

In the non-fiducial approach, the solution with only the coordinates of one station strongly constrained (2 cm) to the ITRF confirms that the network has a orientation deficiency. After applying a seven-parameter transformation relative to the ITRF93, the translation parameters did not change significantly with respect to the solutions in which no constraints were applied (test 1), but the orientation parameter about Z changed.

The free (or non-fiducial) approach has also been carried out to investigate the effects of applying very loose constraints to the station coordinates. When loose and internal constraints were respectively applied to the station coordinates and the covariance matrix, results with an accuracy at the cm level were obtained. This level of accuracy is compatible with that reported by Blewitt *et al* (1992).

Since ITRF errors are expected to be at the 10^{-9} level (Blewitt *et al*, 1992), the scale differences estimated in the transformation from the *free network reference frame* to ITRF93 do appear to be significant. The estimated differences are at the 10^{-8} level. Further investigation should be carried out, but one reason to explain the scale differences may be due to the use of a different earth gravity model. Whereas the solutions submitted to the ITRF make use of earth gravity model GEM-T2, including the first 12 moments, in GAS the

WGS84 model, with coefficients of up to the order and degree 8 is currently used.

The results of the free (or non-fiducial) approach have also shown that by applying constraints of 10 m to the ITRF coordinates and 1000 m to the new stations, highly accurate results can be obtained. The worst RMS after a seven-parameter transformation was 6.4 mm. Additionaly, the transformation parameters estimated from the transformation had no significance when compared with the corresponding standard error. This suggests that applying constraints of 10 m to the stations provides results comparable to those in which the stations are indeed fixed.

There is evidence from the results analysed in this research that GPS can produce a highly accurate global reference frame independent from other positioning systems such as SLR, LLR, VLBI. The geocentric offsets at the decimetre level may be due to mis-modelling of the satellite orbits. The deficiency in orientation, which is also present in the other systems can be tackled by applying respectively loose and internal constraints to some of the station coordinates, fixing one station or by applying internal constraints during the adjustment process.

A new set of coordinates for the Brazilian stations, with at least six-days of data, has been estimated. The precision of the coordinates of these stations is better than 3.5 cm. Comparison of this solution and the Brazilian IGS Epoch '92 solution resulted in RMS discrepancies of a maximum of 6 cm in the height component.

Chapter 9

CONCLUSIONS AND SUGGESTIONS FOR FURTHER WORK

9.1 Conclusions

Software

1 An efficient algorithm for handling 'missing' observations has been implemented in GAS. This algorithm is about 20 times faster than the one previously used in GAS.

2 The *base satellite per baseline* option, which allows for the processing of very large (even global) networks has also been implemented in GAS. Analysing the results obtained from the 'Quasi-network' (sub-division of the network) and 'Full network' processing of the Epoch '92 Campaign in Brazil, it can be concluded from the repeatability and recovery tests that the results improved significantly in the latter approach. This justifies the development and inclusion of the *base satellite per baseline* approach in GAS.

3 Two programs (CONSCOV3 and CONSCOV7) have been developed in order to apply internal constraints to the covariance matrix of the station coordinates estimated by GAS.

The Proposed Brazilian GPS Network

4 The solutions adopted by some countries in the provision of geodetic networks for supporting GPS activities have been described. It has been found that the general tendency is the establishment of new passive networks, retaining some stations of the conventional network, in order to provide a set of parameters to realise the transformation between the two systems. However, the state-of-the-art geodetic network is the so-

called Active Control System (ACS). The ACS provides users equipped with only one receiver with the capability of relative positioning without occupying any control point. The proposed Brazilian GPS network has some characteristics of an ACS.

5 Tests have been carried out to assess the expected precision that can be obtained by a user of the Brazilian GPS Network (RBMC), equipped with only one receiver. The results are given in terms of length and height component recoveries. The former gives an indication of the quality of the three components and the latter represents the component that generally provided the worst recoveries. They have shown results in the range of 1.3 to 0.1 ppm and 2 to 0.1 ppm for the length and height components respectively. With a single frequency receiver collecting 1 hour of data, precision of the order of 2 ppm is expected for height and 1.3 ppm for length, independently of using either broadcast or precise ephemerides. With 5 hours of data, the results improve to about 1 ppm. Once 1 hour of data of a dual frequency receiver is used in conjunction with the precise ephemerides, precision better than 0.2 ppm for the length and height component has been demonstrated. Both components do not improve significantly by increasing the interval of data collection. Dual frequency receiver, broadcast ephemerides and 1 hour of data collection have shown results better than 0.4 ppm for the length and height components. The latter become worse for longer intervals since the broadcast ephemerides were being used beyond the 'valid' (2 hours) interval.

Analysis of the IGS Epoch '92 Campaign in Brazil

6 From the analysis of repeatabilities and recoveries of the 'Full network' results of the IGS Epoch '92 campaign in Brazil, it has been made clear that for large networks, EBT corrections should be applied for achieving the highest accuracies. The application of OTL corrections did not have any significant improvement over the network analysed in Chapter 7. Furthermore, the use of tropospheric delay zenithal scale factors per station, modelled as a second order polynomial, showed better results than with a first order polynomial, suggesting that some un-modelled errors were still present. These could be due to Atmospheric Pressure Loading, multipath, or even a varying thoposphere.

7 All the Brazilian stations occupied during the IGS Epoch '92 Campaign have been integrated into the ITRF93. The repeatability of the worst component, height, was of about 20 mm for baselines of up to 8200 km. The plan components are about twice as good as the height component. The recovery, which gives an indication of the accuracy was worse than the precision. The computed value suggests an expected accuracy better than 8 cm for the stations with at least six days of data.

8 The International GPS Geodynamic Service (IGS) provides an effective way of connecting national and regional networks into a global reference frame.

9 The newly computed ITRF93 coordinates of station CHUA, the origin of SAD-69, differs from the currently used WGS84 values by -0.340, -0.421, 0.171 m in X, Y and Z geocentric coordinates respectively. These differences are well below the 2 m level of the expected accuracy of the Transit-Doppler derived absolute position of station CHUA.

10 The coordinates of the Brazilian stations with at least six-days of GPS data have also been estimated within the context of an inter-continental network (Chapter 8). The repeatabilities of this solution are similar to those of the IGS Epoch '92 Campaign in Brazil (Chapter 7). The results suggested precision better than 3.5 cm, approximately twice as good as the accuracies of the IGS Epoch '92 Campaign in Brazil (8 cm).

11 Comparison of the Brazilian station coordinates estimated in the inter-continental network solution (UEPP, BRAS and PARA) with that of the IGS Epoch '92 campaign in Brazil, resulted in maximum RMS discrepancies of 6.0 cm in the height component. For the north and east components the discrepancies were 1.3 cm and 1.6 cm respectively. These levels of errors are within the expected accuracy of the coordinates estimated in the IGS Epoch '92 campaign in Brazil (8 cm).

12 The coordinates of the Brazilian stations estimated in this research project can be used to support future high accuracy GPS activities in Brazil.

Analysis of the Inter-continental GPS Network

13 For the ordinary network adjustment approach applied to the inter-continental network, three solutions have been tested, namely 'Free Precise Ephemeris', 'Precise Ephemeris with Fiducial Stations', and 'Free Precise Ephemeris Transformed to Fiducial'. As expected, the worst results in terms of repeatabilities and recoveries were obtained using the 'Free Precise Ephemeris' solution, in which only the satellite positions were fixed. The recoveries of this solution provided an indication of the accuracy of the precise ephemeris used in the processing. The ephemeris errors are directly transferred to the station's coordinates, since no stations are fixed in the adjustment. The results showed accuracies compatible with the values claimed in the literature, better than 30 cm.

14 The 'Free Precise Ephemeris' solution was transformed to the same reference frame defined by the stations which were used as fiducial stations in the 'Precise Ephemeris with Fiducial Stations'. The transformed solution, referred to as 'Free Precise Ephemeris Transformed to Fiducial' solution, provided the best accuracies, which were 20, 17 and 22 mm for X, Y and Z respectively, compared with 49, 46 and 31 mm in the 'Precise Ephemeris with Fiducial Stations' approach. The precision, however, was slightly worse than that of the 'Precise Ephemerides with Fiducial Stations'. The maximum discrepancy between the repeatabilities of both approaches was 8 mm in the Z component. The better recoveries of the transformed solution are due to the fact that some errors (eg ephemeris errors) were eliminated in the transformation process.

15 The comparison between the approaches 'Full Fiducial' and 'Precise Ephemeris with Fiducial Stations' demonstrated that from a global point of view in terms of repeatabilities and recoveries, the latter provided slightly better results. The repeatabilities of the 'Full Fiducial' approach were 25, 38 and 19 mm in X, Y and Z respectively and 17, 23 and 15 mm in the 'Precise Ephemeris with Fiducial Stations'. The resulting recoveries of the three components were slightly better in the 'Full Fiducial' approach, ie 72 mm opposed to 74 mm in the latter. Such results show that the precise ephemeris used in the data processing (JPL precise ephemeris) was better determined than in the 'Full Fiducial'

approach used in this test, in which only six fiducial stations were used. The precise ephemerides determined by JPL for the IGS Epoch' 92 involved about 30 IGS core stations, with eight of them fixed as fiducial.

16 The free (or non-fiducial) approach solution was transformed to the reference frame defined by the fiducial stations used in the 'Full Fiducial' approach. This approach is referred to as 'Free Network Transformed to Fiducial'. The recoveries and repeatabilities of both approaches have been compared. In terms of repeatabilities they are quite similar, but the recoveries in the 'Full Fiducial' approach were much worse. They were 35, 43 and 46 mm for X, Y and Z respectively as opposed to 24, 17 and 15 mm for the 'Free Network Transformed to Fiducial' approach. However, analysing the RMS's of the residuals of the fiducial stations after the transformation, ie 36, 50 and 44 mm for X, Y and Z respectively (see Table 8.14), it can be seen that they are quite similar to the recoveries of the 'Full Fiducial' approach. Such results, as expected, showed a good agreement between these two approaches.

17 The results obtained by applying the 'Free Network Transformed to Fiducial' and 'Free Precise Ephemeris Transformed to Fiducial' approaches demonstrated that they provided reliable results. The benefits involved in these two approaches refer to the definition of the reference frame, which is involved in the last stage of the data processing. Therefore, any change of the reference frame is easily adapted in this processing method. The conventional 'Full Fiducial' approach, however, requires all the main steps of the processing to be repeated.

18 A complete free network adjustment (without loose constraints) was carried out with the inter-continental GPS network and the results have shown that the network has a *quasi* rank defect. In this solution, the deficiency of the network orientation about the Z axis is clearly illustrated by a very high orientation parameter (approximately 33") estimated in the transformation between the free network solution and the ITRF framework. When very loose constraints were applied to the station coordinates (1000 m to the ITRF stations), the orientation parameter reduced to 0.0024".

19 In the non-fiducial approach, the solution with only the coordinates of one station strongly constrained (2 cm) to the ITRF confirms that the network has an orientation deficiency. After applying a seven-parameter transformation relative to the ITRF93, the translation parameters did not change significantly with respect to the solutions in which no constraints were applied, but the orientation about Z changed.

20 The free (or non-fiducial) approach has also been carried out to investigate the effects of applying very loose constraints to the station coordinates. Once loose and internal constraints were respectively applied to the station coordinates and the covariance matrix, results with an accuracy at the cm level were obtained. This level of accuracy is compatible with that reported by Blewitt *et al* (1992).

21 The results of the free (or non-fiducial) approach have also shown that by applying constraints of 10 m to the ITRF coordinates and 1000 m to the new stations, highly accurate results can be obtained. The worst RMS after a seven-parameter transformation was 6.4 mm. Additionaly, the transformation parameters estimated from the transformation had no significance when compared with the corresponding standard error. This suggests that applying constraints of 10 m to the stations provides results comparable to those in which the stations are indeed fixed

22 There is evidence from the results analysed in this research that GPS can produce a highly accurate global reference frame independent from other positioning systems such as SLR, LLR, VLBI. The geocentric offsets at the decimetre level may be due to mis-modelling of the satellite orbits. The deficiency in orientation, which is also present in the other systems can be tackled by applying loose constraints to some of the station coordinates, fixing one station or by applying internal constraints to the covariance matrix or directly in the adjustment.

9.2 Suggestion for Further Work

1 The GAS module for cycle slip detection needs to be improved in order to enhance the manual detection of slips and outliers. It is a very time consuming task that could be less tedious, if plots of the residuals were available. By visually inspecting the residual graphs, it would become

very easy to identify undetected cycle slips and outliers, as they produce very distinct patterns in the double and triple difference residuals (Monico, 1992). Although the non-availability of this facility in the Nottingham software is not a limitation, its implementation would enhance significantly the system.

2 In order to obtain a more conclusive assessment of the precision that can be obtained by the users of the proposed Brazilian geodetic system, the tests carried out in this thesis using GPS data collected in Europe should be carried out using data collected in Brazil. The recent SIRGAS campaign (May-June 1995) may provide the data to carry out the tests. Furthermore, it has to be pointed out that although the results of the data processing using only a single baseline have provided very high precision, they are not very reliable. Therefore, the concept of reliability within the context of an ACS must be further investigated.

3 For a more detailed analysis on the establishment of global reference frame using GPS, tests should be carried out with a more representative (global) GPS data set, since the one analysed in this research was not global.

4 The application of internal constraints within the adjustment process (§4.8.3) instead of after the adjustment and only restricted to the covariance matrix is a topic to be investigated in conjunction with suggestion 3.

5 The value of the constraints to be applied to the different sets of parameters should be defined based on statistical analysis, instead of being subjectively chosen as it was in this research. This would involve the variance component estimation method.

6 A module to fix (from the Bulletin A values) or estimate the earth orientation parameter (EOP) or polar motion should be developed and implemented in GAS. The displacements resulting from EOP have non-zero average over any given time and should be considered in global solution at the centimetre level.

7 Although not applied during this research, it is known that Atmospheric Pressure Loading (APL) can induce deformation on the Earth's crust of about 1 cm for high latitude sites. Therefore, for high accuracy global GPS, the use of APL models should be investigated.

8 The ITRF errors are expected to be at the 10^{-9} level. Therefore, the scale differences estimated in the transformation from the *free network reference frame* to ITRF93 do appear to be significant. The estimated differences are at the 10^{-8} level. Further investigation should be carried out to better explain the scale differences. It may be due to the use of a different earth gravity model. Whereas the solutions submitted to the ITRF make use of earth gravity model GEM-T2, including the first 12 moments (order and degree), in GAS, the WGS84 model with coefficients of up to the order and degree 8 is currently used.

10 REFERENCES

Agrotis, L. G. (1984). ***The Determination of Satellite Orbits and the Global Positioning System,*** PhD Thesis, University of Nottingham.

Andersen P. H., Hauge S. and Kristiansen O. (1993) GPS Relative Positioning at a Precision Level of one Part Per Billion, ***Bulletin Géodésique, Vol 67 No 2,*** pp. 91-106.

Ashjaee J. and Lorentz R. (1992) ***Precision GPS Surveying After Y-Code,*** Ashtech Inc.- AN/AFTY(9/92), Sunnyvale, CA

Ashkenazi V., Moore T. and Monico J. F. G. (1995a) Centimetres over thousands of kilometres by GPS: Brazilian Test Network, ***Paper Submitted to Geophysical Research Letters,*** June 1995.

Ashkenazi V., Moore T. and Monico J. F. G. (1995b) High Precision GPS Network in Brazil, ***Revista Brasileira de Cartografia,*** Rio de Janeiro, Brazil, June 1995.

Ashkenazi V., Bingley R. M., Chang C.C., Dodson A. H., Torres J. A., Boucher C., Fagard H., Caturla J. L., Quiros R., Capdevlla J., Calvert C., Baker T.F., Rius A. and Cross P. A. (1994) EUROGAUGE: The West European Tide Gauge Monitoring Project, ***Proceedings of International Symposium on Marine Positioning INSMAP 94,*** Hannover, Germany, 19-23 September 1994.

Ashkenazi V., Bingley R. M., Whitmore G. M. (1993a) ***Reference Framework for Fiducial GPS,*** IESSG Publication, University of Nottingham, UK.

Ashkenazi V., Bingley R. M., Whitmore G. M. and Baker T. F. (1993b) Monitoring Changes in Mean-Sea Level to Millimeters Using GPS, ***Geophysical Research Letters,*** Vol. 20, No. 18, pp 1951-1954, September, 1993.

Ashkenazi V. and Ffoulkes-Jones G.H. (1990) Millimiters Over Hundred of Kilometres by GPS, ***GPS World,*** Vol 1, NO. 6, Nov/Dec/1990.

Ashkenazi, V., Moore, T., Ffoulkes-Jones, G.H., Whalley, S. and Aquino M. (1990). High Precision GPS Positioning by Fiducial Technique. In: Bock Y., Leppard N. (eds): Global Positioning System: An Overview, ***Springer, New York, Berlin, Heidelberg, Lond, Paris, Tokyo, Hong Kong, pp 195-202, [Mueller I.I. (ed): IAG Symposia 102].***

Ashkenazi, V. and Moore T. (1986). The Navigation of Navigation Satellites, ***Journal of Navigation***, Vol.3 No.3.

Ashkenazi V., Crane S. A., W. J., Willians J. W. (1980). The 1980 Readjustment of the triangulation of the United Kingdom and the Republic of Ireland OS(SN)80, ***Ordnance Survey Professional Paper New Series***, No. 31, United Kingdom.

Beamson G. A. (1995) ***Precise Height Determination of Tide Gauges Using GPS***, PhD Thesis, University of Nottingham.

Baker T. F., Curtis D. J. and Dodson A. H. (1995) Ocean Tide Loading and GPS, ***GPS World***, March 1995, pp 54-59.

Baker T. F. (1984) Tidal deformation of the Earth, ***Sci. Prog., Oxf.*** 69, pp 197-233.

Bergamini, E.W. (1993). IGS Service: Epoch '92 Regional Centre in Brazil, ***Proceedings of the 1993 IGS Workshop***, pp 25-31, Ed. by G.Beutler and E. Brockmann, Univ. of Berne, 1993.

Beutler G., Brockmann E., Gurtner W., Hugentobler U., Mervart L., Rothacher M., and Verdun A. (1994) Extended orbit modeling techniques at the CODE processing center of the international GPS service for geodynamics (IGS): theory and initial results, ***Manuscripta geodaetica*** 19, p.367-386.

Beutler G. (1993). The 1992 IGS Test Campaign, Epoch '92 and the IGS Pilot Service: An Overview, ***Proc. of the 1993 IGS Workshop***, pp 3-9, Ed. by G.Beutler and E. Brockmann, Univ. of Berne, 1993.

Beutler G., Gurtner W., Bauresima I. and Rothacher M. (1987) Correlations Between Simultaneous GPS Double Difference Carrier Phase Observations in the Multistation mode: Implementation Considerations and First Expericences, ***Manuscripta geodaetica*** 12, p.40-44.

Beutler G., Gurtner W., Bauresima I. and Rothacher M. (1986) Efficient Computation of the Inverse of the Covariance Matrix of Simultaneous GPS Carrier Phase Difference Observations, ***Manuscripta geodaetica*** 11, p.249-255.

Bingley R. (1994) ***Personal Communication on REPDIF Software***, University of Nottingham, January 1994.

Blewitt G. (1995) ***Personal Communication from University of Newcastle***, UK, June 1995.

Blewitt, G., van Dam T., Heflin M. B. (1994) Atmospheric Loading Effects and GPS Time-Averaged Vertical Positions, ***Proceedings of the 1st International Symposium on Deformation in Turkey***, Istanbul, Turkey (in press, 1994).

Blewitt, G. (1993a) ***Personal Communication*** , An updated solution as presented in: "Blewitt, G., M. Heflin, Y. Vigue, J.F. Zumberge, D. Jefferson, and F. H. Webb, "The Earth viewed as a deforming polyhedron: method and results" in Proc. of the (1993) IGS Workshop, p.165-174, Ed. by G.Beutler and E. Brockmann, Univ. of Berne, (1993).

Blewitt, G., M.B Heflin, Y. Vigue, J.F. Zumberge, D. Jefferson, and F. H. Webb (1993b). The Earth viewed as a deforming polyhedron: method and results. ***Proc. of the 1993 IGS Workshop***, pp 165-174, Ed. by G.Beutler and E. Brockmann, Univ. of Berne, 1993.

Blewitt G., Heflin M. B., Webb F. H., Lindqwister U. J. and Malla R. P. (1992). Global Coordinates with Centimeter Accuracy in the International Terrestrial Reference Frame Using GPS, ***Geophysical Research Letters***, Vol. 19, No.9, pp 853-856.

Blewitt, G., (1989). Carrier Phase Ambiguity Resolution for the Global Positioning System Applied to Geodetic Baselines up to 2000 Km, ***Journal of Geophysical Research***, Vol. 94, No. B8, pp. 10187-10203

Blitzkow D., Netto, N.P., Cintra, J.P., Junior, E.S.F., Bueno, R.F., Schaal, R.E., Fortes, L.P.S., Pereira, K.D. and Campos, M.A. (1993). GPS Network in Brazil, ***Paper Presented at the IAG General Meeting***, Beijing, China.

Boucher C., Altamimi Z. and Duhem L. (1994) ***Results and Analysis of the ITRF93,*** Technical Note 18, October 1994, Observatoire de Paris.

Boucher C.,Altamimi Z. and Duhem L. (1993a) ***ITRF 92 and its associated field,*** Technical Note 15, October 1993, Observatoire de Paris.

Boucher C. and Altamimi Z. (1993b) Contribution of IGS 92 to the Terrestrial Reference Frame, ***Proceedings of the 1993 IGS Workshop***, pp 175-183, Ed. by G.Beutler and E. Brockmann, Univ. of Berne, 1993

Boucher C.,Altamimi Z. and Duhem L. (1992) ***ITRF 91 and its associated field,*** Technical Note 12, October 1992, Observatoire de Paris.

Boucher C. and Altamimi Z. (1991a) ***ITRF 89 and other realizations of the IERS Terrestrial Reference Frame for 1989***, IERS Technical Note 6, April 1991, Observatoire de Paris.

Boucher C. and Altamimi Z. (1991b) ***ITRF 90 and other realizations of the IERS Terrestrial Reference Frame for 1990***, IERS Technical Note 9, December 1991, Observatoire de Paris.

Boucher C. and Altamimi Z. (1989) ***The Initial IERS Terrestrial Reference Frame***, IERS Technical Note 1, June 1989, Observatoire de Paris.

Breach M. C. (1990) The importance of accurate coordinates of a known station in precise relative positioning, ***Survey Review***, 30, 238, pp 398-403.

Brockmann E., Beutler G., Gurtner W., Rothacher M., Springer T. and Mervat L. (1993) Solution using European GPS Observations produced at the "Center for Orbit Determination in Europe" (CODE) during the 1992 IGS Campaign, ***Proceedings of the 1993 IGS Workshop***, pp 251-260, Ed. by G.Beutler and E. Brockmann, Univ. of Berne, 1993.

Christie R. R. (1992) ***Pillars in the sky***, Paper Presented at the Civil Engineering Surveying Conference, Keele University, April 1992.

Costa S. M. A. and Fortes (1991) ***Ajustamento da Rede Planimetrica do Sistema Geodesico Brasileiro***, Departamento de Geodesia, IBGE, Rio de Janeiro, Brasil.

Costa S. M. A and Pereira K. D. (1994) ***Personal Communication*** Processamento da Rede GPS Brasileira e Ajustamento Combinado com a Rede Classica.

Cross P. A. (1983) Advanced Least Squares Applied to Position Fixing, *Working Paper* No6, NELP, 1983.

Curley. R.A. (1988). ***The Use of TI 4100 GPS Receivers and MAGNET Software to Determine Height Differences***. MSc Thesis, University of Nottingham.

Delikaraglou D., Steeves R.R. and Beck N. (1986) Development of a Canadian Active Control System Using GPS, ***Fourth International Geodetic Symposium on Satellite Positioning***, Austin Texas, April 28-May 2 1986.

DMA - Defence Mapping Agency (1987) ***Department of Defence World Geodetic System 1984- Its Definition and Relationships With Local Geodetic Systems***, DMA Technical Report 8350.2

Dodson A. H., Hill C. J. and Shardlow P. J. (1993) The effects of Error Propagation on GPS Measurements, ***Sixth International Seminar on the GPS***. University of Nottingham.

Dong D. and Bock Y., (1989) Global Positioning System Network Analysis with Phase Ambiguity Resolution Applied to Crustal Deformation Studies in California, ***Journal of Geophysical Research***, Vol. 94, No B4, pp 3949-3966.

Ffoukes-Jones G.H. (1990) ***High Precision GPS by Fiducial Techniques***, PhD Thesis, University of Nottingham.

Fliegel H. F., Gallini T. E. and Swift E. R. (1992) Global Positioning System Radiation Force Model for Geodetic Applications, ***Journal of Geophysical Research***, Vol. 97, No. B1, pp. 559-568.

Fortes L. P. S (1991) Brazilian Network for Continuous Monitoring of the Global Positioning System :RBMC, In: Mader G.L. (ed): Permanent Satellite Tracking Networks for Geodesy and Geodynamics, ***Springer, New York, Berlin, Heidelberg, Lond, Paris, Tokyo, Hong Kong, pp 95-101, [Torge W.. (ed): IAG Symposia 109].***

Fortes L. P. S. and Godoy R.A.Z. (1991) ***Rede Brasileira de Monitoramento Continuo do Sistema de Posicionamento Global-GPS***, Departamento de Geodesia, Diretoria de Geociencias, IBGE, RJ, Brazil.

Fortes L.P.S., Cagnin I.F. and Godoy R.A.Z. (1989) Determinação dos Parametros de Transformação entre os Sistemas NWL-10D, NSWC-9Z2, WGS-84 eo SAD-69. ***Anais do XIV Congresso Brasileiro de Cartografia***, Vol I, p. 157-165.

Georgiadou Y. (1990) Ionospheric Delay Modelling for GPS Relative Positioning, ***Second International Symposium on Precise Positioning with the Global Positioning System***, Ottawa, Canada, Sep 3-7, 1990, pp 403-410

Goad C. (1993) IGS Orbits Comparisons, ***Proceedings of the 1993 IGS Workshop***, pp 218-225, Ed. by G.Beutler and E. Brockmann, Univ. of Berne, 1993.

Godoy R. A. Z., Pereira K. D., Oliveira P.M.G. (1991) ***Reprocessamento de Estacoes Doppler no IBGE***, Departamento de Geodesia, IBGE, Rio de Janeiro, Brasil.

Heflin M., Blewitt G., Jefferson D., Vigue Y., Weeb F., Zumberge J., Argus D., Clark T., Gipson J. and Chopō Ma. (1993) ***Global Positions and Velocities from One Year of GPS Data***, Paper presented at AGU Meeting, San Francisco, December 9, 1993.

Heflin M., Blewitt G., Bertiger W., Freedman A., Hurst K., Lichten S., Lindqwister V., Malla R., Vigue Y., Weeb F., Yurck T. and Zumberge J. (1992a) Analysis of Global GPS Experiments Without Fiducial Sites, ***Proceedings of Sixth International Geodetic Symposium on Satellite Positioning***, Volume I, Columbus, Ohio, 17 to 20 March 1992, pp 436-438.

Heflin M., Bertiger W., Blewitt G., Freedman A., Hurst K., Lichten S., Lindqwister V., Vigue Y., Weeb F., Yurck T. and Zumberge J. (1992b) Global Geodesy Using GPS without Fiducial Sites, ***Geophysical Research Letters***, Vol. 19, NO. 2, pp 131-134, January, 24-1992.

Herring T.A., Dong D. and King R. W. Sub-Milliarcsecond Determination of Pole Position Using Global Positioning System Data (1991) ***Geophysical Research Letters***, Vol.18 NO. 10, pp 1893-1896, October, 1991

Hofmann-Wellenhof B., Lichtenegger H. and Collins J. (1992) ***GPS Theory and Practice***, Spring-Verlag, Wien

King R. W., Master E.G., Rizos C., Stolz A. and Collins J. (1985) ***Surveying with GPS***, Monograph No. 9, School of Surveying, The University of New South Wales, Kensigton, NSW, Australia.

Klobuchar J. A. (1986) Design and Characteristics of the GPS Ionospheric Time Delay Algorithm for Single Frequency Users, ***Proceedings of the PLANS-86 conference***, Las Vegas, pp. 280-286.

Koch K.R. (1987) ***Parameter Estimation and Hypothesis Testing in Linear Models***, Springer-Verlag, New York.

Kösters A. J. M (1992) ***Some Aspects of a 3-Dimensional Reference System for Surveying in the Netherlands: Quality Analysis of GPS Phase Observations***, Report 92.1 of the Faculty of Geodetic Engineering, Delft University of Technology.

Kouba J., Tétreault P., Ferland R. and Lahaye F. (1993) IGS Data Processing at the EMR Active Control System Centre, ***Proceedings of the 1993 IGS Workshop***, pp 123-132, Ed. by G.Beutler and E. Brockmann, Univ. of Berne, 1993.

Lachapelle G., Killand P. and Casey M., (1992) GPS For Marine Navigation and Hydrography, ***International Hydrographic Review***, Monaco, LXIX(1), March 1992, pp 43-69.

Leick A. (1990) ***GPS Satellite Surveying***, New York, John Wiley & Sons.

Lowe D. P. (1994) ***CARNET User Guide***. Version 3.13. IESSG Publication, University of Nottingham.

Lowe D. P. (1992) ***Adjustment Models for Integrated Geodesy***. PhD Thesis, University of Nottingham.

McCarthy D. D. (1992) IERS Standards (1992), ***IERS Technical Note 13***, Central Bureau of IERS- Observatoire de Paris

Monico J. F. G., Moore T and Ashkenazi V. (1994) Preliminary results of the IGS Epoch '92 Campaign in Brazil, ***IAG Courier for Development***, Newsletter No. 3, August 94.

Monico J. F. G. (1992) ***Processing Small GPS Network with the Bernese GPS Software Version 3.2-D : Summer Camp 1990***, Delft Geodetic Computing Centre, Delft University of Technology, Delft, The Netherlands.

Monico J. F. G. (1988) ***Ajustamento e Análise Estatística de Observações Aplicados na Detecção de Deformações***, MSc Thesis, Universidade Federal do Paraná, Brasil.

Moore T. (1993) GPS Orbit Determination and Fiducial Networks, ***Sixth International Seminar on the Global Positioning System***, University of Nottingham, Nottingham.

Moore T. (1986) ***Satellite Laser Ranging and the Determination of Earth Rotation Parameters***, PhD Thesis, University of Nottingham.

Mueller I. I. (1993) The International GPS Service for Geodynamics: An Introduction. ***Proceedings of the 1993 IGS Workshop***, pp 1-2, Ed. by G.Beutler and E. Brockmann, Univ. of Berne, 1993.

Muller, I. I. and Beutler (1992) The International GPS Service for Geodynamics - Development and Current Status, In: ***Proceedings Sixth International Geodetic Symposium on Satellite Positioning***, Columbus, Ohio, March 1992, pp. 823-835.

Mueller T. (1994) Wide Area Differential GPS, ***GPS World***, June 1994, pp 36-44.

Mur M. T.J., Dow J.M., Feltens J., Garcia Martinez C. (1993) ESOC Station Coordinate Solutions for the IGS'92 Campaign, Including Epoch,92, ***Proceedings of the 1993 IGS Workshop***, pp 275-284, Ed. by G.Beutler and E. Brockmann, Univ. of Berne, 1993.

Neilan R. E. and Noll C.E. (1993) The IGS Core and Fiducial Networks: Current Status and Future Plans, ***Proceedings of the 1993 IGS Workshop***, pp 32-41, Ed. by G.Beutler and E. Brockmann, Univ. of Berne, 1993.

Newby S. P. and Langley R. B. (1992) Three Alternative Empirical Ionospheric Models- Are They Better Than the GPS Broadcast Model?, ***Proceeding of Sixth International Geodetic Symposium on Satellite Positioning***, 17 to 20 March 1992, Vol 1, pp 240-244.

Newby S. P. and Langley R. B. (1990) Ionospheric Modelling for Single Frequency Users of the Global Positioning System: A Status Report, ***Proceedings of Second International Symposium on Precise Positioning with the Global Position System***, Ottawa, Canada, 3 to 7 September 1990, pp 429-443.

Noll C.E. and Dube M.P. (1993) ***Developing of a GPS Data Catalogue for the IGS Epoch '92 Campaign***, Fall (1993) AGU Meeting, December 06-10, 1993.

Ochieng W. Y. (1993) ***Wide Area DGPS And Fiducial Network Design***, PhD Thesis, University of Nottingham.

Ochieng W. Y. (1990) ***GPS Selective Availability: Implementation and Effects***, MSc Thesis, University of Nottingham.

Schupler B. R. and Clark T. A. (1991) How Different Antennas Affect the GPS Observables, ***GPS Word***, pp 32-36, November/December 1991.

Seeber G. (1993) ***Satellite Geodesy: foundations, methods and applications,*** Berlin, New-York: Walter de Gruyter.

Shardlow P. J. (1994) ***Propagation Effects on Precise GPS Heighting***, PhD Thesis, University of Nottingham, UK.

SIRGAS (1994) ***South America Geocentric Reference System***, Newsletter #2, IAG, IPGH, DMA

Spilker J.J. (1980) GPS Signal Structure and Performance Characteristics, ***Global Positioning System***, Vol I, The Institute of Navigation, ISBN: 0-936406-00-3.

Springer T. A. and Beutler G. (1993) Toward an Official IGS Orbit by Combining the Results of All IGS Processing Centers, ***Proceedings of the 1993 IGS Workshop***, pp 242-249, Ed. by G.Beutler and E. Brockmann, Univ. of Berne, 1993.

Stewart M. P., Ffoulkes-Jones G. H. and Ochieng W. Y. (1994) ***GPS Analysis Software (GAS) Version 2.2 User Manual***, IESSG Publication, University of Nottingham, UK.

Talbot N. C. (1992) ***Recent Advances in GPS Surveying, Applications and Technical Notes***, Publication of Trimble Navigation.

Talbot N. C. (1991) ***Real-Time High Precision GPS Positioning Concepts: Modelling, Processing and Results***, PhD Thesis, Department of Land Information, RMIT Centre for Remote Sensing, Victoria, Australia.

Teunissen P. J. G. and Van der Marel H (1992) ***GPS Work Group Lecture Notes***, Faculty of Geodesy, TU Delft, Delft, The Netherlands.

Teunissen P. J. G. (1990). ***Mathematische Geodesie I***, Faculteit der Geodesie, TU Delft, Delft, The Netherlands.

Teunissen P. J. G. (1989). ***Mathematische Geodesie II***, Faculteit der Geodesie, TU Delft, Delft, The Netherlands.

Underhill and Underhill, Usher Canada Limited and UGC Consulting Ltd. (1993). ***ACS Applications Definition & Feasibility Study***, British Columbia Ministry of Environment and Parks Survey & Resource Mapping Branch, ISBN 0-7726-1626-4.

Van Dam T. M and Wahr J. M. (1987) Displacements of the Earth's Surface Due to Atmospheric Loading: Effects on Gravity and Baseline Measurements, ***Journal of Geophysical Research***, Vol. 92, No. B2, pp 1281-1286.

Vaníc̆ek P. and Krakiwsky E. (1986). ***Geodesy : The Concepts***, North Holland, Amsterdam.

Wanminger L. (1993) Effects of the Equatorial Ionosphere on GPS, ***GPS World***, July 1993, pp 48-54.

Wells D., Beck N., Delikaraoglou D., Kleusberg A., Krakiwsky E. J., Lachapelle G., Langley R. B., Nakiboglu M., Schwarz K.P., Tranquilla J. M., Vanicek P. (1986), ***Guide to GPS Positioning***, Canadian GPS Associates, Fredericton, New Brunswick, Canada.

Whalley, S. (1990). ***Precise Orbit Determination for GPS Satellites***. PhD Thesis, University of Nottingham.

White H. L., Decker B. L. and Kumar M. (1989) WGS 84 Reference Frame, ***Proceeding of 5th International Geodetic Symposium on Satellite Positioning,*** March 13-17 1989, Las Cruces, New Mexico, pp 127-141.

Whitmore G. (1994) ***Coordinate Reference System for High Precision Geodesy***, PhD Thesis, University of Nottingham.

Wilson J. I. and Christie R. R. (1992) ***A New Geodetic Datum For Great Britain: The Ordnance Survey Scientific GPS Network: SCINET92***, Ordnance Survey, Southampton, UK.

Zeigler H. J. (1988) GPS Geodetic Reference System in Tennessee, ***Journal of Surveying Engineering***, Vol. 114 No. 4, November, 1988

Zumberge J. F., Jefferson D. C., Blewitt G., Heflin M. B. and Webb F. H. (1993) Jet Propulsion Laboratory IGS Analysis Center Report, 1992. ***Proceedings of the 1993 IGS Workshop***, pp 154-163, Ed. by G.Beutler and E. Brockmann, Univ. of Berne, 1993.